Formation of the Testicular Immunological Barrier through Immunomodulation and ZIP9 Androgen Signaling in Rat Sertoli Cells

Inaugural Dissertation
Submitted to the
Faculty of Veterinary Medicine
In partial fulfillment of the requirements
for the PhD-Degree
of the Faculties of Veterinary Medicine and Medicine
of the Justus Liebig University Giessen

Submitted by

Hassan Kabbesh,

Veterinarian from Damascus, Syria

Giessen 2022

From the Institute of Veterinary Physiology and Biochemistry

Director / Chairman: Prof. Dr. Martin Diener

Of the faculty of Veterinary Medicine of the Justus Liebig University Giessen

First Supervisor and Committee Member: Prof Dr. Georgios Scheiner-Bobis

Second Supervisor and Committee Member: PD Dr. Lutz Konrad

Committee Members: Prof. Dr. Christine Wrenzycki - PD. Dr. Joachim Weitzel

Date of Doctoral Defense: 24.01.2023

Abbreviation:

ABP: Androgen binding protein

Akt: Protein kinase B

AMH: Anti-Müllerian hormone

AR: Androgen receptor

ASMA: alpha smooth muscle actin

ATF-1: Activating transcription factor-1

BCS: Bovine calf serum

bp: Base pair

BMP: Bone morphogenetic protein

BSA: Bovine serum albumin

BTB: Blood testis barrier

cAMP: Cyclic adenosine monophosphate

CAR: Coxsackievirus-adenovirus receptor

CCL: C-C motif chemokine ligand

CCR2: C-C chemokine receptor type 2

CD: Cluster of differentiation

Cldn: Claudin

CR: Conditional reprogramming

c-Raf: Rapidly accelerated fibrosarcoma

CREB: cAMP response element-binding protein

Cxcl: C-X-C Motif Chemokine Ligand

d: Day

DAPI: 4′,6-diamidino-2-phenylindole

DHT: Dihydrotestosterone

DMEM/F-12: Dulbecco's modified eagle medium/nutrient mixture F-12

DMSO: Dimethyl sulfoxide

DNA: Deoxyribonucleic acid

DNase I: Deoxyribonuclease I

DPBS: Dulbecco′s Phosphate Buffered Saline

DTT: 1,4-Dithiothreitol

ECL: Enhanced chemiluminescence

ECM: Extracellular matrix

EDTA: Ethylenediaminetetraacetic acid

ER: Endoplasmic reticulum

Erk1/2: Extracellular signal-regulated kinases 1 and 2

FACS: Fluorescence activated cell sorting

FCS: fetal calf serum

Fig: Figure

FITC: Fluorescein isothiocyanate

FSH: Follicle stimulating hormone

g: Gradual gravitation

GATA1: Erythroid transcription factor 1

GnRH: Gonadotropin releasing hormone

Gnα11: G protein α11

GPCR: G-Protein coupled receptor

hr: Hour

IFN- γ: Interferon gamma

IGF-1: Insulin-like growth factor 1

IL: Interleukin

ITS: Insulin transferrin selenium

JAM: Junction adhesion molecule

KDa: kilo Dalton

LCs: Leydig cells

LH: Luteinizing hormone

LPS: Lipopolysaccharide

M: Macrophages

MAPK: Mitogen-activated protein kinase

M-CSF: Macrophage colony stimulating factor

MCP1: Macrophage chemoattractant protein 1

MG: Matrigel

mRNA: Messenger RNA

mL: Milliliter

nc-siRNA: negative control siRNA

ng: Nanogram

nM: Nanomolar

NO: Number

OD: Optical density

P: Passage

P450scc: Cytochrome P450 side-chain cleavage enzyme

PA: Plasminogen activator

PASC1: Primary adult rat Sertoli cells-1

PBS: Phosphate Buffered Saline

PCR: polymerase chain reaction

PCs: Peritubular cells

PI3K: Phosphatidylinositol 3-kinase

PKA: Protein kinase A

PKC: Protein kinase C

PMSF: Phenylmethyl sulfonyl fluoride

P/S: Penicillin streptomycin

qRT-PCR: quantitative real time polymerase chain reaction

Raf: proto-oncogene serine/threonine-protein kinase

Ras: sarcoma protein kinase

RBDM: Rat blood derived monocytes

RNA: Ribonucleic acid

Rock inhibitor: Rho kinase inhibitor

RT: Room temperature

SCO: Sertoli cell only syndrome

SCs: Sertoli cells

SDS: Sodium dodecyl sulfate

SEM: Standard error of the mean

Ser: Serine

siRNA: small interfering RNA

SOX9: SRY-Box transcription factor 9

Src: Proto-oncogene sarcoma protein

T: Testosterone

T-BSA-FITC: Testosterone-conjugated bovine serum albumin-labeled fluorescein isothiocyanate

TDA: Tracer diffusion assay

TEMED: Tetramethylethylenediamine

TER: Transepithelial electrical resistance

TGF-β: Transforming growth factor-beta

TIB: Testicular immunological barrier

TM: Testicular macrophages

TNF-α: Tumor necrosis factor-alpha

µg: Microgram

µm: Micrometer

µM: Micromolar

WB: Western blots

ZIP9: a zinc transporter from the family ZRT/IRT-like protein 9 (ZRT=zinc-regulated transporter; IRT=iron-regulated transporter)

ZO: Zonula occludens

HSD17β3: Hydroxysteroid dehydrogenase 17 beta3

Table of Contents

1 Introduction 14

1.1 The male reproductive tract 14

1.1.1 Function and anatomy of the testis 14

1.1.2 Functions of peritubular cells (PCs) 15

1.1.3 Structure and functions of Sertoli cells 15

1.1.4 Spermatogenesis 16

1.2 Formation and regulation of the blood testis barrier (BTB) 17

Figure 2. Illustrative figure of the blood testis barrier. 18

1.3 The testis as an immune privileged organ 20

1.3.1 Maintenance of the testicular immune privilege through structural elements and local immune tolerance 20

1.3.2 The role of testicular macrophages (TMs) and other local immune cells in testis immune privilege 21

1.4 Steroidogenesis and the production of male sex hormones 22

1.4.1 The classical and the non-classical pathway of androgen signaling in testis 23

1.4.2 ZIP9 as a non-classical receptor of androgen signaling 25

1.5 Aims of the study 25

2 Materials and Methods 27

2.1 Chemicals and materials 27

2.1.1 Chemicals 27

2.1.2 PCR Reagents 29

2.1.3 Antibodies 29

2.1.4 Cytokines and toxins 30

2.1.5 kits 31

2.1.6 Enzymes 31

2.1.7 Primers 31

2.1.8 Cell culture reagents 33

2.1.9 siRNA transfection reagents 34

2.1.10 siRNA sequences 34

2.1.11 Equipments 34

2.1.12 Miscellaneous 35

2.2 Buffer solutions and reagent used for western blot 36

2.2.1 Western blots buffers 36

2.3 Cell culture 37

2.3.1 93RS2 Sertoli cells 37

2.3.2 Irradiation of 3T3-J2 mouse fibroblast and preparation of conditioned medium (CM) 37
2.4 Animals 38
2.5 Isolation of primary adult rat Sertoli cells and PCs 38
2.5.1 Isolation of primary adult rat Sertoli cells and PCs using enzymatic digestion 38
2.5.2 Conditional reprogramming of primary adult rat Sertolie cells by culturing freshly isolated SC clusters with CM 39
2.6 Isolation of rat blood-derived-monocytes (RBDM), purity assessment and polarization toward M0, M1 and M2 macrophages 40
2.6.1 Isolation and purity assessment of RBDM 40
2.6.2 Differentiation of RBDM into M0 macrophages and polarization into M1 and M2 macrophages 40
2.7 Immunofluorescence 41
2.8 RNA extraction, RT-PCR and quantitative real time PCR 42
2.8.1 RNA Isolation 42
2.8.2 DNase digestion 42
2.8.3 DNase digestion reaction mix: 42
2.8.4 cDNA synthesis 43
2.8.5 Denaturation of RNA and primer annealing: 43
2.8.6 RT mix: 44
2.8.7 RT-PCR 44
2.8.8 Quantitative real-time PCR (qRT-PCR) 44
2.9 Transmigration assay of macrophages 45
2.10 Measurement of transepithelial resistance (TER) 46
2.11 Tracer diffusion assay (TDA) 46
2.12 Silencing expression of ZIP9 or AR via siRNA 47
2.13 Plasma membrane labeling with testosterone-BSA-FITC 47
2.14. Treatments and sample preparations for western blots (WB) 48
2.14.1 Preparation of cell lysates from PASC1 48
2.14.2 SDS-polyacrylamide gel electrophoresis 48
2.14.3 Western blotting 49
2.14.4 Reprobing of the membrane 50
2.15 Statistical analysis 50
3 Results 51
3.1.1 Isolation, characterization and purity assessment of adult rat Sertoli cells 51
3.1.2 Characterization of PASC1 and expression of testicular markers 56
3.1.3 Formation of the SC barrier to a functional characterize PASC1 59
3.1.4 Expression of the androgen receptor (AR) in PASC1 60

3.1.5 Effects of T on PASC1 barrier integrity 61
3.1.6 Effects of T on the tight junction proteins zonula occludens-1 (ZO-1) and junctional adhesion molecule (JAM-3) 62
3.1.7 Effects of different cytokines on the TJ barrier of PASC1 64
3.2 Characterization of the testicular immunological barrier (TIB) formed between PASC1 65
3.2.1 Isolation and characterization of rat blood-derived-monocytes (RBDM) 65
3.2.2 Characterization of M0, M1, and M2 after polarization 69
3.2.3 The role of macrophage chemoattractant protein-1 (MCP1) in the transmigration assay 70
3.2.4 Transmigration assay of macrophages through testicular cells 70
3.2.5 Influence of cytokines on macrophage transmigration through the testicular barrier formed between PASC1 72
3.3 Contribution of the classical AR or Zrt- and Irt-like protein 9 ZIP9 on TJ formation between PASC1 cells 74
3.3.1 Silencing AR or ZIP9 expression by siRNA to investigate their role in androgen signaling 74
3.3.2 Investigation of the responsiveness of the PASC1 AR towards T or towards the ZIP9-targeting androgenic tetrapeptide IAPG 76
3.3.3 Binding of the IAPG peptide or of T to the androgen binding site of ZIP9 77
3.3.4 Stimulation of Erk1/2 phosphorylation by T or IAPG 79
3.3.5 Identification of the receptor for androgen involved in Erk1/2 phosphorylation 80
3.3.6 Involvement of AR or ZIP9 in stimulation of CREB/ATF-1 phosphorylation by T or IAPG .. 82
3.3.7 Involvement of AR or ZiP9 in stimulation of ZO-1 expression by T or IAPG 84
3.3.8 Participation of AR or ZIP9 in stimulation of Cldn-1 and JAM-3 expression by T or IAPG . 85
3.3.9 Investigation of the involvement of AR or ZIP9 in T- or lAPG-induced TJ formation 87
4 Discussion 89
4.1 Isolation and characterization of the primary adult rat Sertoli cell line-1 (PASC1) 89
4.2 Establishment and characterization of the TJ barrier formed between PASC1 91
4.3 Effects of some testicular cytokines on the TJ barrier of PASC1 91
4.4 Studying the TJ barrier between PASC1 from an immunological aspect 92
4.5 Effects of different testicular cytokines on transmigration of macrophages through the TJ barrier between PASC1 94
4.6 Investigation of the involvement of the classical AR or ZIP9 in androgen signaling and TJ formation in PASC1 95
4.7 Investigation of the involvement of either the classical AR or ZIP9 in PASC1 androgen signaling in stimulation of Cldn-1 or JAM-3 and of the TJ integrity 96
4.8 ZIP9, the non-classical androgen receptor and its future therapeutic application 98
4.9 Conclusion 99
5 Summary 101
6 Zusammenfassung 102

7 References 104
8 Acknowledgements 125
9 Declaration 126
10 Erklärung 126
11 Own publications 127

List of figures:

Figure 1. The stages of spermatogenesis are illustrated. 17
Figure 2. Illustrative figure of the blood testis barrier..... 18
Figure 3. Schematic overview of the hypothalamic pituitary gonadal axis in males. 23
Figure 4. The classical and the non-classical signaling pathway of T. 24
Figure 5. Brightfield microscopic photos of freshly isolated SCs. 52
Figure 6. Comparison of freshly isolated SC clusters with complete CM compared to complete DMEM/F12 in collagen-coated flasks..... 53
Figure 7. Overview of the CR method for the isolation of adult rat SCs. 56
Figure 8. Immunofluorescence staining of PASC1 against SOX9, ASMA or both..... 57
Figure 9. qRT-PCR analysis of mRNA expression of SC-specific and/or -maturation markers in PASC1. 59
Figure 10. Time-dependent effects on the barrier integrity of SCs and PCs in mono-or co-cultures. 59
Figure 11. Conditionally reprogrammed PASC1 express the androgen receptor (AR) on the protein (A–D) and mRNA level (A) in passages P4 and P16. 61
Figure 12. Time-dependent effects of T on the PASC1 TJ barrier. 62
Figure 13. Effects of T on JAM-3 mRNA expression and protein presence. 63
Figure 14. Effects of T on ZO-1 mRNA expression (A) and protein presence (B–D). 64
Figure 15. Effects of IL-6, BMP2 or TGF-β3 on barrier integrity of PASC1..... 65
Figure 16. Morphology and characterization of RBDM with CD68 and TNF-α mRNA. 67
Figure 17. Overview of the isolation of RBDM, their differentiation, and polarization into M0, M1, and M2 macrophages. 68
Figure 18. Expression of macrophage-specific genes after polarization analyzed with qRT-PCR. 69
Figure 19. Concentration-dependent effects of MCP1 as macrophage chemoattractant in the transmigration assay. 70
Figure 20. Transmigration of macrophages M0, M1 and M2 through a barrier of PASC1 or PC, alone or both with or without matrigel (MG). 71
Figure 21. Characterization of PASC1 transmigration after treatment with different cytokines. 73
Figure 22. Detection of AR mRNA or protein in PASC1 cells. 75
Figure 23. Detection of ZIP9 mRNA or protein in PASC1 cells. 76
Figure 24. Localization of AR in PASC1 cells with T or IAPG treatment. 77

Figure 25. Testosterone-BSA-FITC (T-BSA-FITC) membrane labeling of PASC1 cells.78
Figure 26. Western blot analysis of phospho-Erk1/2 after stimulation of PASC1 cells with various concentrations of T or IAPG for 24 hrs. 80
Figure 27. Immunofluorescence of phospho-Erk1/2 in PASC1 cells. 81
Figure 28. Immunofluorescence of p-CREB/p-ATF-1. 83
Figure 29. Immunofluorescence of ZO-1 expression in PASC1..... 85
Figure 30. Detection of Cldn-1 by immunofluorescence. 86
Figure 31. Detection of JAM-3-specific mRNA by qRT-PCR. 87
Figure 32. Transepithelial electrical resistance (TER) across adult Sertoli cell layers. .. 88

List of tables:

Table 1: Chemicals 27
Table 2: Standard PCR and qRT-PCR reagents 29
Table 3: Primary antibodies used for immunofluorescence (IF) and western blots (WB) 29
Table 4: Secondary antibodies used for IF or WB 30
Table 5: Chemokines, cytokines and toxins 30
Table 6: Kits 31
Table 7: Enzymes 31
Table 8: List of primer sequences used for Standard PCR or qRT-PCR 32
Table 9: List cell culture reagents 33
Table 10: List of transfection reagents 34
Table 11: List of siRNA sequences 34
Table 12: List of equipments 34
Table 13: List of Miscellaneous 35
Table 14: Western blot buffers 36
Table 15: DNase digestion reaction mixture 42
Table 16: RNA mix 43
Table 17: RT mix 44
Table 18: qRT-PCR MIX 45
Table 19: Separating gel, SDS –PAGE gel preparation. 48
Table 20: Stacking Gel 49

1 Introduction

1.1 The male reproductive tract

All living beings undergo reproduction through which they produce progeny. The male reproductive system of humans and rodents consists of the penis, urethra, seminal vesicles, vas deferens, epididymis, testis and accessory glands (prostate). The main function of the male reproductive system is to sustain the continuous production and the transport of sperms in addition to the synthesis of sex hormones (Bilinska, 2006; Hedger & Hals, 2006).

1.1.1 Function and anatomy of the testis

Testes are oval shaped, paired, descended outside of the abdominal cavity and are located inside the scrotum, as it is outside of the body; the temperature is slightly lower from the core temperature (Cooper, 2007; Nieschlag et al., 2010). The primary function of the histologically and functionally compartmented testis is to generate sperms and produce androgens, especially testosterone. Spermatogenesis takes place in the seminiferous tubules, whereas testosterone (T) synthesis occurs in the interstitium by Leydig cells which are located between the testis seminiferous tubules. The tubules are surrounded by a lamina propria, which contains 3 parts: a basal membrane, collagens and peritubular cells (PCs). PCs form a structural support and transport the immotile spermatozoa by generating a peristaltic motion through contractions along the tubules (Fijak & Meinhardt, 2006; de Krester et al., 2016). In men, several layers of PCs together with the extracellular matrix (ECM) proteins are forming the wall of the tubules (Mayerhofer, 2013).

The germinal epithelium is the epithelial layer of the seminiferous tubules of the testis and it consists of different stages of germ cells: primarily spermatogonia, primary and secondary spermatocytes, spermatids and spermatozoa which are all located within invaginations of Sertoli cells (SCs). SCs are also called the nursery cells as they provide structural support, nutrients and different growth factors to the developing germ cells in addition to their other trophic functions. The progressively maturation of spermatogonia occurs as spermatocytes go through meiosis and transit to haploid spermatozoa and advance from the base toward the lumen of the tubules continuously while they are surrounded by SC cytoplasmic protrusions (Petersen & Soder, 2006).

The interstitial space consists of various types of cells like fibroblasts, Leydig cells, and different kinds of immune cells like T cells, testicular macrophages and few B cells and mast cells, which protect the microenvironment of the tubules against pathogens and sustain adequate conditions to support spermatogenesis (Loveland et al., 2017; Hedger, 1997; Heffner & Schust, 2010).

1.1.2 Functions of peritubular cells (PCs)

PCs are smooth muscle-like cells with a spindle-shaped morphology and are surrounding the seminiferous tubules. In addition to SCs, they secrete ECM components. The peristaltic waves resulting from PC contractions and relaxations are vital for the successful transportation of the immotile spermatozoa along the lumen, which show clearly their inevitable role in spermatogenesis and hence, male fertility (Welsh et al., 2009; Welter et al., 2013). PCs express alpha-smooth muscle actin (ASMA), a contractile protein responsible for the movement of PCs. It is also used as a specific marker of these kind of cells (Schell et al., 2010).

In cases with diminished spermatogenesis resulting from abnormalities in the testis like Sertoli cell only syndrome (SCO) or mixed atrophy, the accompanied infertility is usually associated with increased secretion of ECM proteins resulting in a fibrotic process in the seminiferous tubules wall in addition to changes in the PC layers (Welter et al., 2013). Previous investigations revealed more abnormalities in the morphology of the nucleus of the PCs, the cell size, faint staining of actin as well as an increase of vimentin staining associated with tubular sclerosis (Welter et al., 2013).

1.1.3 Structure and functions of Sertoli cells

The early appearance of SCs in the gonad initiates the first developmental stages of the testis as they express the SRY gene, which determines sexual differentiation. Sertoli cells produce various substances that are important for male physiology such as ceruloplasmin, plasminogen activator (PA), transforming growth factors a & B (TGF-a & TGF-B), insulin- like growth factor (IGF-I) and various hormones like inhibin, anti-Mullerian hormone (AMH) and androgen binding protein (ABP) (Holstein et al., 2003). AMH produced solely in SCs suppresses the development of the female gonads (Holstein et al., 2003; Petersen & Soder, 2006).

Immature and mature SCs are different from each other in both morphological and biochemical aspects. At puberty, SCs become elongated, establish the TJs and secrete the seminiferous fluid, which allow lumen formation. At puberty, SC lose their ability to proliferate and they begin to express a new pattern of proteins e.g., transferrin and the inflammatory cytokine interleukin-1a (IL-1a) (Holstein et al., 2003; Petersen & Soder, 2006).

SC form an epithelium which encloses the various stages of spermatocytes and forms a centrally located seminiferous tubule. Tight junctions (TJs) formed between SCs divide the seminiferous tubules into a basal and an adluminal compartment and form the blood testis barrier (BTB) (Holstein et al., 2003).

1.1.4 Spermatogenesis

Spermatogenesis is a complicated process comprised of three main stages: mitotic proliferation which increases cell numbers; meiotic division resulting in genetic diversity; and spermiogenesis, which involves extensive reshaping to allow swimming and penetration of the egg by the sperm (Heffner & Schust, 2010).

Before puberty, the spermatogonial stem cells are dormant. At puberty, they start developing on two different aspects: they increase their numbers through mitotic division; then they differentiate into spermatogonia type A/B, which go through meiotic divisions before they differentiate into primary spermatocytes. The first meiotic division leads to secondary spermatocytes and the second mitotic division results in the spermatids (de Krester et al., 1998). Finally, the round spermatids undergo a transformation to a microtubule-base tailed sperm with a head rich with chromatin and an anterior acrosome, which releases lytic enzymes during oocyte fertilization. By the end of this process, most of the spermatid cytoplasm is removed (de Krester et al., 1998; Fijak & Meinhardt, 2006; Heffner & Schust, 2010; Fig. 1).

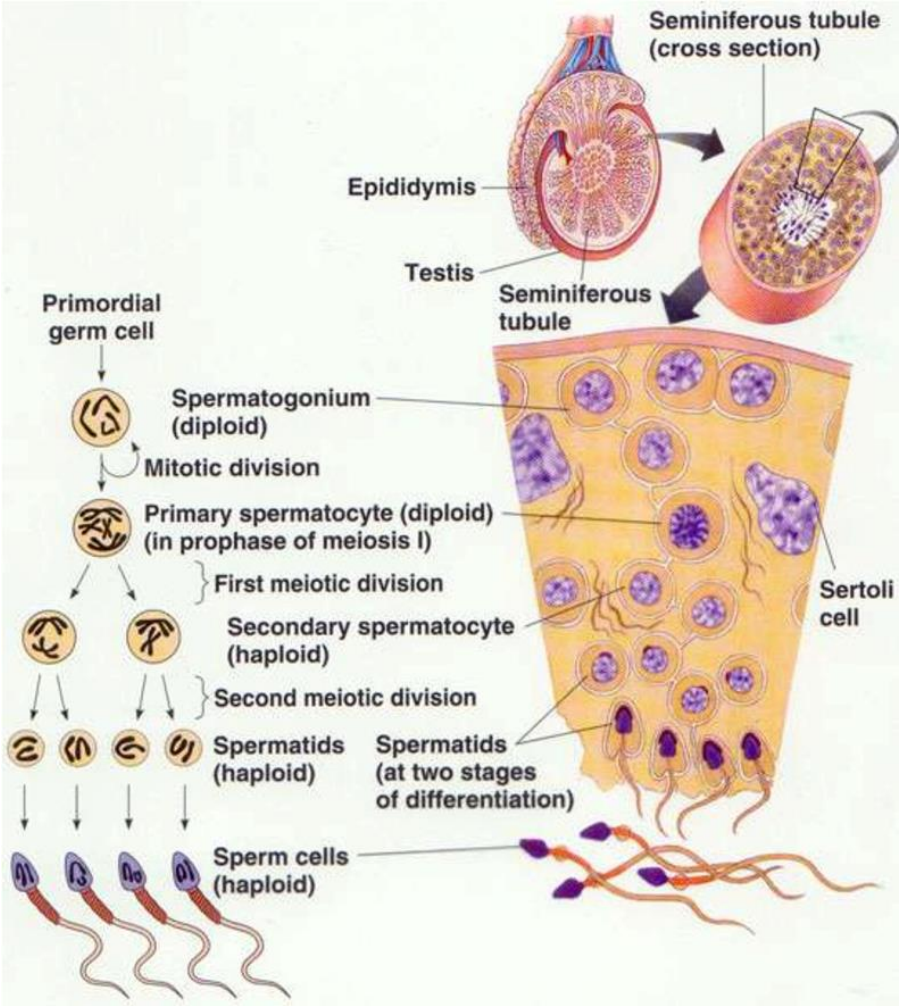

Figure 1. The stages of spermatogenesis are illustrated.

A diagram summarizing the stages of meiosis during spermatogenesis. (Figure http://iceteazegeg.wordpress.com/2009/02/25/gametogenesis/spermatogenesis/).

1.2 Formation and regulation of the blood testis barrier (BTB)

The BTB is formed between SCs and it separates the advanced meiotic and post-meiotic germ cells from the immune system. It is a dynamic structure that allows the passage of the various stages of) germ cells from the adluminal to the luminal compartment. At the same time, the formation of TJ at the BTB restrict the uncontrolled paracellular flow of water and nutrients across the SC epithelia and protect at the same time the developing haploid forms of male germ cells by establishing an immune-privileged environment Impairments of the BTB causes infertility in men (Mruk & Cheng, 2015).

The BTB is formed and maintained by the establishment of TJs located between SCs. TJs are mainly formed by interactions of occludin with claudins (Cldn), which in turn associate with signaling proteins and proteins of the cytoskeleton inside the cell membrane (Mruk & Cheng, 2004; Morrow et al., 2010; Cheng & Mruk, 2012; Fig.2).

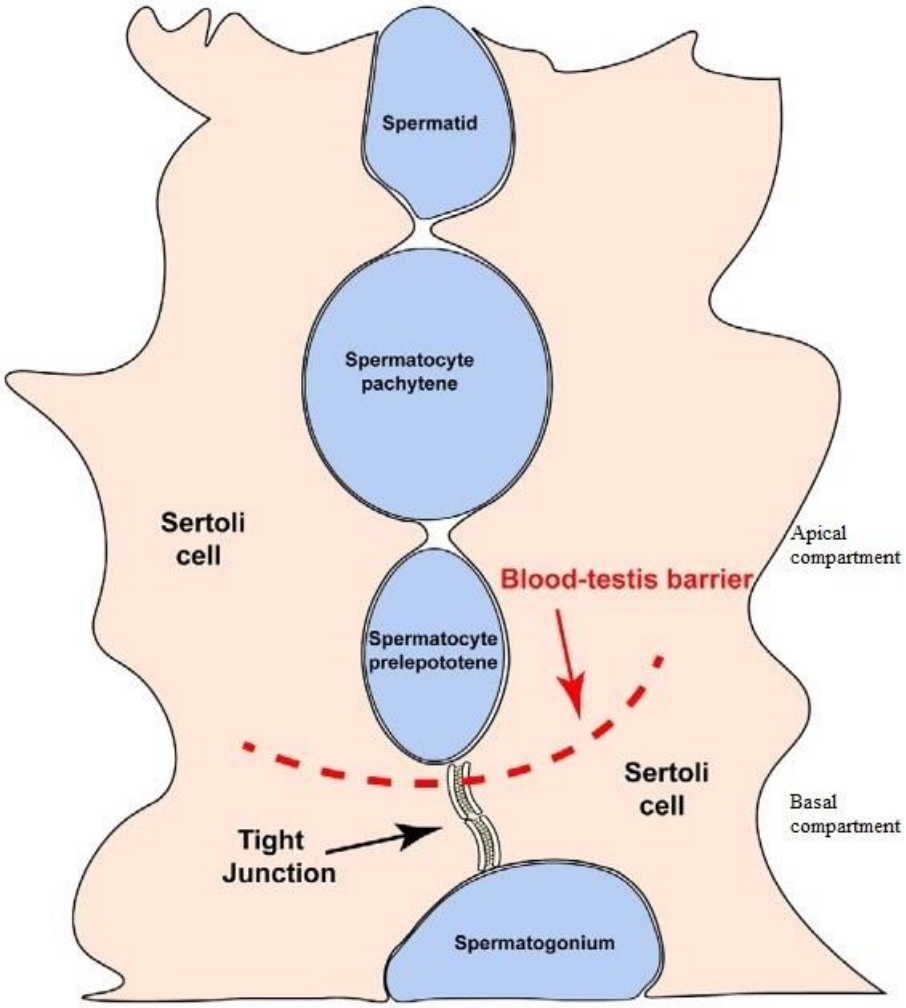

Figure 2. Illustrative figure of the blood testis barrier.

The BTB is located near the tunica propria and is formed between Sertoli cells (SCs). It divides the seminiferous tubules into apical and basal compartments. Spermatogonial cell division and differentiation to preleptotene spermatocytes occur in the basal compartment, whereas meiosis, spermiogenesis and spermiation happens in the apical compartment (Figure taken from Gao et al., 2020).

Numerous fundamental tight junction proteins were described among SCs; these include the Cldn family, Cldn-1, -3, -5, -11, -12 and -13 (Gow et al., 1999; Morrow et al., 2009; 2010;

Komljenovic et al., 2009; Haverfield et al., 2013; Chakraborty et al., 2014; Dietze et al., 2015), occludin (Moroi et al., 1998), the junctional adhesion molecule (JAM) family (Gliki et al., 2004), tricellulin (Smith & Braun, 2012) and coxsackievirus and adenovirus receptor (CAR) (Su et al., 2012). These proteins bind to the actin cytoskeleton via cytoplasmic plaque proteins including zonula occludens-1, -2 and -3 (ZO-1, ZO-2 and ZO-3) and provide links to the other different types of junctions (gap- , adherens-) in the BTB (Mruk & Cheng, 2015).

There are numerous studies implementing the importance of the Cldns in the establishment of TJs. For instance, mice with Cldn-1 deficiency die shortly after birth because of dehydration resulting from disruption of many blood-tissue barriers (Furuse et al., 2002). Cldn-2 has also a vital role in the establishment of TJs in the proximal tubule in kidneys (Muto et al., 2010), and Cldn-5 is important in the establishment of the blood-brain barrier (Nitta et al., 2003).

Among all types of Cldns, it appears that only Cldn-11 is pivotal for spermatogenesis as inactivation of Cldn-11 protein causes infertility as spermatogenesis does not proceed beyond spermatocytes (Mazaud-Guittot et al., 2011; Gow et al., 1999), whereas Cldn-3, CAR and JAM-A knockouts are fertile with no testicular phenotype (Cera et al., 2004; Chakraborty et al., 2014). Cldn-11 was also proven to be present in high levels in rat, mouse and human testis (Morita et al., 1999; Fink et al., 2009; Dietze et al., 2015; Stammler et al., 2016), whereas occluden or Cldn-3 presence in human testis is still controversial (Moroi et al., 1998; Ilani et al., 2012). The role of Cldn-5 in spermatogenesis is unknown because the knockout causes post-natal death (Nitta et al., 2003).

In rat testis, numerous Cldns were identified to participate in BTB formation (Furuse et al., 1998; Morita et al., 1999a). The expression of Cldn-3 and Cldn-5 is highly increased at stage VIII of spermatogenesis in mice at day 20 post-partum, which suggests their importance in the formation of the BTB (Meng et al., 2005; Morrow et al., 2009). The expression of Cldn-1 also increases postnatally between days 16 and 35 until adulthood where it stops increasing (Yan et al., 2008).

T is a key regulator of BTB dynamics (Meng et al, 2005; Morrow et al, 2010). It was also found to promote TJ formation between SCs by stimulating expression of Cldn-1 and Cldn-11 (Gye, 2003; Florin et al., 2005). Cldn-3 was found to be dependent on signaling of the androgen receptor (AR) in Sertoli cell specific-knockout mice. Moreover, AR downregulation negatively affected testicular immune privilege (Meng et al., 2005; 2011). Nevertheless, it was never clear whether the T effects on the membrane-bound Cldns and on establishment of TJs

are mediated by the classical AR or through a G-protein coupled receptor (GPCR). Understanding this mechanism may open new concepts regarding causes of infertility and its treatment.

1.3 The testis as an immune privileged organ

An immune privileged organ is characterized by its ability to tolerate certain events from causing an inflammatory immune response in the long term (Forrester et al., 2008). A number of immune privileged organs, other than the testis, have been described and include the centeral nervous system, the anterior chamber of the eye and tumor-draining lymph nodes (Fijak & Meinhardt, 2006; Mellor & Munn, 2008; Asano et al., 2015). These organs are believed to protect themselves from the immune system by inhibiting access of innate and adaptive immune cells to these sites (Benhar et al., 2012). Testicular immune privilege is critical to protect developing germ cells from the auto-immune attack of immune cells, as foreign antigens are expressed during spermatogenesis (Fijak & Meinhardt, 2006; Arck et al., 2014; Zhao et al., 2014).

In specific pathological incidents, the testicular immune privilege is compromised. As a result, anti-sperm antibodies are produced in large quantities which may lead to infertility (Wenes et al., 2016). Numerous studies in the last decades have demonstrated that multiple mechanisms including the testicular immunological barrier (TIB), local immunosuppression and tolerance of the immune system are involved in testis immune privilege (Zhao et al., 2014; Bhushan & Meinhardt, 2017).

1.3.1 Maintenance of the testicular immune privilege through structural elements and local immune tolerance

As previously mentioned, the BTB is formed between SCs and it divides the seminiferous tubules into basal and adluminal compartments, which separates the advanced germ cells form the immune system (Arck et al., 2014; Jiang et al., 2014). Moreover, SCs have also immunosuppressive characteristics by secreting specific factors including anti-inflammatory proteins like TGF-β1, complement factors and some proteinase inhibitors (Suarez-Pinzon et al., 2000; Sipione et al., 2006; Lee et al., 2007; Fallarino et al., 2009). SC co-transplantation studies revealed more facts about the SC immunosuppressive factors, where pancreatic islets

survived longer when applied together with SCs (Lan et al., 2001). Additionally, SC get rid of apoptotic germ cells and of the residual bodies of the spermatids, which may cause an inflammatory response and thus maintain normal spermatogenesis (Li at al., 2012; Zhao et al., 2014; Asano et al., 2015).

Leydig cells are the largest cell population in the interstitial space, they secrete androgens which are pivotal for normal spermatogenesis and are also known to have anti-inflammatory characteristics (Fijak & Meinhardt, 2006; Zhao et al., 2014). Testosterone increases polarization of immature T cells to regulatory T cells and inhibit production of tumor necrosis factor-alpha (TNF-α) in SCs and PCs in case of inflammation (Fijak et al., 2015). Additionally, several studies have shown that T treatment stopped some auto-immune diseases like rheumatoid arthritis by suppression of local immune reactions (Cutolo, 2009). Furthermore, numerous clinical studies have demonstrated that T downregulated secretion of pro-inflammatory cytokines including TNF-α, interleukin-1 (IL-1) and interleukin-6 (IL-6). In contrast, secretion of anti-inflammatory cytokines like IL-10 was upregulated (Bhushan et al., 2015). Taken together, androgens maintain the testis immune privilege by suppressing the local immune reaction and inducing immune tolerance.

1.3.2 The role of testicular macrophages (TMs) and other local immune cells in testis immune privilege

TMs are immune cells which are found in the interstitial space of the testis (Bhushan & Meinhardt, 2017). In contrast to macrophages found in other tissues, TMs have only a weak ability to secrete pro-inflammatory cytokines like TNF-α, concomitant with a strong secretion of anti-inflammatory cytokines like IL-10, which help to maintain the testis immune privilege (Bhushan et al., 2015). In normal conditions, 80% of TMs demonstrate an immunosuppressive M2 phenotype characterized by expression of CD-163, a marker of M2 macrophages (Meinhardt & Hedger, 2011; Winnall & Hedger, 2013; Bhushan & Meinhardt, 2017).

Dendritic cells are also found in the testicular interstitial space and are known to play a vital role in the regulation of adaptive immune response (Guazzone et al., 2011). They can induce lymphocytes differentiation in response to antigens which reduces their immune response (Banchereau & Steinman, 1998; Rival et al., 2006). They are also found in huge numbers in the testis in post-experimental autoimmune orchitis (EAO) which indicates their role in suppressing inflammation (Rival et al., 2006).

Mast cells participate to the immune response against parasites and allergy (Hussein et al., 2005). They can also induce tissue fibrosis and sclerosis by activating fibroblast proliferation and collagen synthesis (Abe et al., 1998). Several studies have demonstrated that cases accompanied with abnormal spermatogenesis or infertility are associated with higher numbers of mast cells which caused fibrosis in testis later on (Jezek et al., 1999; Meineke et al., 2000; Fijak & Meinhardt, 2006).

1.4 Steroidogenesis and the production of male sex hormones

Steroids are lipophilic compounds comprised of cholesterol and the two classes of its derivatives, the bile acids and the steroid hormones. Since cholesterol can be found in all cell membranes of animal cells, thus, they are involved in most of the physiological processes in the body (Silvius, 2003). Steroids help also to regulate and control immune responses, stress, bone and muscular metabolism and even mood (Coutinho & Chapman, 2011; Kuo et al., 2013; Carson & Manolagas, 2015; Sanjuan et al., 2016). Despite that cholesterol synthesis takes place in all animal cells, steroidogenesis (the production of steroid hormones), happens only in few organs: the adrenal cortex, the placenta and the gonads (New & White, 1995). The first enzymatic reaction in the mitochondria which catalyzes the conversion of cholesterol to pregnenolone is activated by the removal of the cholesterol side chain. After that, pregnenolone enters the endoplasmic reticulum (ER) for synthesis of either sex steroids or corticoids and becomes hydroxylated on Carbon-17 by P450scc to form 17α-hydroxy-pregnenolone or it gets converted to progesterone (Hall, 1985; Arukwe et al., 2008; Sewer & Li, 2008). The later processing of either of both leads to the synthesis of androgens and estrogens, T or 17β-estradiol. T is converted in the target tissue to the more active dihydrotestosterone (DHT) (Randall, 1994).

Synthesis of sex hormones is regulated by the hypothalamus through pulsatile secretion of Gonadotropin-releasing hormone (GnRH), which stimulates the pituitary gland to release of luteinizing hormone (LH) and follicle stimulating hormone (FSH) (Drummond, 2006). In testis, expression of P450scc and thus pregnenolone synthesis is increased by stimulation of LH in Leydig cells. After puberty, this leads to increased synthesis of T by the continuous pulsatile release of GnRH and LH. FSH is essential in stimulating both LH receptor expression in Leydig cells and the production of androgen binding protein in SCs (Ramaswamy & Weinbauer, 2014; Fig. 3).

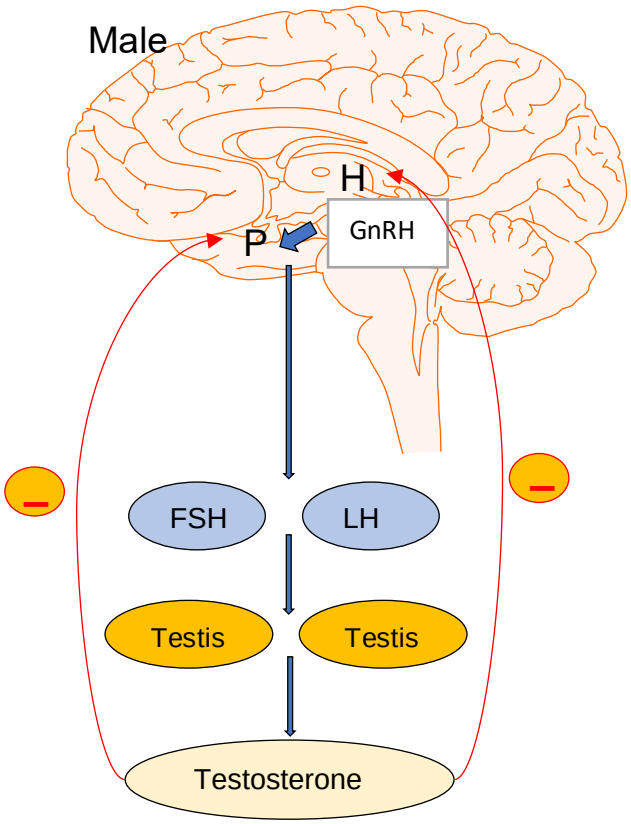

Figure 3. Schematic overview of the hypothalamic pituitary gonadal axis in males.
LH and FSH are secreted from the pituitary gland (P) in response to GnRH secreted from hypothalamus (H). LH stimulates testosterone production and FSH stimulates expression of the androgen binding protein and also of LH receptors on Leydig cells. Feedback mechanism of testosterone helps to regulate secretion of GnRH and thus synthesis of LH and FSH.

1.4.1 The classical and the non-classical pathway of androgen signaling in testis

T is primarily synthesized in Leydig cells in addition to small amounts produced in the adrenal glands. T serum concentration is age related (Kelsey et al., 2014). T acts via 2 different pathways, the classical and the non-classical pathway. In the classical pathway, T activates the cytosolic AR causing its translocation to the nucleus there it regulates protein biosynthesis by activating transcription factors (Mangelsdorf et al., 1995; Ochiai et al., 2004). The non-classical pathway is characterized by rapid events which lead to activation of cytosolic signaling cascades that are normally activated by growth factors such as the tyrosine kinases (Src)/phosphatidylinositol 3-kinase (PI3K)/ protein kinase B (Akt) and/or the Src/rat sarcoma protein kinase (Ras)/ proto-oncogene serine/threonine-protein kinase (Raf)/ extracellular signal-regulated protein kinase 1/2 (ERK1/2) cascade (Kato et al., 2000; Valverde & Parker,

2002). Nevertheless, the receptor involved in the non-classical signaling is still debeted. Some investigators even suggested that the cytosolic AR is involved in both the classical and the non-classical pathway of T signaling (Walker, 2010).

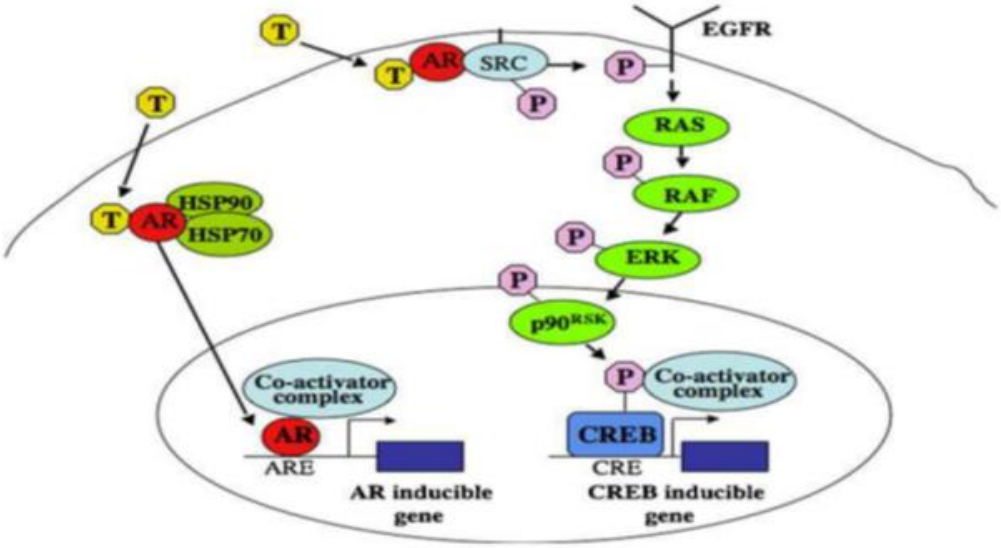

Figure 4. The classical and the non-classical signaling pathway of T.

The cytosolic and nuclear AR is involved in both testosterone signaling pathways in this model of Walker (2009).

Others suggested a membrane-bound receptor of the family G-protein coupled receptor (GPCR) is a possible mediator of the non-classical pathway (Kampa et al., 2002; 2005; Estrada et al., 2003; Dambaki et al., 2005; Fu et al., 2012). Activation of ERK1/2 and other mitogen-activated protein kinase (MAPK) is also pivotal for spermatogenesis (Sette et al., 1999; Di Agostino et al., 2004).

Non-classical action of T is essential for spermatogenesis and maturation of germ cells towards spermatozoa (Walker, 2010). Moreover, activation of cyclic AMP response element binding protein (CREB) in SCs which is vital for spermatocytes and spermatozoa production (Scobey et al., 2001), is triggered by T via the activation of the c-Src/c-RAF/ERK1/2 signaling cascade of the non-classical T signaling pathway (Rahman & Christian, 2007; Walker, 2010; 2011; Fig. 4).

1.4.2 ZIP9 as a non-classical receptor of androgen signaling

Recent studies in our laboratory demonstrated that in spermatogenic GC-2 cells, the non-classical T signaling pathway is mediated by a membrane-bound protein interacting with the G-protein Gnα11 (Shihan et al., 2014). Further studies by other investigators in the same year indicated that the female Atlantic croaker ZIP9, a zinc transporter from the family ZRT/IRT-like protein (ZRT=zinc-regulated transporter; IRT=iron-regulated transporter) serves as a membrane-bound androgen receptor (Berg et al., 2014; Thomas et al., 2014).

More findings in our laboratory revealed that the membrane-bound protein that interacts with Gnα11 as a mediator of the non-classical pathway of androgen signaling in GC-2 cells is ZIP9, and not the classical cytosolic AR (Shihan et al., 2015). More recent investigations have also revealed that ZIP9 is the sole mediator of the non-classical pathway of T represented by activation of ERK1/2, CREB and ATF-1 and regulation of TJs in the rat prepubertal Sertoli cell line 93RS2, which lacks AR expression (Bulldan et al., 2016).

1.5 Aims of the study

Despite numerous studies performed to analyze the BTB in vitro, very few have been focused on its establishment, the key cell molecules of its formation or how the TIB can prevent the infiltration of the immune cells into the lumen of the seminiferous tubules. Moreover, most of the BTB studies performed using SCs from immature animals because of the easiness to achieve it. However, only very few studies were focused on studying the BTB between adult SCs with limited success regarding the isolation of adult SC or even establishing a functional barrier in vitro. T is the main player in all stages of testis development, it has pivotal role in spermatogenesis and tightening of the BTB to form an immune privileged environment in the testis. Recently published manuscripts demonstrated that the ZIP9 is the sole receptor to mediate the non-classical pathway of T signaling in immature rat SC, however, would it be also the same in case of adult rat SC?

However, because the BTB formed by immature SCs is weak, thus we decided to start with adult SCs and the formation of the barrier by addressing the following aims:

- Creating a successful isolation protocol of adult rat SCs in which the main characteristics of adult rat SCs are maintained in the long term.
- Unveil the contribution SCs, PCs or co-culture of both cells to the integrity of the BTB.

- Achieving a tighter barrier in vitro between adult rat SCs by treatment with known testicular hormones or cytokines.
- Establishment of a transmigration model with macrophages which might help us to understand the situation in vivo.
- Study the effects of T on the BTB integrity and the mechanism of androgen signaling by testing both the classical and the non-classical pathway of androgen signaling to investigate whether ZIP9 or AR is the main mediator of androgen signaling in adult rat SCs by treatment of SCs with androgenic peptide designed to target ZIP9 only.

2 Materials and Methods

2.1 Chemicals and materials

2.1.1 Chemicals

Table 1: Chemicals

Chemicals	Manufacturer	City, Country
Acetic acid	Roth	Karlsruhe, Germany
Acrylamide 30% (w/v)	Roth	Karlsruhe, Germany
Amphotericin B	Sigma-Aldrich	Steinheim, Germany
Agarose	Roth	Karlsruhe, Germany
Biotinylated protein ladder	Cell signaling	Leiden, Holland
Calcium chloride ($CaCl_2$)	Merck	Darmstadt, Germany
Chloroform	Merck	Darmstadt, Germany
Collagen I 354236	Corning	Frickenhausen, Germany
4′,6-diamidino-2-phenylindole (DAPI)	Invitrogen	Karlsruhe, Germany
DNA ladder (100 bp)	Promega	Mannheim, Germany
Dimethyl sulfoxide (DMSO)	Merck	Darmstadt, Germany
di-potassium hydrogen phosphate	Merck	Darmstadt, Germany
di-sodium hydrogen phosphate	Merck	Darmstadt, Germany
1,4-Dithiothreitol (DTT)	Roche	Mannheim, Germany
Ethanol	Sigma-Aldrich	Steinheim, Germany
Ethylene diaminetetraacetic acid disodium salt (EDTA)	Merck	Darmstadt, Germany
Fluorescein isothiocyanate conjugate (FITC) coupled dextran FD4	Sigma-Aldrich	Steinheim, Germany
Glycerol	Merck	Darmstadt, Germany
Halt ™ protease inhibitor cocktail	Thermo Scientific	Frankfurt, Germany
Hydrogen peroxide	Roth	Karlsruhe, Germany
Glycine	Sigma-Aldrich	Steinheim, Germany
Isofluran	Abbott	Wetzlar, Germany

4-(2-hydroxyethyl)-1-piperazineetha-nesulfonic acid	Roth	Karlsruhe, Germany
Leukotracker ™	Cell biolabs	San Diego, USA
Lymphoprep gradient	Stem cell	Cologne, Germany
Lysis buffer X10	Cell signaling	Frankfurt, Germany
Magnesium chloride ($MgCl_2$)	Merck	Darmstadt, Germany
Magnesium sulfate ($MgSO_4$)	Sigma-Aldrich	Steinheim, Germany
Matrigel (MG)	Corning	Frickenhausen, Germany
β-Mercaptoethanol	AppliChem	Darmstadt, Germany
Methanol	Roth	Karlsruhe, Germany
Non-fat dry milk	Bio-Rad	München, Germany
Paraformaldehyde	Merck	Darmstadt, Germany
Pepstatin A	Tocris	Wiesbaden, Germany
Percoll gradient	Sigma-Aldrich	Steinheim, Germany
Phenylmethylsulfonyl fluoride (PMSF)	Sigma-Aldrich	Steinheim, Germany
Ponceau S	Roth	Karlsruhe, Germany
Protease inhibitor cocktail	Roche	Mannheim, Germany
Rho kinase (ROCK) inhibitor	Enzo life sciences	Lörrach, Germany
Sodium acetate	Roth	Karlsruhe, Germany
Sodium azide	Merck	Darmstadt, Germany
Sodium chloride	Sigma-Aldrich	Steinheim, Germany
Sodium dodecyl sulfate (SDS)	Merck	Darmstadt, Germany
N,N,N',N'-Tetramethylethylenediamin (TEMED)	Roth	Karlsruhe, Germany
Tris (hydroxymethyl) aminomethane hydrocholride	Roth	Karlsruhe, Germany
Triton X-100	Sigma-Aldrich	Steinheim, Germany
Trypan blue Dye, 0,4%	Bio-rad	Munchen, Germany
Tween-20	Roth	Karlsruhe, Germany
Testosterone	Sigma-Aldrich	Steinheim, Germany

Testosterone 3-(O-carboxymethyl) oxime bovine serum albumin-fluorescein isothiocyanate conjugate (T-BSA-FITC) and BSA-FITC	Sigma-Aldrich	Steinheim, Germany

2.1.2 PCR Reagents

Table 2: Standard PCR and qRT-PCR reagents

Item	Manufacturer	City, Country
DNase I	Invitrogen	Karlsruhe, Germany
dNTPs	Promega	Mannheim, Germany
iTaq universal SYBR green supermix	Biorad	Munich, Germany
Oligo dT	Promega	Mannheim, Germany
MMLV RT	Promega	Mannheim, Germany
Nuclease-free water	Qiagen	Hilden, Germany
Reverse Transcription-System first strand cDNA synthesis kit	Invitrogen	Karlsruhe, Germany
Taq DNA polymerase	Promega	Mannheim, Germany
Taq DNA Polymerase	Bio&Sell	Feucht, Germany

2.1.3 Antibodies

Table 3: Primary antibodies used for immunofluorescence (IF) and western blots (WB)

Primary Antibody	Manufacturer	Catalogue No.	Dilution
AR	Santa Cruz	SC-7305	1:300 IF
ASMA	DAKO	M0851	1:300 IF
Beta actin	Cell Signaling	4970S	1:3000 WB
CD68	Abcam	ab283654	1:100 IF
Claudin-1	Invitrogen	37-4900	1:300 IF
JAM-3	Invitrogen	AB_2533486	1:300 IF
SOX9	Merck Millipore	AB5535	1:300 IF

p-CREB	Cell Signaling	9198S	1:300 IF
p-Erk1/2	Cell Signaling	4370S	1:2000 WB 1:300 IF
t-Erk1/2	Cell Signaling	9102S	1:1000 WB
ZIP9	Thermo Fisher Sientific	PA5-21074	1:300 IF
ZO-1	Invitrogen	61-7300	1:300 IF

Table 4: Secondary antibodies used for IF or WB

Secondary antibody	Manufacturer	Catalogue No.	Dilution
Alexafluor 488-conjugated donkey anti-rabbit	Life Technologies	A-21206	1:250 IF
Alexafluor 488-conjugated donkey anti-mouse	Life Technologies	A-21202	1:250 IF
Alexafluor 555-conjugated donkey anti-mouse	Life Technologies	A-31570	1:250 IF
Donkey anti mouse IgG–HRP	Cell signaling	7076S	1:2500 WB
Goat anti rabbit IgG –HRP	Cell signaling	7074S	1:2500 WB

2.1.4 Cytokines and toxins

Table 5: Chemokines, cytokines and toxins

Name	Manufacturer	Catalogue Number
Bone morphogenetic protein 2 (BMP2)	Promokine	C-67309
Cholera toxin	Sigma-Aldrich	C8052
Interleukin-6 (IL-6)	Promokine	D-61632
Lipopolysaccharide (LPS)	Sigma-Aldrich	L2630
Macrophage colony stimulating factor (M-CSF)	Miltenyi Biotec	130-101-700
Recombinant interferon gamma (IFN-γ)	Promocell	C-60724

Recombinant interleukin-4 (IL-4)	Promocell	C-61421
Recombinant interleukin-13 (IL-13)	Promocell	C-62312
Transforming growth factor beta-3 (TGF-β3)	Promokine	C-63508
Tumor necrosis factor-alpha (TNF-α)	Promokine	C-63719

2.1.5 kits

Table 6: Kits

Name	Manufacturer	Catalogue Number
Cytoselect™ leukocyte transmigration assay kit (8 µm)	Cell Biolabs	CBA-212
Bicinchoninic acid protein assay reagent kit	Thermofisher	23225

2.1.6 Enzymes

Table 7: Enzymes

Name	Manufacturer	City, country
Collagenase type I	Sigma-Aldrich	Taufkirchen, Germany
Hyaluronidase	Sigma-Aldrich	Taufkirchen, Germany
Deoxyribonuclease I (DNASE I)	Sigma-Aldrich	Taufkirchen, Germany
Trypsin	Pan-Biotech	Aidenbach, Germany

2.1.7 Primers

All primers were designed with http://www.ncbi.nlm.nih.gov/tools/primer-blast (last accessed February 28, 2022) and were all intron-spanning (Table 8).

Table 8: List of primer sequences used for Standard PCR or qRT-PCR

Genes (species) and acc. No	Sequence (5'-3')	Annealing temperature	Size of PCR product (bp)
AMH (rat) NM_012902.1	5' AACTGACCAATACCAGGGGC 3' 5' GGCTCCCATATCACTTCAGCC 3'	59°C	334
AR (rat) NM_012502.2	5' GCCAGTGGCTGAGGATGAG 3' 5' GGTGAGCTGGTAGAAGCGC 3'	59°C	236
CCL17 (rat) NM_057151.1	5' TGATGTCACTTCAGATGCTGC 3' 5' GGACAGTCTCAAACACGATGG 3'	59°C	201
CCL22 (rat) NM_057203.1	5' AGGATGCTCTGGGTGAAGAA 3' 5' TAGGGTTTGCTGAGCCTTGT 3'	59°C	98
Clusterin (rat) XM_039092999.1	5' AGGAGCTAAACGACTCGCT 3' 5' GCTTTTCCTGCGGTATTCC 3'	59°C	362
CXCL11 (rat) NM_182952.2	5' GCAGCAATCAAGGAAGTTTCTG3' 5' CAGAAACTTCCTTGATTGCTGC 3'	59°C	22
GAPDH (rat) XM_039107008.1	5' GACCCCTTCATTGACCTCAAC 3' 5' GATGACCTTGCCCACAGCCTT 3'	59°C	561
GATA1 (rat) NM_012764.2	5' ATAGCAAGACGGCGCTCTACfwd 5' CACTCTCTGGCCTCACAAGG 3'	59°C	319
HSD17B3 (rat) NM_054007	5' GGAAGCCGTGTGAAGGTT 3' 5' GACACTCTGGCTCTCACC 3'	58°C	171
JAM-3 (rat) NM_001004269.1	5' CTTCTTCCTGCTGCTGCTCT 3' 5' TCTTGGCATTGCAGTGTTGC 3'	59°C	435
SOX9 (rat) NM_080403.2	5' CATCAAGACGGAGCAACTGAG 3' 5' GTGGTCGGTGTAGTCATACTGC 3'	59°C	148
TNF-α (rat) XM_034524600.1	5' GAACTCAGCGAGGACACCAA 3' 5' GCTTGGTGGTTTGCTACGAC 3'	59°C	460
Transferrin (rat) NM_001013110.1	5' TATTGGCCCAGCAAAATGTG 3' 5' CCGGAACAAACAGAAATTGC 3'	59°C	370
ZIP9 (rat) NM_001034929.1	5' GCTGCATGCCTACATTGGTG 3' 5' GTTAGTGCTGGTGTCCTCAGGG 3'	58°C	502
ZO-1 (rat) XM_0391053461	5' CTTGCCACACTGTGACCCTA 3' 5' GGGGCATGCTCACTAACCTT 3'	59°C	262

Acc. No., Accession number; bp, base pairs; GAPDH, Glyceraldehyde 3-phosphate Dehydrogenase; ASMA, alpha smooth muscle actin; HSD17B3, hydroxy-delta-17-beta dehydrogenase 3; AMH, Anti-

Mullerian Hormone; AR, Androgen Receptor; JAM-3, Junctional Adhesion Molecule-3; ZO-1: Zonula occludens-1; CXCL11, C-X-C motif chemokine ligand 11; TNF-α, tumor necrosis factor alpha; CCL17, CC chemokine ligand 17; CCL22, CC chemokine ligand 22; ZIP9, Zinc transporter; ZIP9.

2.1.8 Cell culture reagents

Table 9: List of cell culture reagents

Cell culture reagents	Manufacturer	City, Country
Accutase (0.25%)	Gibco	Frankfurt, Germany
Bovine calf serum (BCS)	GE Health-Thermofisher	Frankfurt, Germany
Bovine serum albumin (BSA)	Sigma-Aldrich	Taufkirchen, Germany
phosphate-buffered saline (PBS)	Gibco	Frankfurt, Germany
DMEM medium high glucose	Gibco	Frankfurt, Germany
DMEM/F-12 medium	Gibco	Frankfurt, Germany
Dulbecco's phosphate-buffered saline (DPBS)	Gibco	Frankfurt, Germany
F-12 nutrient mix	Gibco	Frankfurt, Germany
Fetal calf serum (FCS)	Gibco	Frankfurt, Germany
HEPES	Gibco	Frankfurt, Germany
Insulin transferrin selenium (ITS)	Thermofisher	Frankfurt, Germany
L-glutamine	Gibco	Frankfurt, Germany
Mercaptoethanol	Gibco	Frankfurt, Germany
MEM non-essential amino acid solution	Sigma-Aldrich	Taufkirchen, Germany
Penicillin/streptomycin (P/S)	Gibco	Frankfurt, Germany
RPMI 1640 medium	Gibco	Frankfurt, Germany
Sodium pyruvate	Gibco	Frankfurt, Germany
TrypLE	Gibco	Frankfurt, Germany

2.1.9 siRNA transfection reagents

Table 10: List of transfection reagents

Name	Manufacturer	City, Country
Lipofectamine™ RNAiMAX	Invitrogen	Karlsruhe, Germany
Negative control siRNA	Invitrogen	Karlsruhe, Germany
Opti-MEM™	Thermofisher Scientific	Frankfurt, Germany
siRNA Silencer ® Select	Invitrogen	Karlsruhe, Germany

2.1.10 siRNA sequences

Table 11: List of siRNA sequences

siRNA oligo (Species)	Sequence (5′→3′)	Catalogue number
ZIP9 siRNA (rat)	5′ GGAUUAAGUAAGAGCAGUAtt 3′ 5′ UACUGCUCUUACUUAAUCCta 3′	4392420
AR siRNA (rat)	5′ CCGGAAAUGUUAUGAAGCAtt 3′ 5′ UGCUUCAUAACAUUUCCGGag 3′	4390771

2.1.11 Equipments

Table 12: List of equipments

Equipment	Manufacturer	City, Country
Cell culture CO_2 incubator	Memmert	Schwabach, Germany
Desktop centrifuge Biofuge Fresco balance SPB50	Hettich Electronic	Tuttlingen, Germany
Heat block DB-2A	Techne	Cambridge, UK
Elekta 6-MV Synergy photon linear accelerator	Elekta	Stockholm, Sweden
Herasafe™ KS biological safety cabinet	Thermo Electron Co.	Berlin, Germany
Horizontal mini electrophoresis system	PEQLAB	Erlangen, Germany
Labsystems plate reader	Labsystem	Helisinki, Finland
Microwave oven	Samsung	Schwabach, Germany

Millicell ERS-2 Volt-ohm Meter	Merck Millipore	Darmstadt, Germany
Mini centrifuge Galaxy	Heathrow Scientific	San Diego, USA
Mini-rocker shaker MR-1	PEQLA	Erlangen, Germany
MiniOpticon™ Real-Time PCR	BioRad	Munich, Germany
NANODROP ND 2000	Promega	Mannheim, Germany
Olympus X81 Fluorescence Microscope	Olympus	Hannover, Germany
PCR thermo cycler	Biozyme	Oldendor, Germany
Power supply units	Consurs	Reiskirchen, Germany
SDS gel electrophoresis chambers		
Semi-dry-electroblotter	BioRad	Munich, Germany
T10 automatic cell counter	BioRad	Munich, Germany
Tecan infinite M100 Microplate reader	Tecan	Crailsheim, Germany
Ultrasonic homogenizer Bandelin Sonopul	Bandelin	Berlin, Germany

2.1.12 Miscellaneous

Table 13: List of Miscellaneous

Item	Manufacturer	City, Country
Black 96-well plates	Greiner	Frickenhausen, Germany
Cell culture 12-24-48 well plates	Greiner	Frickenhausen, Germany
Cell inserts 0,4 µm of 24 well plate	Greiner	Frickenhausen, Germany
Cell strainers 100-µm	Corning/Greiner	Frickenhausen, Germany
Enhanced chemiluminescence (ECL) reagents	Amersham	Freiburg, Germany
Filters 0,22 µm	Sigma-Aldrich	Steinheim, Germany
Protein size markers	Invitrogen	Karlsruhe, Germany
PVDF membranes	Merck Chemicals	Schwalbach, Germany
S-Monovette 2,7 mL tubes prepared with EDTA K3	Sarstedt	Nümbrecht, Germany
T 75 cell culture flasks	TPP	Frankfurt, Germany

2.2 Buffer solutions and reagent used for western blot

2.2.1 Western blots buffers

Table 14: Western blot buffers

Cell Lysis buffer	2 ml: 200 µL 10x Lysis buffer 1750 µL of distilled water 1 mM PMSF 25 µL of Protease Inhibitor 25 µL of Phosphatase Inhibitor, *: prepare fresh every time before cell lysis
10X Phosphate buffered saline (PBS)	4 g KCl 4 g KH_2PO_4 160 g NaCl 23 g Na_2HPO_4 * H_2O Dissolved in 1L H_2O, pH to 7.4 with HCl
10X Tris base buffered saline (TBS)	24.2 g Tris base 80 g NaCl Dissolved in 1L H_2O, pH to 7.4 with HCl
Washing buffer TBS/T	1 X TBS 0.1% (v/v) Tween-20
Blocking buffer (100 ml)	100 ml 1 X TBS 0.1 ml Tween-20 5 g Non-fat dry milk
10 X Electrophoresis buffer	30.3 g Tris base 144 g Glycine 10 g SDS Dissolved in 1L distilled water

Stripping buffer	6.25 ml 1 M Tris-HCl 2 ml 10% SDS 700 µl β-mercaptoethanol* Make volume up to 100 ml with water * added freshly just before stripping of membrane

2.3 Cell culture

2.3.1 93RS2 Sertoli cells

The prepubertal rat Sertoli cells (SCs) line without androgen receptor (AR) expression 93RS2 (Jiang et al., 1997) are cultured in DMEM/F-12 with L-glutamine supplemented with 10% FCS, 1% penicillin/streptomycin (P/S), and 1% insulin transferase selenium (ITS) in a humidified incubator (37 °C, 5% CO_2). The media were changed every 2 days. After the medium was removed by aspiration, cells were washed with Dulbecco's phosphate-buffered saline (PBS) without Ca^{2+} and Mg^{2+} and subsequently harvested by incubation with accutase (0.25%) for 4 min at 37°C.

2.3.2 Irradiation of 3T3-J2 mouse fibroblast and preparation of conditioned medium (CM)

The 3T3-J2 mouse fibroblast cell line (KER-EF3003) were purchased from Kerafast (USA) and were cultured as advised by the manufacturer in a humidified incubator (37°C, 5% CO_2). Complete DMEM (+ 2 mM L-glutamine, 10% bovine calf serum (BCS) and 1% P/S was replaced every 2 days until the cells reached 60-80% confluency in a T175 flask. Cells were washed with DPBS, incubated with TrypLE for 5 min at 37°C until detachment, and filled up to 10 mL F medium [375 mL complete DMEM/F-12 and 125 mL of F12 nutrient mix]. The cell suspension (1.0-2.5 X 10^6 cells/mL) was irradiated with a total dose of 30 Gy (=3,000 rad) with a Synergy Elekta 6-MV photon linear accelerator and cultured in a T175 flask (7.0 X 10^6 cells/30 mL F medium) and incubated at 37°C and CO2. After 72 hrs, medium was collected and centrifuged at 300xg for 5 min at 4°C. The supernatant was filtered through 0.22 µm filters. For immediate use, one part of fresh F medium was mixed with three parts of CM (filtered supernatant) supplemented with 10 µM ROCK inhibitor (diluted in water) and 0.1 nM cholera toxin (diluted in water) resulting in complete CM, which can be stored for up to 1 week at 4°C or up to 6 months at -80°C.

2.4 Animals

11-13 week-old adult male Sprague Dawley rats ((Crl:CD (SD)IGS) weighing 150-200 g were purchased from Charles River (Germany). The study was approved by the local committee on the Ethics of Animal Experiments of the Justus Liebig University (permit number: M_695 Giessen, Germany) and all experiments were performed in accordance with relevant guidelines and regulations.

2.5 Isolation of primary adult rat Sertoli cells and PCs

2.5.1 Isolation of primary adult rat Sertoli cells and PCs using enzymatic digestion

Adult male Sprague Dawley rat weighing 150-200 g was anesthetized with 5% isoflurane. Testes were removed, briefly rinsed in 70% ethanol, washed with sterile Dulbecco's phosphate buffered saline (DPBS) and placed in Dulbecco Modified Eagle Medium/Nutrient Mixture F-12 (DMEM/F-12). After removal of the tunica albuginea, tubules of one testis were disaggregated without rupturing them, transferred to enzymatic solution 1 (10 mL DPBS and 1.5 mg/10 mL collagenase type I) and agitated for 3 min in a shaking water bath at 35°C (120 oscillations/min). The suspension was allowed to settle by gravity for 5 min at room temperature (RT) and the supernatant, containing mostly Leydig cells (LCs), carefully aspirated. Tubules were rinsed gently thrice with 10 ml DPBS and incubated for 15 min in enzymatic solution 2 [10 mL DPBS with 0.5 mg/mL collagenase, 0.5 mg/mL hyaluronidase and 0.2 mg/mL deoxyribonuclease I (DNASE I)] in a shaking water bath at 35°C (120 oscillations/min) to dislodge peritubular cells (PCs) from the tubules until they were free from surrounding tissue, but still intact. Then 15 mL DPBS was added and tubules allowed to settle. The supernatant enriched in PCs was collected and centrifuged (500xg, 10 min). The cell pellet was suspended in complete DMEM/F-12, seeded into a T75 flask (~ 5 X 10^6 cells/flask) and maintained in a humidified incubator (37°C, 5% CO_2). After 3 days, the PCs reached confluency and were used for further experiments.

The tubules were transferred to 2 ml DPBS, added slowly on top of 38 mL 5% Percoll (in DPBS) in a 50 mL centrifuge tube and allowed to settle for 20-30 min at room temperature (RT). After discarding the top 35 mL Percoll, the tubules were washed 3 times with DPBS and incubated in enzymatic solution 3 (10 mL DPBS with 1 mg/mL trypsin and 0.2 mg/mL DNase I) for 15 min in a shaking water bath at 35°C (120 oscillations/min). Tubules were shaken

vigorously every 3 min by hand for 5 sec until complete digestion, which was stopped by adding 3 mL 100% fetal calf serum (FCS). The SC-enriched tubule suspension was transferred to a new 50 mL centrifuge tube containing 25 mL complete DMEM/F-12 [10% FCS, 1% P/S, 1% insulin transferrin-selenium (ITS) to decrease the viscosity prior to filtration through 100-µm cell strainers. The filters were inverted over a 50 mL centrifuge tube and collected by washing with complete DMEM/F-12, and centrifuged (500xg, 5 min, RT). After washing twice with DPBS, cells were resuspended in 10-15 mL complete DMEM/F12 and cell viability examined by trypan blue staining using a TC10 cell counter. Approximately 18-36 × 10^6 cells were obtained from one testis of one adult rat.

2.5.2 Conditional reprogramming of primary adult rat Sertolie cells by culturing freshly isolated SC clusters with CM

The conditional reprogramming (CR) was done according to (Liu et al., 2017) with modifications. Briefly, enriched SC clusters (~3.5-5.0 × 10^6) were suspended in 5 mL complete CM supplemented with 10 µM ROCK inhibitor, seeded into a collagen-coated T25 flask and were cultivated in a humidified incubator at 37°C and 5% CO_2. Coating was done with 5 mL collagen type I (50 µg/mL) in DPBS in the presence of 1% 1 M acetic acid for 1 hr in a humidified incubator at 37°C and 5% CO_2. After washing with DPBS flasks were sterilized with UV light for 1 hr before use. 48 hrs after seeding, medium was discarded and hypotonic shock was performed with 4 mL autoclaved hypotonic solution (20 mM Tris-HCl, pH 7-7.4) for exactly 2 min at RT. After washing with DPBS, 5 mL fresh complete CM was added and cell growth was monitored regularly with a Leica microscope. After 4 days, SCs were washed with DPBS, detached with 3 mL TrypEL for 3 min at RT, collected, centrifuged (600×g, 3 min) and then seeded on a fresh collagen-coated T25 flask in 5 mL fresh complete CM. SCs were sub-cultured every 4-5 days and complete CM was replaced every 2 days. After 5-12 days SCs reached confluency.

2.6 Isolation of rat blood-derived-monocytes (RBDM), purity assessment and polarization toward M0, M1 and M2 macrophages

2.6.1 Isolation and purity assessment of RBDM

RBDM were isolated according to de Almeida et al. (2000) with some modifications. Adult male Sprague Dawley rats ((Crl:CD (SD)IGS; Charles River, Germany) weighing 150-200 g were anesthetized with 5% isoflurane and sacrificed (Abbott, Germany). Peripheral blood was collected directly from the heart into S-Monovette 2,7 mL tubes prepared with EDTA as an anti-coagulant. The collected blood was diluted 1:2 with phosphate buffered saline (PBS, Gibco) and mononuclear cells were purified with gradient centrifugation (800×g, 20 min, no brakes) with Lymphoprep™ gradient (Stemcell, Norway) at room temperature (RT). Then cells were aspired from the middle white layer of the interface and washed 2 times with PBS with gradually decreasing centrifugation (600×g followed by 450×g) to remove the lymphocytes. The enriched RBDM fraction was cultured in RPMI 1640 medium (Gibco) supplemented with 10% fetal calf serum (FCS, Gibco), 1% P/S (Gibco), 1 mM sodium pyruvate (Gibco), 1% HEPES (Gibco), 1 % MEM non-essential amino acid solution (Sigma-Aldrich) and 50 µM 2-mercaptoethanol (Gibco) in a humidified incubator (37°C, 5% CO_2). Cell viability was examined by trypan blue (Gibco) staining using a TC10 cell-counter (BioRad). Approximately 1×10^6 cells were seeded into each well of a 24-well-plate and after 6 hrs, cells were carefully washed with PBS. The attached cells were stained with Cluster of differentiation 68 (CD68, a cytoplasmic marker specific for rat monocytes) to assess purity of the RBDMs, which was > 95% with very few contaminating lymphocytes which could be distinguished from RBDM by their weak staining of CD68 in addition to their small size.

To test the response of monocytes to LPS, 5×10^5 RBDM cells were seeded into a 24-well-plate and incubated with RPMI 1640 medium containing 10% FCS, 1% P/S and 10 ng/mL LPS (Sigma-Aldrich) for 48 hrs. The controls were only incubated in medium without LPS. After 48 hrs RNA was collected and gene expression analyzed with qRT-PCR.

2.6.2 Differentiation of RBDM into M0 macrophages and polarization into M1 and M2 macrophages

For differentiation and polarization of RBDM the protocol of Spiller et al. (2016) and the recommendations of the manufacturer Promocell™ were used with some minor modifications. Briefly, 1×10^6 RBDM cells/mL were cultured for 5 days in RPMI 1640 containing 10% FCS

and 50 ng/mL mouse macrophage colony stimulating factor (M-CSF; premium grade; Miltenyi Biotec) in 25 cm^2 ultra-low attachment flasks in a humidified incubator (37°C, 5% CO_2) to differentiate them into M0 macrophages. Medium was changed after 5 days.

At day 6, different substances were added to achieve polarization: To get M1 macrophages, M0 macrophages were treated with 10 ng/mL LPS and 50 ng/mL recombinant interferon gamma (IFN-γ; Promocell); and for M2 macrophages, 40 ng/mL recombinant interleukin-4 (IL-4; Promocell) and 20 ng/mL recombinant interleukin-13 (IL-13; Promocell) were used. Macrophages were polarized for 48 hrs in ultra-low attachment 25 cm^2 flasks. Afterwards RNAs were collected for qRT-PCR or the cells were detached using PBS containing 5 mM EDTA for 40 min at 4°C. Instead of enzymatic detachment, we used EDTA to avoid alterations in the macrophages as indicated by Chen et al. (2015). After counting with TC10, cells were used in the transmigration assay.

2.7 Immunofluorescence

Primary adult Sertoli cells (PASC1) or RBDMs were plated into 24-well-plates (1 mL/well) and incubated for 6 hrs at 37°C and 5% CO_2. Cells were plated at a density of 3.0×10^4 into 24-well-plates (1 mL/well) and incubated 48 hrs at 37°C and 5% CO_2. After stimulation of PASC1 with 10 nM testosterone (T) for 24 hrs, cells were rinsed with DPBS and fixed with 100% ice-cold methanol on ice for 10 min. Cells were washed with PBS three times for 5 min, and then incubated in blocking solution (PBS with 3% BSA and 0.3% Triton X-100) for 1 hr at RT. Then blocking solution was replaced by fresh blocking solution containing the primary antibodies with the indicated dilutions (Table 3) and incubated overnight at 4°C. Cells were washed 3 times with DPBS for 3 min each at RT on an orbital shaker, and fresh blocking solution with the appropriate secondary antibody (Table 4) was added for 1 hr at RT. After washing 3 times with DPBS, images were obtained using an inverse Olympus IX81 microscope equipped with a fluorescence system.

ImageJ was used for IF measurements according to the protocol http://www.slu.se/PageFiles/388774/Pacho%-20ImageJ%20measuringcell-fluorescence.pdf, freely available at http://rsbweb.nih.gov/ij/. (Accessed between Apr 2019 and Sep 2021). Six cells with surrounding TJs from 3 independent experiments within or closest to the diagonals of the square optical field were quantified and analyzed with GraphPad Prism5.

2.8 RNA extraction, RT-PCR and quantitative real time PCR

2.8.1 RNA Isolation

For all qRT-PCR studies, immortalized 93RS2 cells and one adult rat testis were used as controls. RNAs were collected directly or from confluent PASC1 cells treated with T. Total RNA was isolated from 93RS2 and testosterone treated PASC1 by the RNeasy Mini kit. Briefly, cells were lysed with 700 µl RLT buffer after washing 2 times with ice-cold PBS. Lysed cells were transferred into a microcentrifuge tube, and homogenized by passing through a 24-gauge needle attached to a 1 ml plastic syringe for 4-5 times. These lysates were transferred into a new Eppendorf tube and mixed thoroughly with an equal volume of 70% ethanol. Samples up to 700 µl of mixture were transferred to another RNeasy spin column placed in a 2-ml collection tube and centrifuged for 15 s at 16,000 ×g. The runoff was discarded and the RNeasy spin column are washed with 700 µl of RW1 by centrifuging for 15s at 16,000×g. Then the RNeasy spin column was carefully removed, transferred to new collection tube and washed with 500 µl RPE buffer. This step was repeated one more time by centrifugation for 2 min at 10,000×g. Any possible contamination of RPE buffer in the RNeasy spin column was removed by an additional centrifugation at full speed. To elute total RNA, 30-50 µl of RNase-free water were added directly to another RNeasy spin column membrane and centrifuged at 10,000×g for 1 min. The concentration and quality of RNA was measured spectrometrically by Nano drop (Promega, Mannheim).

2.8.2 DNase digestion

RNA preparations should be free of DNA contamination prior to reverse transcription-PCR (RT-PCR). DNA contamination was removed by treating each RNA sample with DNase I (Invitrogen, Karlsruhe) at room temperature for 15 min in the reaction mixture given below.

2.8.3 DNase digestion reaction mix:

Table 15: DNase digestion reaction mixture

Volume	Component
X µl	2 µg RNA

1 µl	DNase I (10 U/µl)
2 µl	10 X DNase I buffer
to 20 µl	RNase free water

After DNA digestion, DNase I was inactivated by adding 2 µl of 25 mM EDTA (pH 8.0) to each sample and subsequently heat inactivated at 65°C for 10 min.

2.8.4 cDNA synthesis

DNA digested samples were reverse transcribed by using kit H-Minus (PeqLab/VWR, Erlangen, Germany). Briefly, oligo-dTs and dNTPs were mixed with RNA samples as given in Table 15. The reaction mixture was heated at 65°C for 5 min and quickly chilled on ice.

2.8.5 Denaturation of RNA and primer annealing:

Table 16: RNA mix

Volume	Component
21µl	2.5 µg of DNase I digested RNA
2 µl	Oligo dT
2 µl	dNTPs (A,C, G and T, each 10 mM)

To the RNA mix sample, RT mix was added as shown in Table 16, pre-heated for 2 min at 42°C and 1 µl of the reverse transcriptase enzyme was added to each sample. The reaction mixtures were incubated for 50 min at 42°C. Subsequently reactions were inactivated by heating at 75°C for 15 min. Samples were stored at -20°C for further analysis.

2.8.6 RT mix:

Table 17: RT mix

Volume	Component
8 µl	5 X M-MLV RT buffer
2 µl	RNase-free water
4 µl	0.1 M DTT

2.8.7 RT-PCR

A total of 1×10^5 cells of each cell line were grown as described above. Total RNA was extracted with the RNAeasy kit (Qiagen, Hilden, Germany) in accordance to the user manual. Reverse transcription was performed using a cDNA synthesis kit H-Minus (PeqLab/VWR, Erlangen, Germany) according to the supplier's instructions. Primers were designed on the NCBI Primer-Blast algorithm and purchased from Invitrogen/Thermo Scientific (Table 8). The other PCR reagents were purchased from Bio&Sell (Nuremberg, Germany). Semi-quantitative PCR was performed with 1 µg cDNA. GAPDH was used as a positive control. After an initial heating to 95°C for 4 min, each cycle consisted of denaturing at 95°C for 30 sec, annealing at 58°C for 20 sec and elongation at 72°C for 40 sec except for the final extension which lasted 5 min. The program consisted of 35 cycles.

2.8.8 Quantitative real-time PCR (qRT-PCR)

The mixture of qRT-PCR differs from a normal PCR with addition of the double strands DNA (dsDNA) specific fluorescent reporter probes such as SYBR green. The reporter probes can bind to the dsDNA every time the DNA is polymerized, and emit fluorescence detected by a detector. The increasing fluorescence signal is directly related to the exponential increase of DNA product in each cycle and recorded in the real-time PCR thermocycler, which is used to determine the threshold cycle (Ct) value and facilitates quantifying gene expression. Real-time PCR amplification was done in duplicates with iQTM SYBR Green Super-mix on the iCycler iQ System. After an initial heating at 94°C for 5 min, 40 cycles were performed: denaturation at 94°C for 14 sec, annealing at 59°C for 30 sec, and extension at 72°C for 15 sec. A final extension at 72°C was done for 10 min. Gene expression was measured after reaching the ct

value and calculated using the Delta – Delta Ct method. GAPDH was used for normalization (Table 8).

The primers were designed by primer Table 8. Gradient PCR was employed to determine the optimal annealing temperature for individual genes. According to it the temperature of each gene is set. All primers' efficiencies were between 100 ± 15 %.

The preparation of a typical 25 µl qRT-PCR reaction mix is given below.

Table 18: qRT-PCR MIX

Component	Volume per reaction
cDNA	1 µl
2X iQ SYBR green super mix	12.5 µl
Forward and reverse primer mix (10 pM/µl)	1 µl
DNase/RNase free water	10.5 µl
Total volume	25 µl

Realtime PCR amplification with iQ™ SYBR® Green Supermix was performed in duplicate by using the MiniOpticon cycler System (Bio-Rad) according to manufacturer's procedure.

2.9 Transmigration assay of macrophages

The Cytoselect™ transmigration assay kit (Cell Biolabs) was used following the manufacturer's protocol. Briefly, PASC1 cells, PC or a co-culture of both were seeded on pre-coated inserts with matrigel (Corning) or without coating in 500 µl complete DMEM/F12. Controls were performed with medium only. For coating, 9 µg/cm^2 MG in cold medium was added on top of the inserts and incubated in a humidified incubator (37°C, 5% CO_2) for 1 hr until solidification of MG. Washing with PBS was done before use. After 48-72 hrs, the cells or the co-cultures formed monolayers and PASC1-only (without MG coating) inserts were treated with 10 nM T, 10 ng /mL TNF-α or 200 pg/mL IL-6 for 48 hrs. Then, treatments and controls were used for the transmigration assay.

For this, M0, M1 or M2 macrophages were detached as previously mentioned and collected separately at a concentration of 1.0×10^6 cells/mL in RPMI 1640 containing 0.5% FCS (serum-low medium). 2 µl of 500X LeukoTracker™ (Cell Biolabs) to 1 mL of macrophages was added and macrophages were incubated for 1 hr at 37°C and 5% CO_2. Next, macrophages were centrifuged at 400×g for 2 min, the medium aspired and cells were washed twice with serum-low medium and reconstituted at 1.0×10^6 cells/mL with serum-low medium. The medium was removed from the inserts without disturbing the monolayer and transferred to a new 24-well plate containing 500 µl of RPMI 1640 (plus additives) in addition to 100 ng/mL Macrophage chemoattractant protein-1 (MCP1). For the transmigration assay, 100 µl of 1×10^5 labeled M0, M1 or M2 macrophages were added to each insert and incubated for 6 hrs at 37°C and 5% CO_2. 400 µl of the bottom medium containing the transmigrated macrophages were transferred to a new well containing 150 µl of 4X lysis buffer (Cell Biolabs), incubated for 5 min at RT with shaking (100 oscillations/min) and then 150 µl of the mixture were transferred to black 96-well plates (Greiner). Fluorescence intensity was measured at 480/520 nm (extinction/emission) in an ELISA reader (Tecan). Quantification was done by serial dilutions of LeukoTracker™-labeled macrophages, which after lysing were measured in the ELISA reader as described. The blank of serum-low medium with lysis buffer was subtracted from the results.

2.10 Measurement of transepithelial resistance (TER)

TER measurement was performed as reported by Stammler et al. (2013). Briefly, 6.0×10^4 PASC1 cells/cm^2 were seeded on 0.4-µm inserts for 24-well plates (Greiner) and cultured for 48 hrs until they reached confluency. Then, T (10 nM), IL-6 (200 pg/ml), BMP2 (25 ng/ml), or TGF-β3 (3 ng/ml) were added to the inserts. Controls received only vehicle. For TER measurement of PCs, 3.0×10^5 PCs (cells/cm^2) were seeded on inserts for 2 days. For co-culture, 6.0×10^4 PASC1 (cells/cm_2) were seeded on inserts for 2 days, then 2.0×10^5 PCs (cells/cm^2) were seeded on top of them and cultured for 2 days. TER measurements were done with a Millicell ERS-2 epithelial Volt-Ohm meter (Merck Millipore). Ω/cm_2 was calculated according to the protocol of the manufacturer and by setting the resistance of cell-free inserts to zero.

2.11 Tracer diffusion assay (TDA)

The tracer diffusion assay was performed as published by Stammler et al. (2013). In brief, cells cultured for 48 hrs on inserts as described above were incubated with fresh medium containing

5 mg/mL FITC-coupled Dextran, molecular weight 4 kDa (FD4, Sigma-Aldrich) and loaded into the upper compartment of the inserts. After 4 hrs a 100 µl sample was taken from the lower compartment and fluorescence intensity was measured at 490 nm/520 nm (extinction/emission) in an ELISA reader (Tecan) in black 96-well plates (Greiner).

2.12 Silencing expression of ZIP9 or AR via siRNA

For silencing ZIP9 or AR expression, PASC1 cells were treated with commercially available siRNA directed against ZIP9 or AR by following the manufacturer's protocol (Invitrogen). The oligonucleotides mentioned in Table 11 were used. Negative control siRNA (nc-siRNA) was provided in the siRNA kit from the same manufacturer. After incubation of PASC1 for 48 hrs with ZIP9-siRNA, AR-siRNA, or nc-siRNA, preparation of samples for qRT-PCR, TER measurement, or immunofluorescence experiments were carried out as described above.

2.13 Plasma membrane labeling with testosterone-BSA-FITC

PASC1 cells were cultured as described above in 24-well plates at a density of 3×10^3 cells/well until reaching a confluency of approximately 80%. The cells were then treated with either 10 nM testosterone or 1 µM of IAPG for 1 hr. Controls received only the testosterone vehicle ethanol. Thereafter, testosterone 3-(O-carboxymethyl)-oxime:bovine serum albumin-fluorescein isothiocyanate conjugate (T-BSA-FITC; Sigma-Aldrich, Steinheim, Germany) dissolved in Tris buffer (pH 7.2) was added to each well at a final concentration of 10 µM, and incubation was continued at room temperature for another 20 min. The medium was then removed by aspiration. In order to label nuclei, cells were fixed at room temperature with 3.7% formaldehyde that contained 20 ng of 4,6-diamino-2-phenylindole (DAPI). After 15 min, the formaldehyde/DAPI solution was removed by aspiration. Cells were washed with DPBS (Gibco) and then overlayed with 400 µL PBS before imaging. Images were taken by an inverse Olympus IX81 microscope (Olympus). Non-specific binding was assessed by incubating the cells with 10 µM BSA-FITC without testosterone dissolved in Tris buffer (pH 7.2) for 20 min at room temperature.

2.14. Treatments and sample preparations for western blots (WB)

2.14.1 Preparation of cell lysates from PASC1

A total of 3×10^4 PASC1 cells/dish were grown in 5 cm culture dishes as described above. Cells were then incubated for 24 hrs with 1% FCS before testosterone or IAPG were added to the medium to reach the desired final concentration. Ethanol vehicle for testosterone was added to the IAPG-treated cells and untreated controls at the same concentration as in cell cultures treated with testosterone. After 24 hrs, the medium was aspirated and the cells were washed twice with ice-cold DPBS. Cells were then incubated with 400 µL lysis buffer (Cell Signaling) containing 1 µM PMSF, 1× protease inhibitor cocktail (Roche), and 2 µg/mL pepstatin which was added immediately before use. All further steps were carried out on ice. After 5 min of incubation, cells were detached using a cell scraper. The suspensions were then transferred into 1.5 mL vials and sonicated 5 times for 1 sec each with intervals of 1 sec. After centrifugation of the lysates at 4°C and 13,000×g for 10 min, the protein concentration in the supernatants was determined at 540 nm using the bicinchoninic acid protein assay reagent kit (Pierce) and a plate reader (Tecan). The BSA protein standard contained lysis buffer at the same concentration as in the samples from the cell lysates. Supernatants were then aliquoted and maintained at −20 °C until further use.

2.14.2 SDS-polyacrylamide gel electrophoresis

The SDS polyacrylamide gel electrophoresis (SDS-PAGE) technique separate the proteins according to their size. The gels were prepared freshly, depending on the size of investigated proteins; Separating gel and Stacking gel were made according to the recipe given below.

Table 19: Separating gel, SDS –PAGE gel preparation

Solutions	**7.5%***	**10%***	**12.5%***	**15%***
Water	4.85 ml	4.01 ml	3.17 ml	2.35 ml
1.5 M Tris-HCl pH 8.8	2.5 ml	2.5 ml	2.5 ml	2.5 ml
10% (w/v) SDS	100 µl	100 µl	100 µl	100µl
Acrylamide	2.5 ml	3.34 ml	4.17 ml	5 ml

10% (w/v) APS**	50 µl	50 µl	50 µl	50 µl
TEMED	5 µl	5 µl	5 µl	5 µl
Total	10 ml	10 ml	10 ml	10 ml

Table 20: Stacking gel

Solutions	**4%***
Water	3 ml
0.5 mM Tris-HCl pH 6.8	1.25 ml
10% (w/v) SDS	50 µl
Acrylamide	0.65 ml
10% (w/v) APS**	25 µl
TEMED	5 µl
Total	**5 ml**

*The gel percentage depends on the molecular weight of the protein of interest (based on 5:1 acrylamide/bisacrylamide ratio).

** Ammoniumpersulfate (APS) –prepared freshly every time.

2.14.3 Western blotting

A total of 10 µg protein from PASC1 cell lysates was run on SDS-PAGE gels containing 10% acrylamide and 0.3% N,N′-methylene-bis-acrylamide (Table 19). Biotinylated proteins (Cell Signaling) were run in parallel as molecular weight markers. After electrophoresis, proteins were semi-dry electro-blotted onto PVDF membranes (Merck Chemicals) for 30 min at 0.5 V/cm^2. The membranes were then incubated for 1 hr at room temperature in 5% (w/w) non-fat dry milk. Primary antibodies against phospho-Erk1/2, total-Erk1/2, or beta-actin (Table 3) were diluted according to the recommendations of the manufacturers and then poured on the PVDF membranes which were incubated overnight at 4°C for all antibodies with dilutions and

manufacturers. After washing with DPBS, the membranes were incubated under continuous mild agitation on an orbital shaker for 60 min at room temperature with a horseradish peroxidase-conjugated secondary antibody (Table 4). An anti-biotin HRP-conjugated antibody at a dilution of 1:2000 was also included in the mixture containing the secondary antibody in order to detect the biotinylated molecular weight marker. Antibody-labeled protein bands were visualized by enhanced chemiluminescence.

2.14.4 Reprobing of the membrane

The membrane was washed 3 times for 5 min each in 1X TBST buffer and incubated with the stripping buffer at 60°C for 3 min (Table 13). Again, the membrane was washed with 1X TBS/Tween and blocked with 5% milk buffer for 1 hr at room temperature and subsequently the western blot procedure was repeated with other primary antibodies (Table 3, 4)

2.15 Statistical analysis

All experiments were repeated at least three times. The means and the standard error of the means (SEM) of all experiments were used for analysis. The comparison of the means between groups was performed by one-way analysis of variance (ANOVA) using GraphPad prism software (Version 5.0, Graph Pad Inc) followed by the post – hoc test of Dunnett, Tucky, t-test etc…. and P values of ≤ 0.05 were considered significant.

3 Results

3.1.1 Isolation, characterization and purity assessment of adult rat Sertoli cells

Up to date, SCs isolation methods have shown only limited improvements to provide primary SCs that can be cultured long-term. Thus, continuous animal sacrifice is inevitable. This is why we sought to develop a new protocol for isolation and long-term cultivation of adult rat SCs without the need of repeated animal sacrifices, based upon conditional reprogramming (CR). We started to culture irradiated feeder layers of 3T3-J2 mouse fibroblast with primary SCs as described (Liu et al., 2017), and found that single SCs rarely formed typical colonies of SCs (Fig 5A). On the other hand, using cell-strainers with larger pores (100 µm instead of 40 µm or 70 µm strainers as published by Chang et al., (2011), showed that more SCs clusters attached and formed colonies (Fig 5B). Moreover, co-culturing of SCs clusters with 3T3-J2 irradiated feeder cells for 3 days resulted in small colonies (Fig 5C). However, separation of feeder cells from SCs was challenging and contaminating PCs/LCs were phenotypically indistinguishable from the irradiated feeder cells (Fig 5C).

In our next attempts, the use of conditioned medium (CM) and/or in DMEM/F12 rather than an irradiated feeder layers, showed small SCs clusters, as early as 2 days after seeding (Fig. 6A,B). After 3 days, larger presumable SCs clusters in complete CM compared to those in DMEM/F12 only could be monitored (Fig. 6C,D). The observations showed the disappearance of SCs clusters in DMEM/F12 (Fig. 6E). In contrast, complete CM supported presumable SCs clusters to reach almost confluency (Fig. 6F). Compared to DMEM/F12 (Fig. 6C,E), the complete CM inhibited the growth of non-epithelial testicular cells during 5 days (Fig. 6D,F).

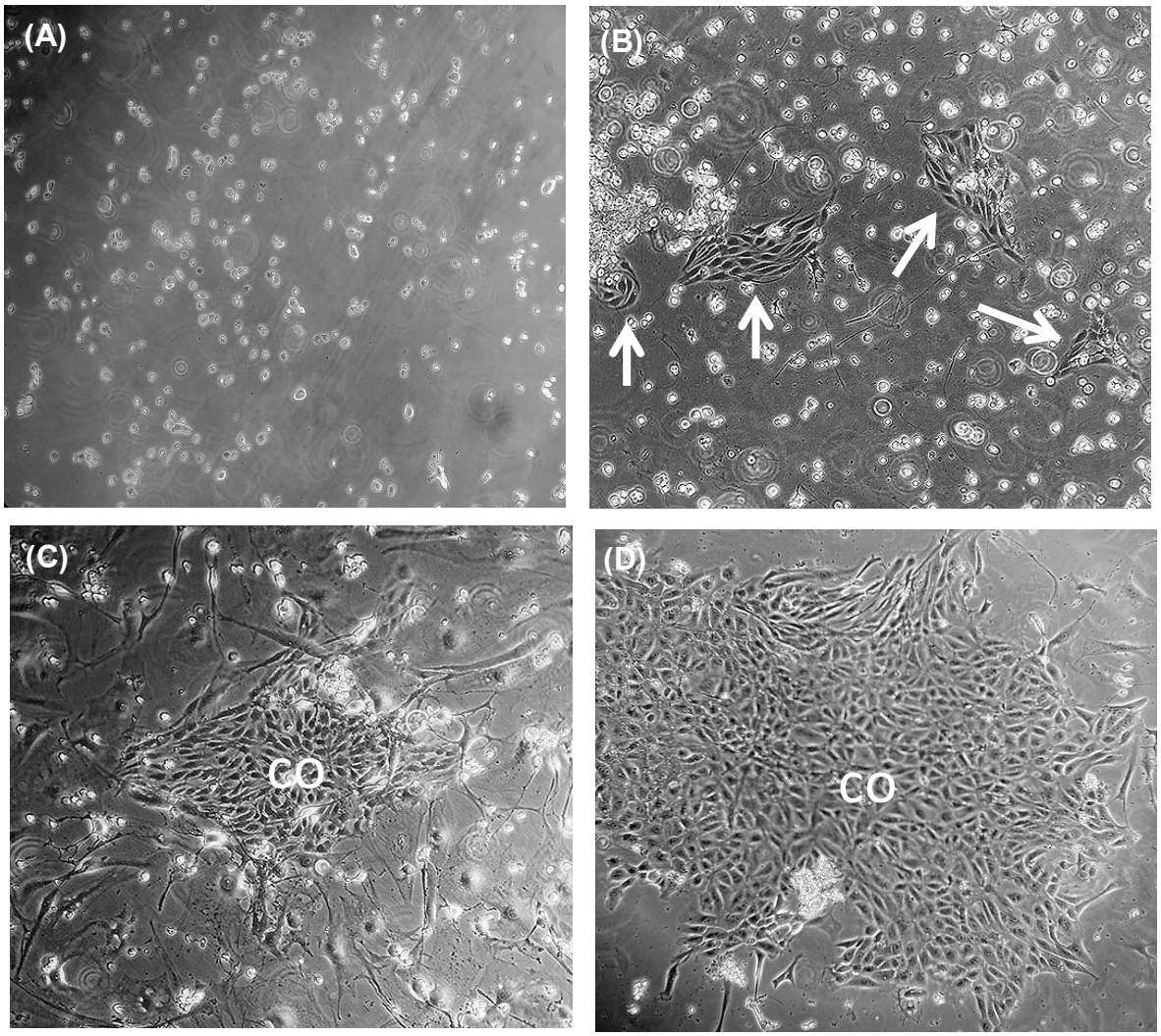

Figure 5. Brightfield microscopic photos of freshly isolated SCs.

Freshly isolated single SCs (A) or SC clusters (B–D) were seeded on collagen-coated T25 flasks with (C) or without irradiated feeder cells (A,B,D). After 24 hrs (A,B) or 72 hrs (D) complete CM was added. Starting with single SCs resulted in less cell numbers and patches (A) compared to starting with SC clusters which formed larger patches of SCs after 24 hrs (B, arrows). After 72 hrs, SC clusters with complete CM only (D) formed larger colonies (co) compared to SC clusters seeded onto irradiated feeder cells (C) (magnification 100×).

Altogether, the complete CM did support attachment and growth of SCs which were easily identifiable due to the lack of contaminating feeder cells and other cells, thus the use of complete CM is preferable to layers of irradiated feeder cells.

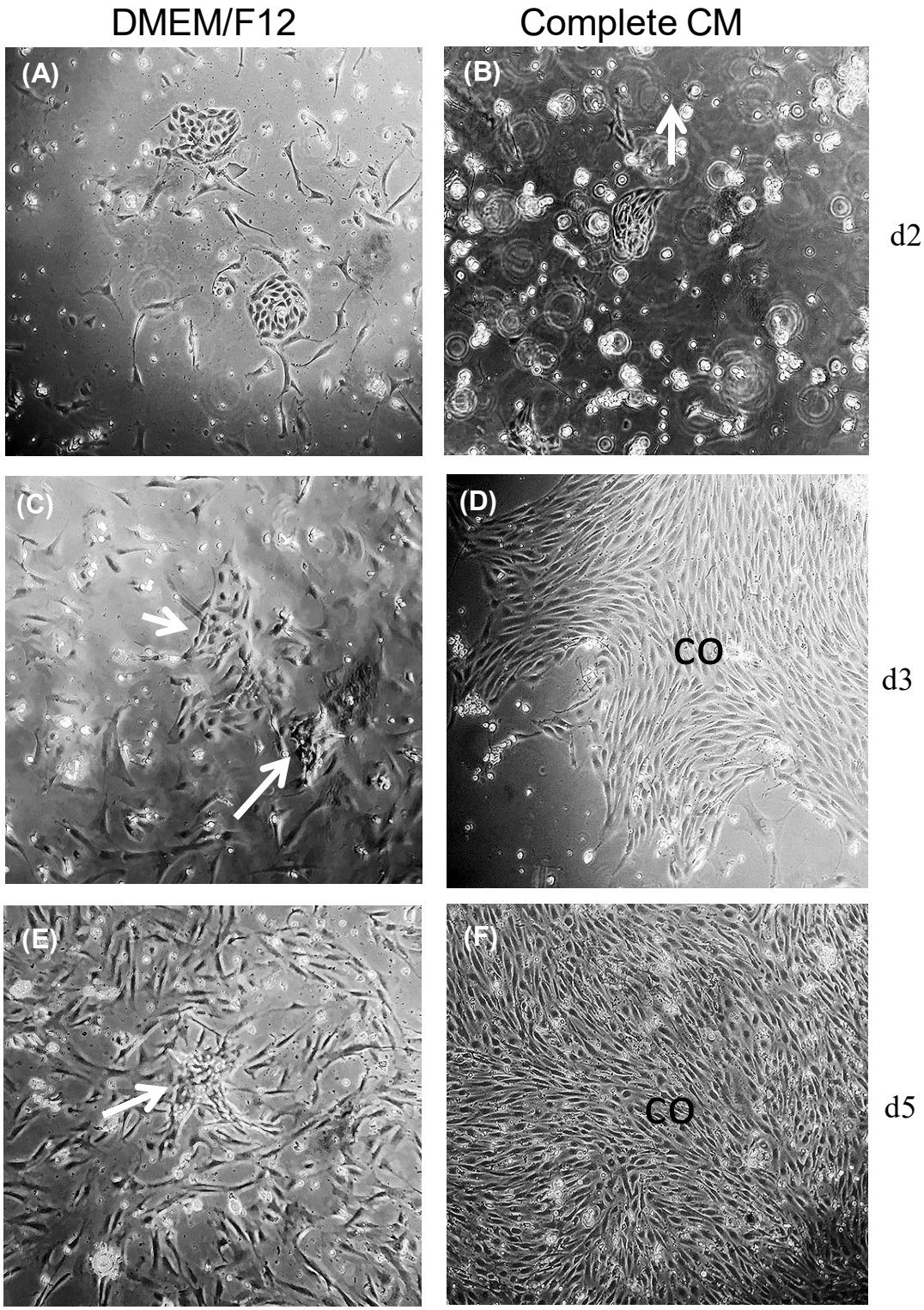

Figure 6. Comparison of freshly isolated SC clusters with complete CM compared to complete DMEM/F12 in collagen-coated flasks.

At day 2 (d2), SC clusters generated with complete DMEM/F12 compared to complete CM demonstrated no significant differences in the numbers and sizes of patches (A,B, arrows). However, a higher number of contaminating PCs/LCs is visible in complete DMEM/F12 (A)

compared to complete CM (B), which seems to inhibit the growth of PCs. At day 3 (d3), SC clusters in complete CM formed larger clusters (co) with fewer contaminating PCs/LCs (D) compared to SC clusters in complete DMEM/F12 (C). At day 5 (d5), contaminating PCs/LCs had overgrown the SC colonies in complete DMEM/F12 (E, arrow) in contrast to the confluent SC monolayer (co) in complete CM (F) (magnification 100×).

The modified and optimized protocol based on the protocol of Liu et al. (2017) is summarized in Fig. 7. Finally, we generated three independent, conditionally reprogrammed adult rat SCs populations with a doubling time of almost 20 hrs, which have been named primary adult rat SCs 1–3 (PASC1–3). PASC1 has now undergone 210 doublings in 175 days and reached passage 31. In addition, the conditionally reprogrammed SCs can be easily frozen and thawed without any problems, with a cell viability of at least ≥ 93% (Kabbesh et al., 2021).

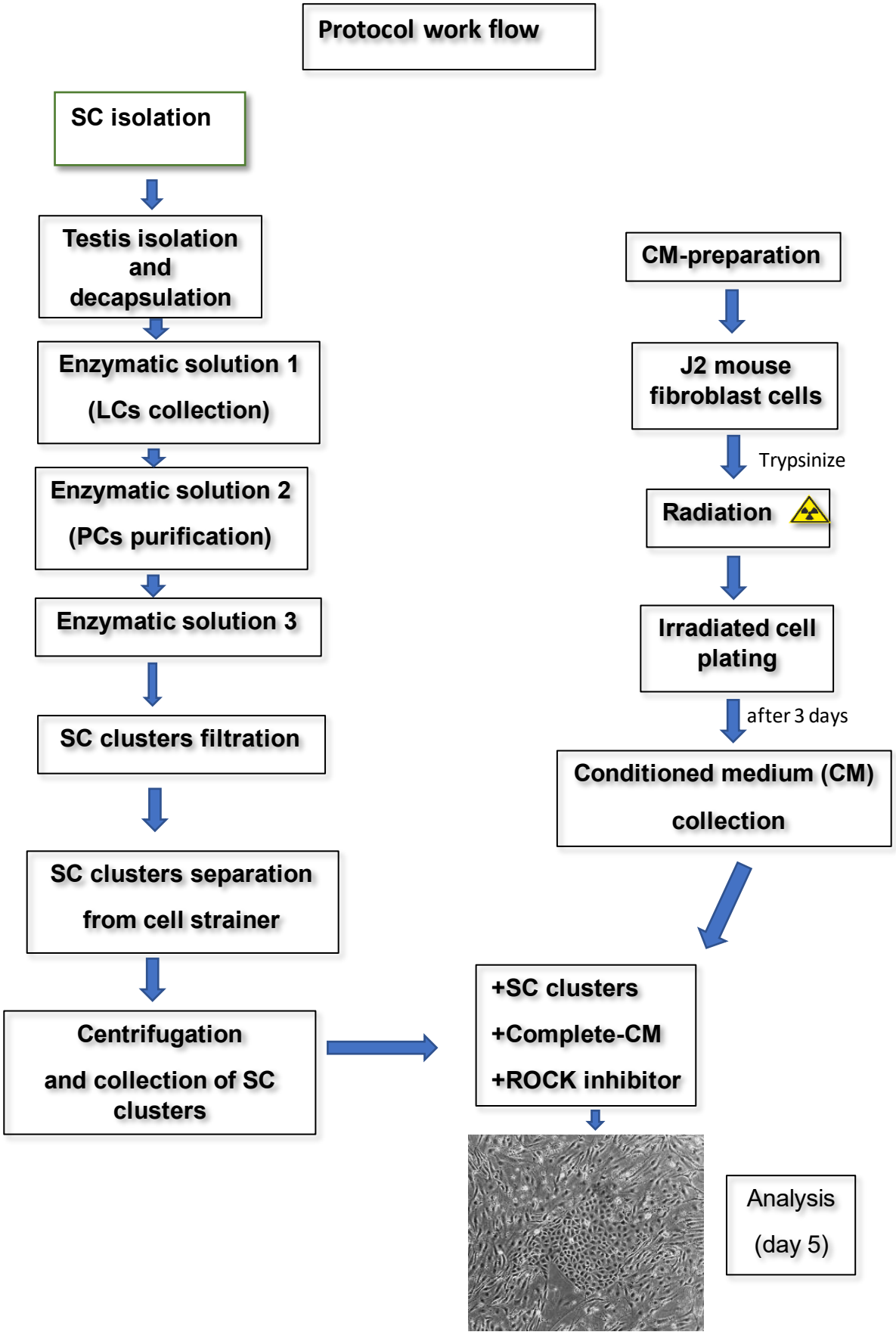
Protocol work flow
SC isolation
Testis isolation and decapsulation
Enzymatic solution 1 (LCs collection)
Enzymatic solution 2 (PCs purification)
Enzymatic solution 3
SC clusters filtration
SC clusters separation from cell strainer
Centrifugation and collection of SC clusters
CM-preparation
J2 mouse fibroblast cells
Trypsinize
Radiation
Irradiated cell plating
after 3 days
Conditioned medium (CM) collection
+SC clusters
+Complete-CM
+ROCK inhibitor
Analysis (day 5)

Figure 7. Overview of the CR method for the isolation of adult rat SCs.

3.1.2 Characterization of PASC1 and expression of testicular markers

Immunofluorescence staining against the SC-specific marker SOX9 and the PC-specific marker ASMA were used in order to address the purity of PASC1. Almost all PASC1 cells expressed SOX9 and not ASMA resulting in a purity of ~99% (Fig. 8). In addition, viability was clearly improved after 6-9 days of culturing and was maintained over time (Fig. 9A). Next, we analyzed expression of SC-specific and SC-maturation genes using qRT-PCR. The results demonstrated that PASC1 cells express SC-specific genes SOX9, transferrin, and clusterin (Fig. 9B–D) (Skinner & Griswold, 1980; Baily & Griswold, 1995; Fröjdman et al., 2000). Moreover, erythroid transcription factor 1 (GATA1), a post-pubertal SC maturation gene (Jegou & Sharpe, 1993; Yomogida et al., 1994), was highly expressed in PASC1 compared to 93RS2 indicating that PASC1 cells maintained differentiation even without CM (Fig. 9E). On the other hand, anti-Müllerian hormone (AMH), a marker of prepubertal SCs (Beau et al., 2000), was very weakly expressed in PASC1 compared to the immature 93RS2 cells (Fig. 9F). One of the most important characteristics of conditional reprogramming, in addition to the long-term viability of epithelial cells, is the selective support and growth of epithelial cells, whereas non-epithelial cells growth is inhibited in the early passages (Liu et al., 2012; 2017). As shown in Fig. 9G, LCs were no longer detectable in passage 4, whereas very small amounts of ASMA-positive PCs were found, which were no longer detectable in the later passages (Fig. 9H).

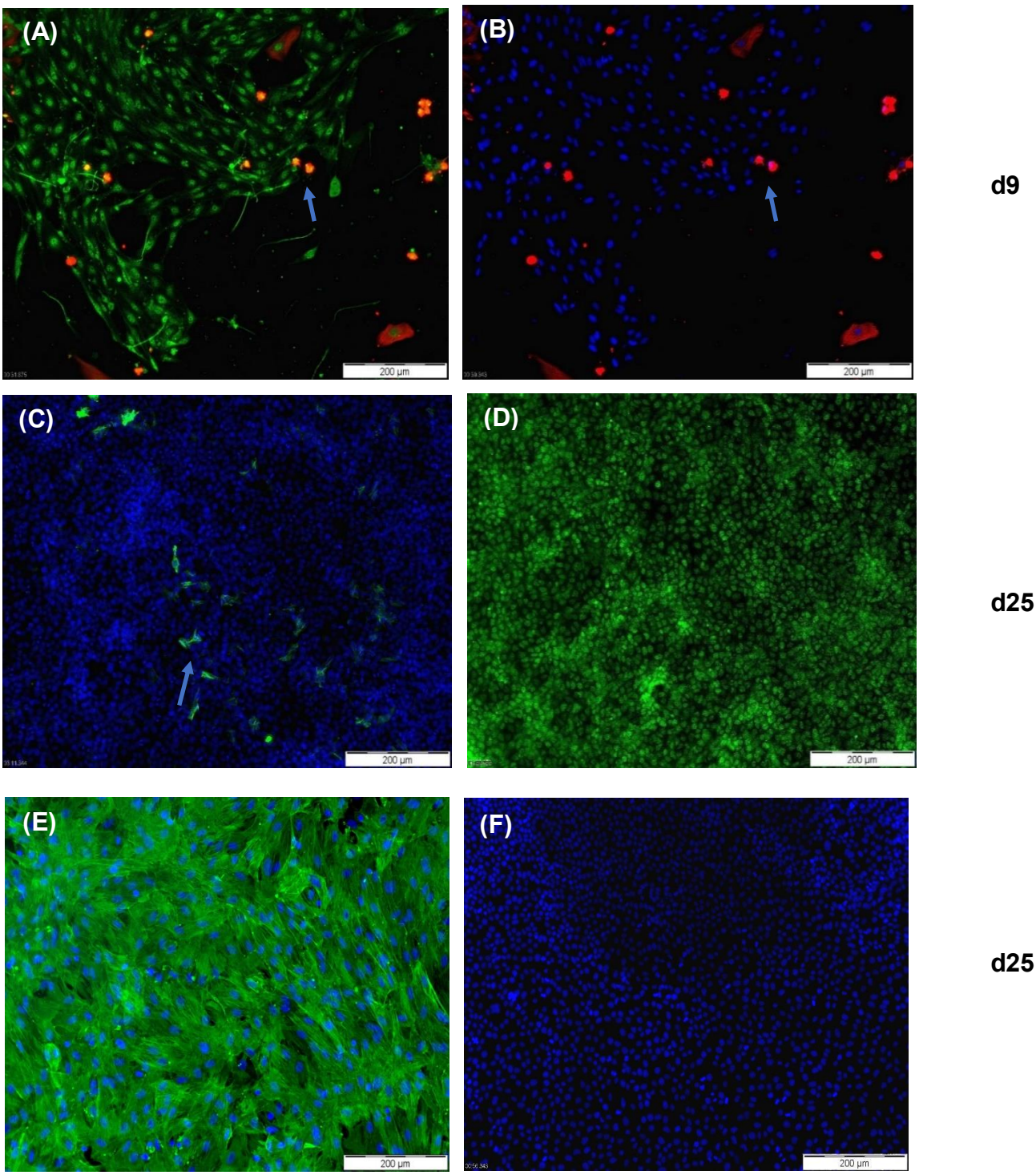

Figure 8. Immunofluorescence staining of PASC1 against SOX9, ASMA or both.

PASC1 cultivated in complete CM for 9 (A,B), and 25 days (C,D), and primary PCs for 18 days (E) were stained with antibodies against SOX9 (A,D, green) and ASMA (A,B, red, C,E green). At day 9 (d9), PASC1 positive for SOX9 (green) are shown in addition to very few contaminating ASMA-positive PCs (red) (A,B, arrows); the round phenotype indicates that the PCs are dying. At day 25 (d25), the purity of SCs is increased, with only very few ASMA-

positive PCs (C, arrows, green) with ~99% of the cells positive for SOX9 (D, green). Primary PCs stained with ASMA were used as a positive control (E); in (F), the negative control without any primary antibody is shown. The nuclei were stained with DAPI (blue). Scale A-F 200µm.

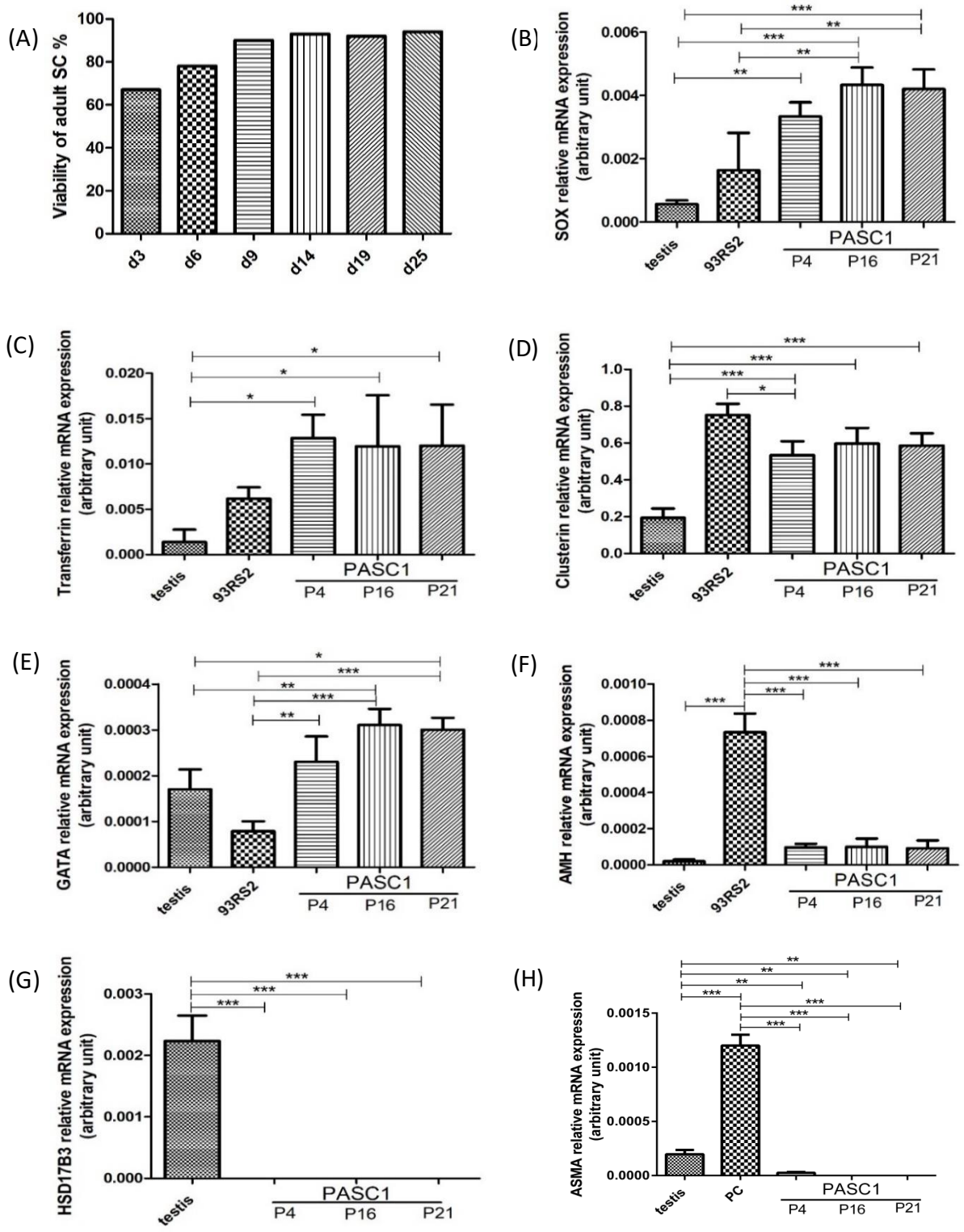

Figure 9. qRT-PCR analysis of mRNA expression of SC-specific and/or -maturation markers in PASC1.

The viability of PASC1 increased strongly after 9 days (d9) after isolation from 63.5% at day 3 to 93% at day 25 (A). Gene expression of SC-specific and SC-maturation genes in passages 4 (P4), 16 (P16), and 21 (P21) was monitored with qRT-PCR. Immortalized immature rat 93RS2 SCs and adult rat testis were used as positive controls. In contrast to a strong expression of SOX9 (B), transferrin (C), clusterin (D), and GATA1 (E), PASC1 showed weak expression of AMH, a marker of immature SCs (F). Contamination of PASC1 by LCs was excluded using HSD17B3 (G) and by ASMA for PCs (H). Each bar represents the mean ± SEMs of three independent experiments performed in duplicates; * $p \leq 0.05$; ** $p < 0.01$; *** $p < 0.001$.

3.1.3 Formation of the SC barrier to a functional characterize PASC1

Next, we sought to test whether PASC1 are representing an appropriate model to study the junction of the adult SCs in vitro, by analyzing both expression and establishment of the TJ barrier as a proof-of-principle. Moreover, we aimed at elucidating the contribution of PCs to the formation of the TJ barrier by measuring the TER. In order to do that, PASC1 or PCs were cultured on cell culture inserts individually or in co-cultures until confluency was achieved. We could show that PASC1 cells contributed mainly to the formation of barrier, whereas PCs alone only formed a very weak barrier (Fig. 10A), similarly to co-cultures, where also PCs only contributed slightly to the barrier (Fig. 10A). As a confirmation, the tracer diffusion assay also showed that in contrast to PCs and co-cultures, mainly PASC1 contributed to the TJ barrier (Fig. 10B).

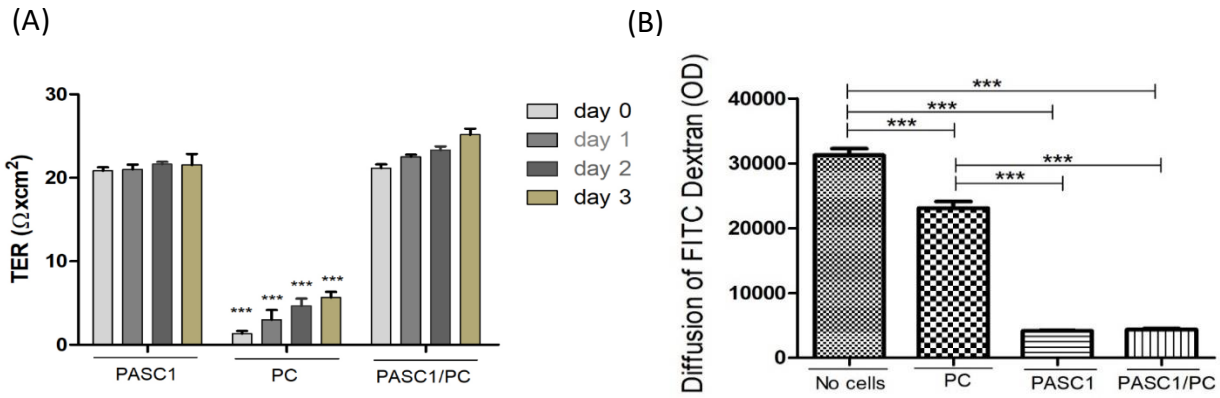

Figure 10. Time-dependent effects on the barrier integrity of SCs and PCs in mono-or co-cultures.

Mono-cultures of PASC1 showed a strong barrier, which was only slightly improved by co-cultures of PASC1/PCs, as shown by TER values (A). Statistical tests were performed to evaluate differences between the distinct days and the distinct mono- and co-cultures; for example, day 0 showed a significant reduction only for PC compared to PASC1, and for the PASC1/PC co-culture, but the difference between PASC1 and PASC1/PC was not significant. Monocultures of PASC1 showed the strongest reduction of the diffused FITC-dextran after day 2 compared to PCs only (B). Co-cultures of PASC1/PCs only showed slightly higher reductions compared to mono-cultures of PASC1. Data points represent the mean values ± SEMs obtained from three independent repetitions performed in duplicates (n = 6); *** $p < 0.001$.

3.1.4 Expression of the androgen receptor (AR) in PASC1

As previously shown, formation of TJs is hormone-dependent (Chakraborty et al., 2014; Bulldan et al., 2016), this is why, AR expression and T responsiveness were investigated. We could show that PASC1 strongly and stably expressed AR on both mRNA and protein levels in the three different passages (P), P4, P16, and P21 (Fig. 11) also indicating SC maturation as published (Regadera et al., 2001). The AR was located in untreated cells mainly in the cytoplasm (Fig. 11B,C), but translocated to the nucleus after treatment with T (Fig. 11D) (Kabbesh et al., 2021).

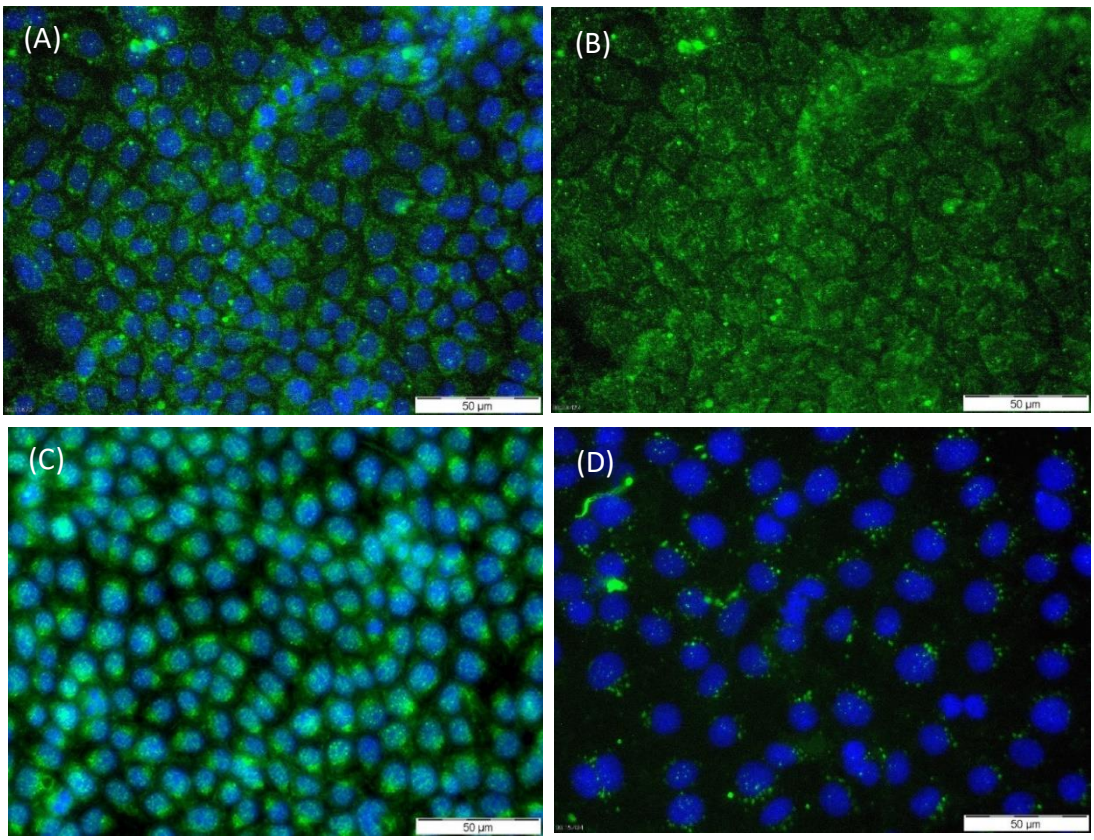

(E)

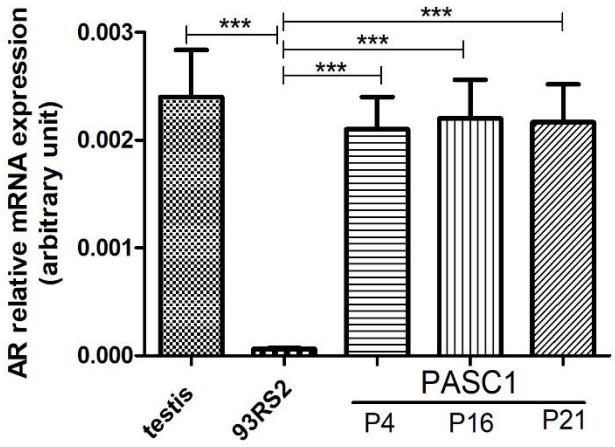

Figure 11. Conditionally reprogrammed PASC1 express the androgen receptor (AR) on the protein (A–D) and mRNA level (A) in passages P4 and P16.

The majority of AR (green) was detected in the cytoplasm of PASC1 and rarely in the nuclei (A,B) of untreated cells. After treatment with T, the AR translocated into the nuclei and was concentrated in the perinuclear region (C). The negative control with Alexa Fluor showed a negligible background and DAPI was used to stain the nuclei (blue) (D). The mRNAs of 93RS2 and adult rat testis were used as negative and positive controls, respectively (E). Each bar represents the mean ± SEMs of three independent experiments performed in duplicates; *** $p < 0.001$.

3.1.5 Effects of T on PASC1 barrier integrity

Next, PASC1 seeded on cell culture inserts were treated with T in order to show the effects of androgens on the SC barrier. As clearly seen in Fig. 12A, T upregulate the TER values of PASC1 in a time-dependent manner compared to the untreated cells. As a confirmation, TDA showed also that T remarkably decreased the permeability (Fig. 12B), indicating that T promoted the TJ integrity of PASC1 in vitro.

(A)

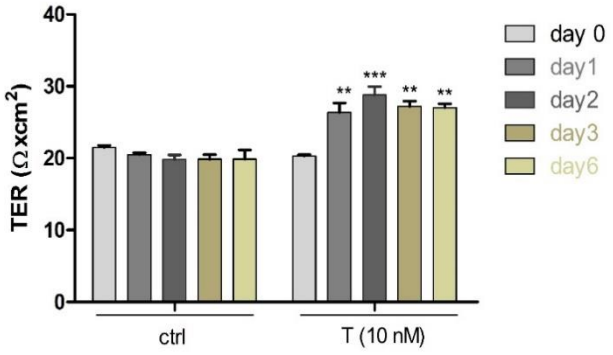

(B)

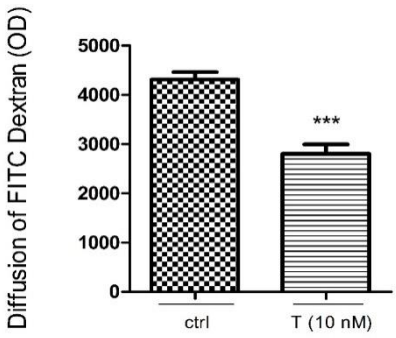

Figure 12. Time-dependent effects of T on the PASC1 TJ barrier.

T increased the TJ integrity in a time-dependent manner as shown by the increased TER values compared to the untreated controls (ctrl) (A). Stimulation of PASC1 with T for 2 days resulted in a significant reduction of FITC-dextran diffusion (B). Data points represent the mean values ± SEMs obtained from three independent repetitions performed in duplicates (n = 6); ** $p < 0.01$; *** $p < 0.001$ (A) and the unpaired t-test was used for statistical analysis; *** $p < 0.001$ (B). OD: Optical density.

3.1.6 Effects of T on the tight junction proteins zonula occludens-1 (ZO-1) and junctional adhesion molecule (JAM-3)

JAM-3 and ZO-1 are both important TJ proteins involved in SC cell-to-cell contacts (Gliki et al., 2004) and both are regulated by androgens (Willems et al., 2010; Lui & Cheng, 2012; De Gendt et al., 2014; Bulldan et al., 2016). Treatment of PASC1 with T strongly increased mRNA expression of JAM-3 (Fig. 13A,B) as well as the cytoplasmic and cell membrane localization of JAM-3 protein significantly (Fig. 13C–E).

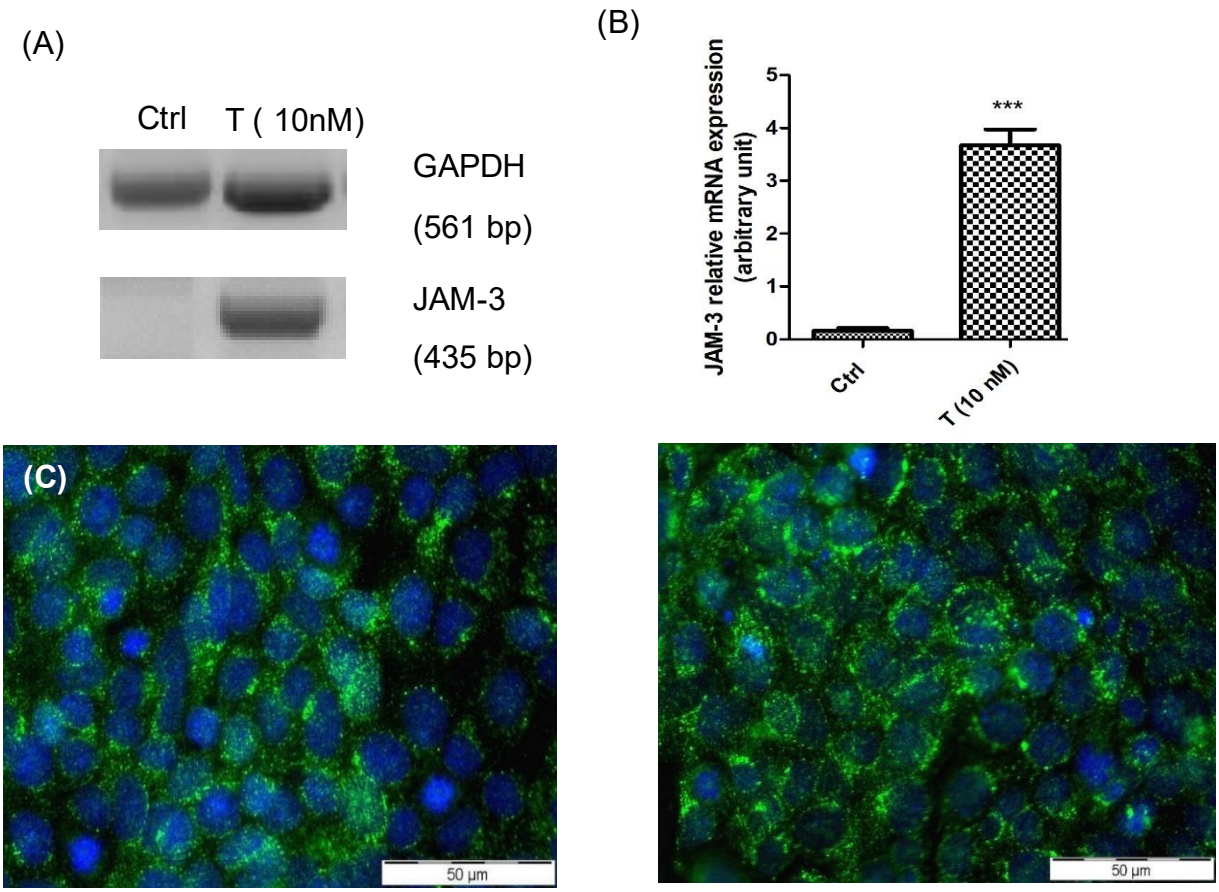

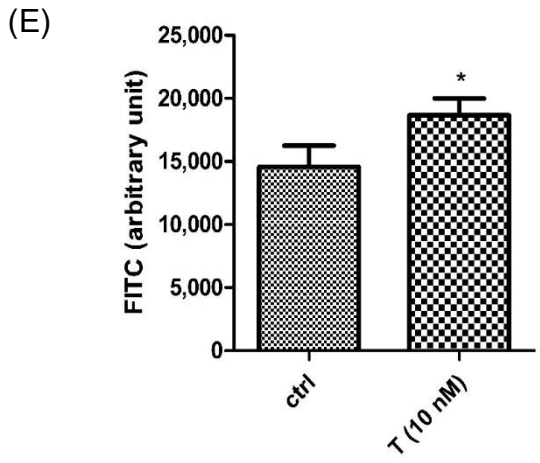

Figure 13. Effects of T on JAM-3 mRNA expression and protein presence.

PASC1 (2×10^5 cells/well) were treated with T for 24 hrs. JAM-3 mRNA expression was strongly increased in PASC1 after T treatment compared to the control (ctrl) (A,B). JAM-3 is localized mainly in the cell membrane in a punctate pattern but can be also found in the cytoplasm (C). T stimulated JAM-3 protein expression strongly (D) and significantly (E). DAPI was used to stain the nuclei (blue). Each bar represents the mean ± SEMs of three independent experiments performed in duplicates. The unpaired t-test was used for statistical analysis; * $p \leq 0.05$; *** $p < 0.001$.

Similarly, T treatment also upregulated ZO-1 mRNA expression (Fig 14A) and ZO-1 protein abundance (Fig 14B–D) at cell-to-cell contacts significantly compared to the untreated controls. Of note, T treatment changed the cell morphology slightly from more elongated (Fig. 14B) to mostly cobblestone-like (Fig 14C) (Kabbesh et al., 2021).

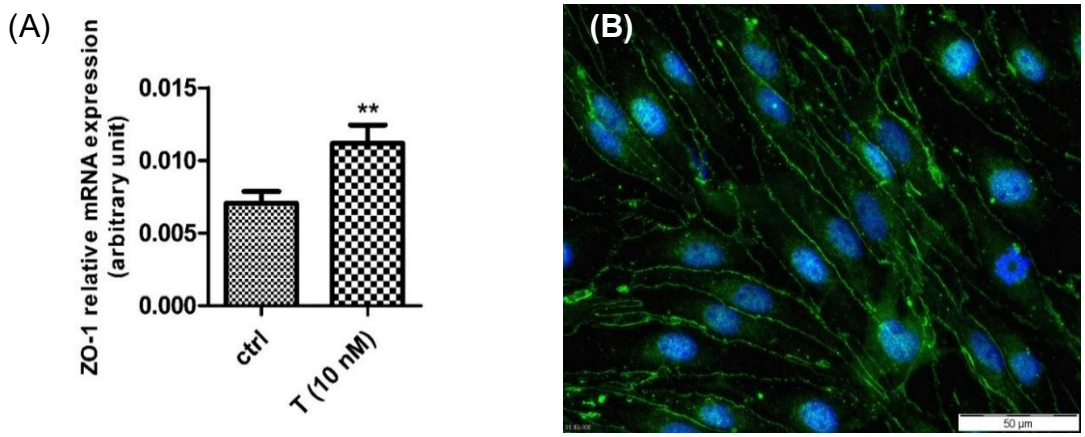

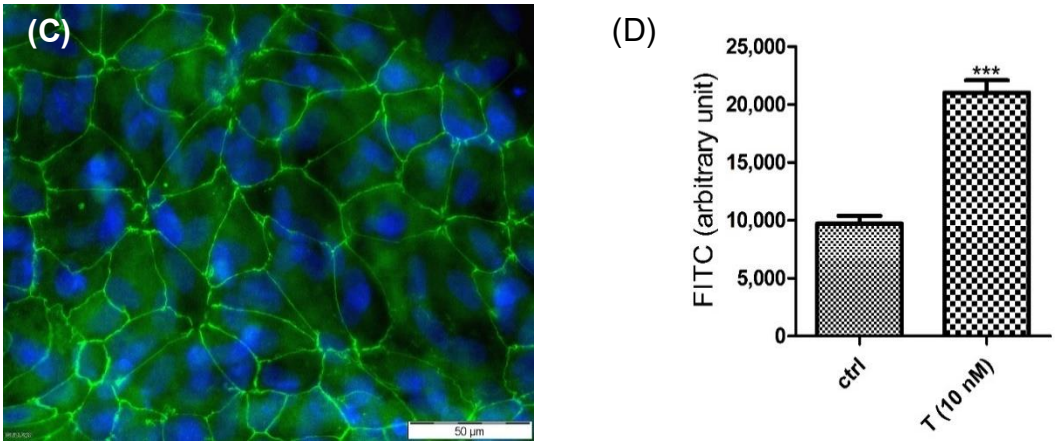

Figure 14. Effects of T on ZO-1 mRNA expression (A) and protein presence (B–D).

PASC1 (2×10^5 cells/well) were treated with T for 24 hrs. ZO-1 mRNA expression was significantly increased by T treatment (A) compared to the untreated cells (B). A stronger protein presence was observed between cell-to-cell contacts in T-treated cells (C). Quantification showed a significant increase (D). DAPI was used to stain the nuclei (blue). Each bar represents the mean ± SEMs of three independent experiments performed in duplicates. The unpaired t-test was used for statistical analysis; ** $p < 0.01$; *** $p < 0.001$.

3.1.7 Effects of different cytokines on the TJ barrier of PASC1

It has been reported that some of the cytokines expressed also in testis have a strong effect on the formation of the BTB (Xia et al., 2009). This is why we used interleukin-6 (IL-6) (Zhang et al., 2014) and TGF-β3 (Lui et al., 2001; 2003), in addition to bone morphogenetic protein-2 (BMP2) (Ciller et al., 2016) to test the effects of these cytokines individually on PASC1. To do that, PASC1 on cell culture inserts were treated individually with the three cytokines for 24–72 hrs. The integrity of the TJ barrier was downregulated strongly after 48 hrs by each substance compared to the untreated controls (Fig 15A). TDA measurements confirmed the TER results (Fig 15B) (Kabbesh et al., 2021).

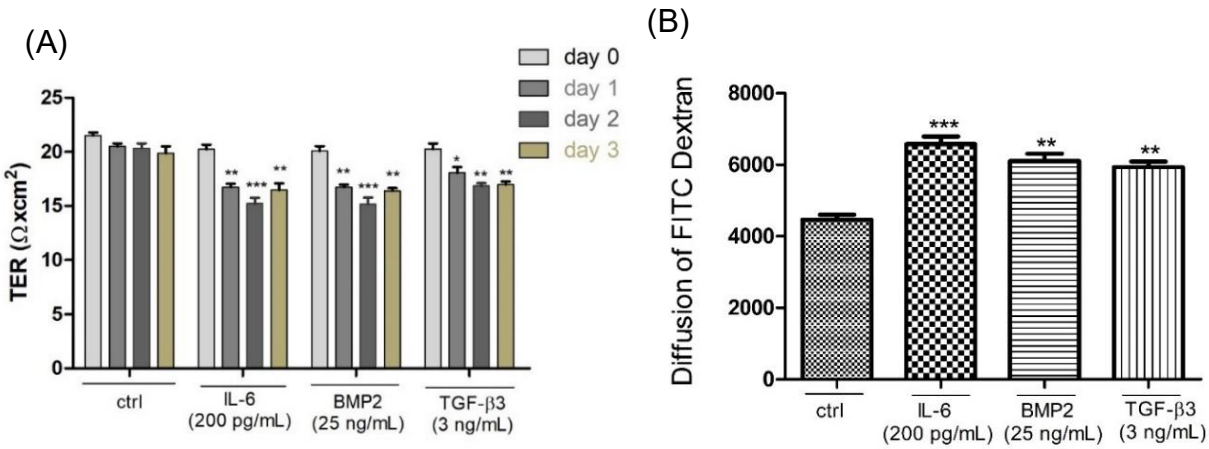

Figure 15. Effects of IL-6, BMP2 or TGF-β3 on barrier integrity of PASC1.

(A). After treatment of PASC1 with IL-6, BMP2 or TGF-β3 for 48 hrs, a significant increase of diffusion of FITC-dextran was observed. The values are normalized to the control (=100) (B). Data points represent the mean values ± SEMs obtained from three independent repetitions performed in duplicates (n = 6); * $p \leq 0.05$; ** $p < 0.01$; *** $p < 0.001$. OD: Optical density.

3.2 Characterization of the testicular immunological barrier (TIB) formed between PASC1

In the next experiments, we sought to test the integrity of the TJ barrier formed between PASC1 cells from an immunological perspective. To do that, we established a new transmigration model of macrophages through a layer of PASC1 cells to study the transmigration of macrophages through the TJ barrier between PASC1 cells (Kabbesh et al., 2022).

3.2.1 Isolation and characterization of rat blood-derived-monocytes (RBDM)

Primary RBDM were isolated from adult rats' fresh blood. In order to test monocyte purity, freshly isolated primary RBDMs were stained against the monocyte marker cluster of differentiation-68 (CD68) (Dijkstra et al., 1985; Grau et al., 2000) which exhibited a cytoplasmic localization (Fig. 16A). The very few contaminating lymphocytes could be easily identified as they showed only DAPI staining in addition to their remarkably smaller size compared to RBDM (Fig. 16A,B). The resulting purity of the isolated RBDM was > 95% and the final yield was ~5-6 × 10^6 RBDM/rat. Moreover, we treated RBDM with lipopolysaccharide

(LPS) and found a strong upregulation of tumor necrosis factor-alpha (TNF-α) gene expression compared to the untreated control monocytes. This indicates that the isolated RBDM react to LPS stimulation by upregulation of TNF-α (Fig. 16C) which is a common characteristic of monocytes as reported in Van der Bruggen et al., (1999) and de Almeida et al., (2000).

After isolation RBDM appeared small and round in shape with a diameter of ~6-22 μm (Figs. 16A-D). After 5 days of macrophage colony stimulating factor (M-CSF) treatment, the differentiated M0 macrophages showed elongated larger cell shapes and adhered tightly to the surface of the plates (Fig. 16E).

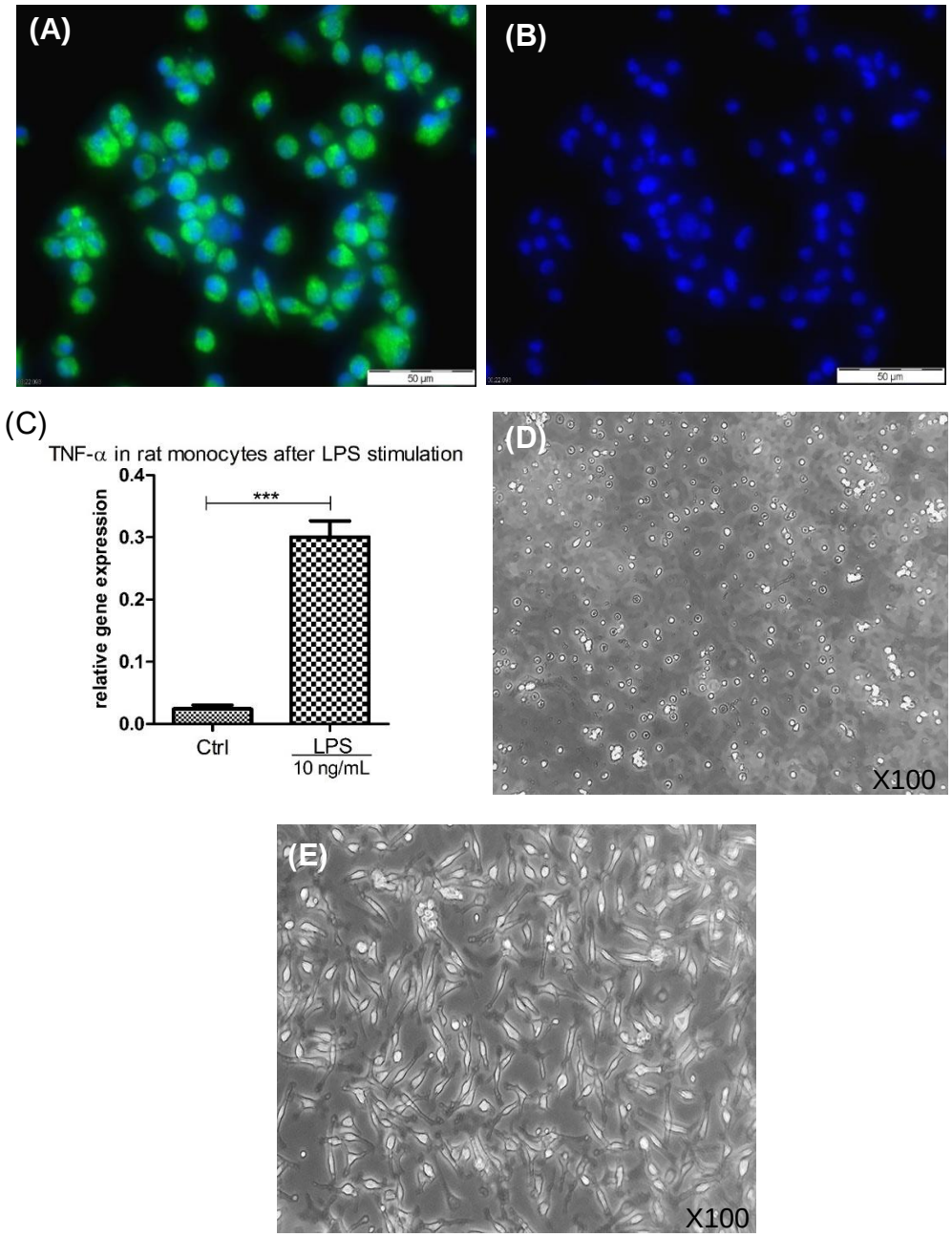

Figure 16. Morphology and characterization of RBDM with CD68 and TNF-α mRNA.

Staining of RBDM with an antibody against CD68 showed positively stained monocytes (green) in addition to very few unstained lymphocytes (only DAPI-positive) indicating that the purity of RBDM was > 95%. (A,B). Nuclei were stained with DAPI (blue in A,B). Gene expression of TNF-α was highly increased after stimulation with LPS compared to the untreated control indicating functional monocytes (C). Incubation with M-CSF showed morphological changes occurring to monocytes (D) after differentiation into M0 macrophages at day 6 (E). The M0 macrophages are bigger, more elongated and attach tightly to the plastic surface compared to monocytes (D,E). Each bar represents the mean ± SEMs of three independent experiments performed in duplicates. Tukey's multiple comparison test was used for statistical analysis; ***$p < 0.001$.

All isolation, differentiation and polarization steps are summarized in Fig. 17.

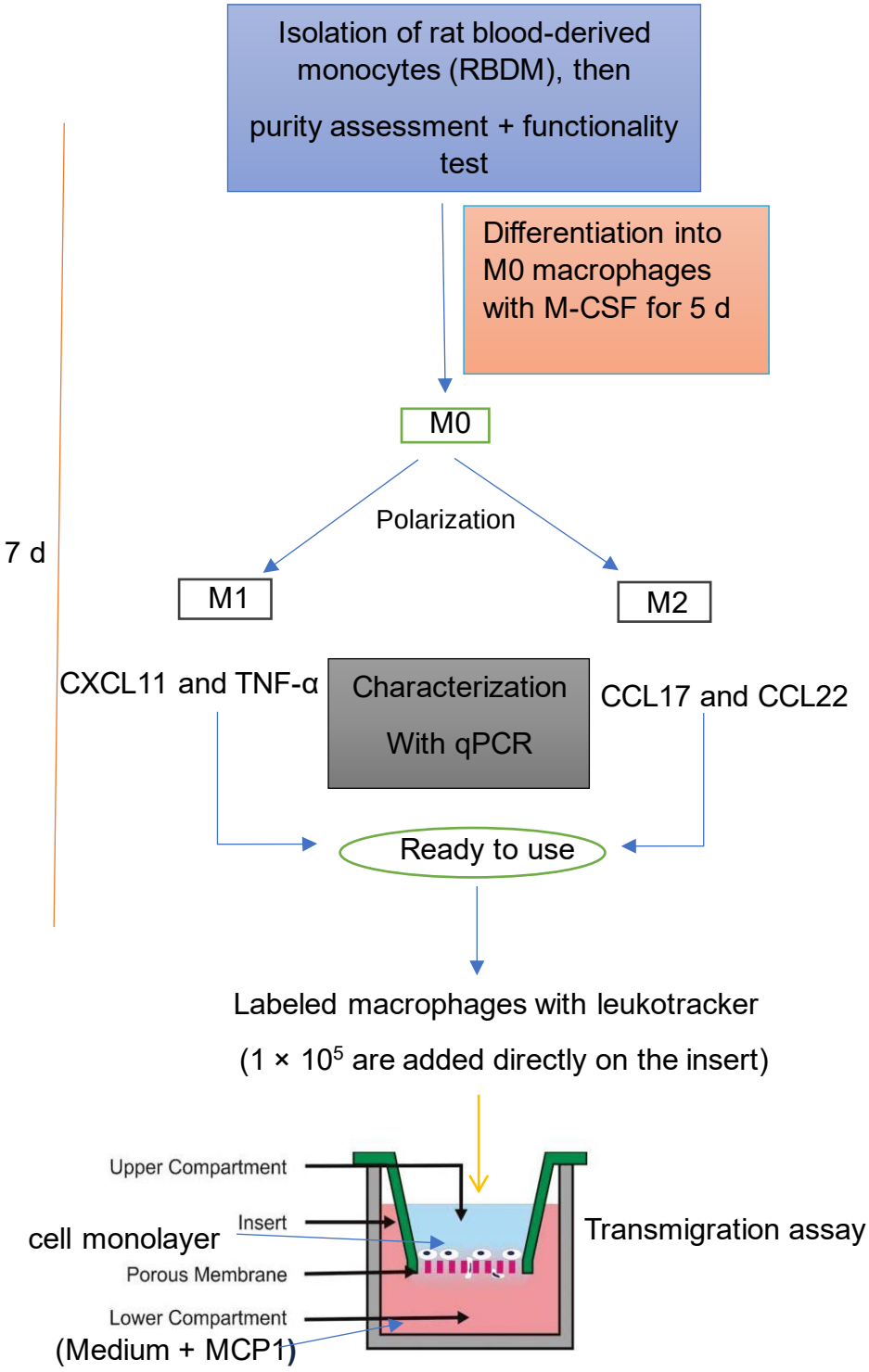

Figure 17. Overview of the isolation of RBDM, their differentiation, and polarization into M0, M1, and M2 macrophages.

The resulting macrophages were then used in a transmigration assay through a monolayer of primary adult Sertoli cells (PASC1) or co-cultures of PASC1 and PC.

3.2.2 Characterization of M0, M1, and M2 after polarization

M0 macrophages were polarized into pro-inflammatory M1 or anti-inflammatory M2 macrophages. In order to confirm the success of the polarization protocol, gene expression of M1-specific markers C-X-C motif chemokine ligand 11 (CXCL11) and TNF-α (Jaguin et al., 2013; Spiller et al., 2016), M2-specific markers CC chemokine ligand 17 (CCL17) (Spiller et al., 2016) and CC chemokine ligand 22 (CCL22) (Jaguin et al., 2013; Spiller et al., 2016) were analyzed using qRT-PCR. Both CXCL11 and TNF-α gene expression was highly and significantly increased in the pro-inflammatory M1 macrophages compared to M0 or M2 macrophages (Fig. 18A,B). In contrast, gene expression of CCL17 and CCL22 was significantly increased in the anti-inflammatory M2 macrophages compared to M0 or M1 macrophages (Fig. 18C,D).

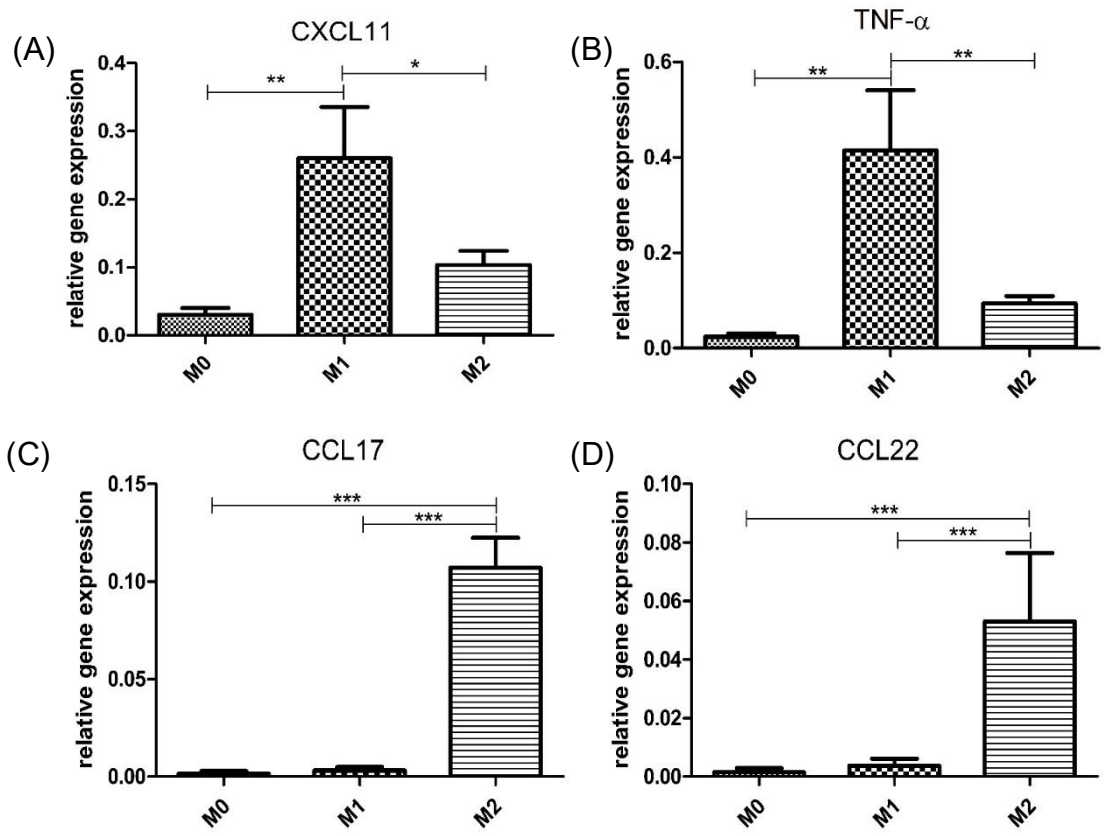

Figure 18. Expression of macrophage-specific genes after polarization analyzed with qRT-PCR.

M1 macrophages showed a stronger gene expression of CXCL11 (A) and TNF-α (B) compared to a very weak expression in M0 and M2 macrophages. In contrast, M2 macrophages showed a stronger gene expression of CCL17 (C) and CCL22 (D) compared to a very weak expression in M0 and M1 macrophages. Each bar represents the mean ± SEMs of three independent

experiments performed in duplicates. Tukey's multiple comparison test was used for statistical analysis; *p ≤ 0.05; **p < 0.01; ***p < 0.001.

3.2.3 The role of macrophage chemoattractant protein-1 (MCP1) in the transmigration assay

MCP1 is one of the chemokines produced by many cell types and it regulates migration and infiltration of monocytes (Brown et al., 1992; Sørensen et al., 2004). Thus, MCP1 was tested as a chemoattractant in the transmigration model and showed that MCP1 successfully increased the number of transmigrated macrophages through the membrane inserts in a dose-dependent manner (Fig 19).

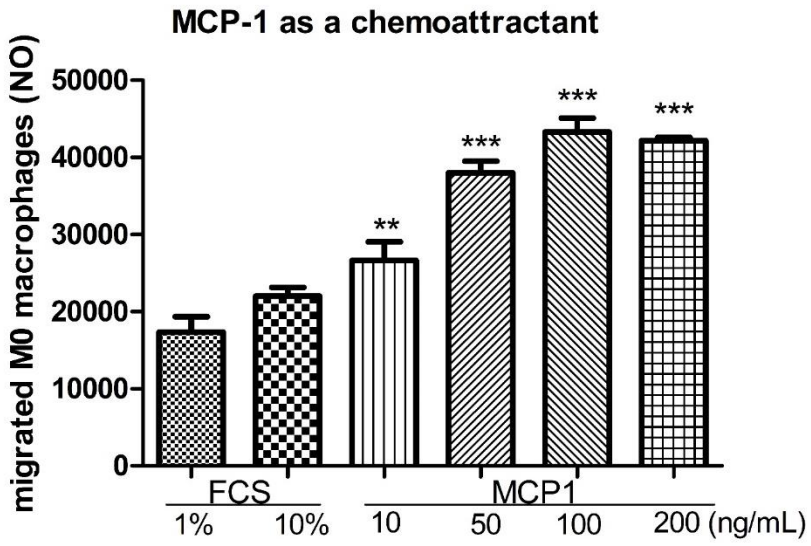

Figure 19. Concentration-dependent effects of MCP1 as macrophage chemoattractant in the transmigration assay.

A concentration of 100 ng/mL of MCP1 showed the best results regarding the number of transmigrated M0 macrophages compared to medium with 1% FCS.

3.2.4 Transmigration assay of macrophages through testicular cells

As shown in the last results, PASC1 are the main constituents of the TJ barrier in vitro. Thus, we sought to investigate the transmigration of polarized M0, M1, and M2 macrophages through a monolayer of cells consisting of PASC1 and PC, alone and together with or without matrigel (MG), to test the contribution of each cell type to the TIB in vitro.

The results showed that PC with or without MG had only a negligible effect on transmigration of macrophages M0, M1, and M2 (Fig. 20A,B). Moreover, transmigration of M2 macrophages was always significantly reduced compared to M0 and M1 macrophages in all settings (Fig. 20A,B). On the other hand, PASC1 strongly and significantly reduced transmigration of M0, M1, and M2 macrophages (Fig. 20A,B). Of note, addition of MG or PCs with or without MG did not improve the barrier generated by PASC1 alone (Fig. 20A,B).

(A)

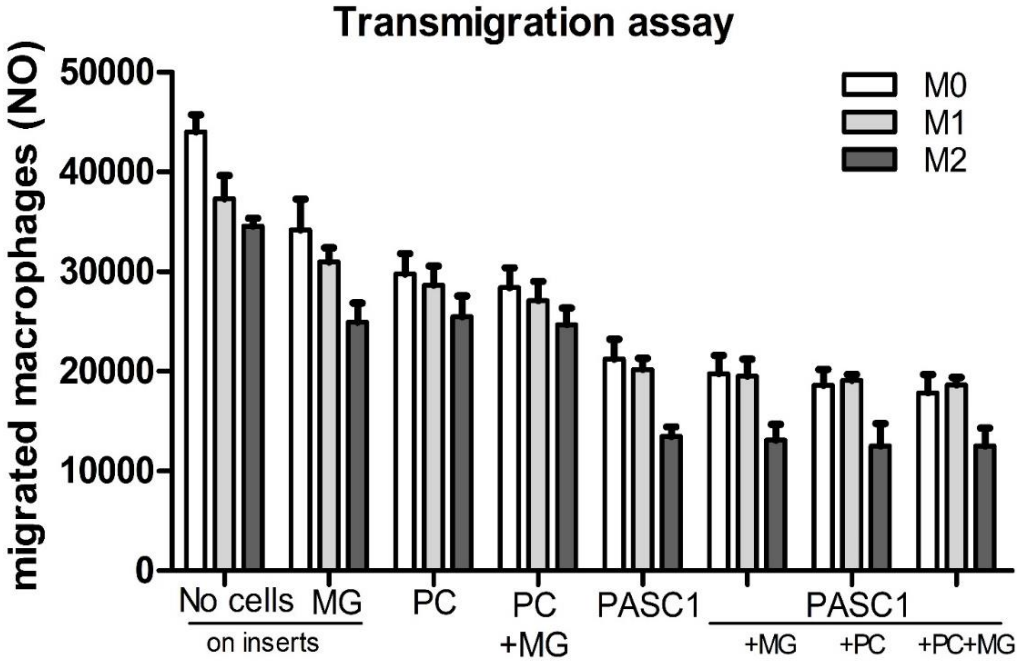

(B)

Comparison between all different setups with no cells, with PASC1, with PC, with MG, and between transmigrated macrophages

	No cells (a)	MG (b)	PC (c)	PC/MG (d)	PASC1 (e)	PASC1/MG (f)	PASC1/PC (g)	PASC1/PC/MG (h)
M0		a/b <0.0001	a/c <0.0001	a/d <0.0001	a/e <0.0001	a/f <0.0001	a/g <0.0001	a/h <0.0001
					b/e <0.001	b/f <0.0001	b/g <0.0001	b/h <0.0001
						c/f <0.01	c/g <0.001	c/h <0.001
							d/g <0.01	d/h <0.01
M1		n.s	n.s	a/d <0.01	a/e <0.0001	a/f <0.0001	a/g <0.0001	a/h <0.0001
					b/e <0.01	b/f <0.001	b/g <0.001	b/h <0.001
								c/h <0.01
M2		n.s	n.s	a/d <0.01	a/e <0.0001	a/f <0.0001	a/g <0.0001	a/h <0.0001
					b/e <0.001	b/f <0.001	b/g <0.001	b/h <0.001
					c/e <0.001	c/f <0.001	c/g <0.001	c/h <0.01
						d/f <0.001	d/g <0.001	d/h <0.001
	No cells	**MG**	**PC**	**PC/MG**	**PASC1**	**PASC1/MG**	**PASC1/PC**	**PASC1/PC/MG**
	M0/M2 <0.01	M0/M2 <0.01	M0/M2 <0.01	M0/M2 <0.01	M0/M2 <0.01	M0/M2 <0.001	M0/M2 <0.001	M0/M2 <0.001
	M1/M2 <0.01				M1/M2 <0.01	M1/M2 <0.01	M1/M2 <0.01	M1/M2 <0.01

PC, peritubular cells; MG, matrigel. The statistical test of Tukey was used.

Figure 20. Transmigration of macrophages M0, M1 and M2 through a barrier of PASC1 or PC, alone or both with or without matrigel (MG).

(A) The numbers of transmigrated M0, M1, and M2 macrophages showed that more M0 and M1 macrophages transmigrated through the PASC1 monolayer compared to M2 macrophages. The influence of PC with or without MG on transmigration was negligible. In contrast, PASC1 demonstrated the highest reduction on transmigration of all macrophage types. Co-culturing of PASC1 with PC with or without MG did not further improve the PASC1 barrier. Each bar represents the means ± SEMs of three independent experiments performed in duplicates. (B) Statistical analysis for Fig. 20A showed significance in reducing the numbers of transmigrated macrophages when PASC1 was part of the cell layer. On the other hand, no significance was shown while using PC, MG or both as a part of the cell layer.

3.2.5 Influence of cytokines on macrophage transmigration through the testicular barrier formed between PASC1

T, IL-6 and TNF-α have different impacts on the SC barrier (Li et al., 2006; Zhang et al., 2014; Kabbesh et al., 2021). Thus, we aimed to elucidate the impacts of these cytokines on the number of transmigrated macrophages. Compared to the untreated controls, T significantly increased the TER values, in contrast, IL-6 and TNF-α decreased the TER values (Fig. 21A,B). Moreover, the number of the transmigrated M0, M1, and M2 macrophages was clearly decreased through T-treated PASC1 cells (Fig. 21C,D). On the other hand, the number of transmigrated M0, M1, and M2 macrophages was highly increased after treatment with IL-6 or TNF-α (Fig. 21C,D) which correlated well with the decreased TER values (Fig. 21A,B). In all settings, significantly less M2 macrophages transmigrated through the PASC1 barrier (Fig. 21C,D).

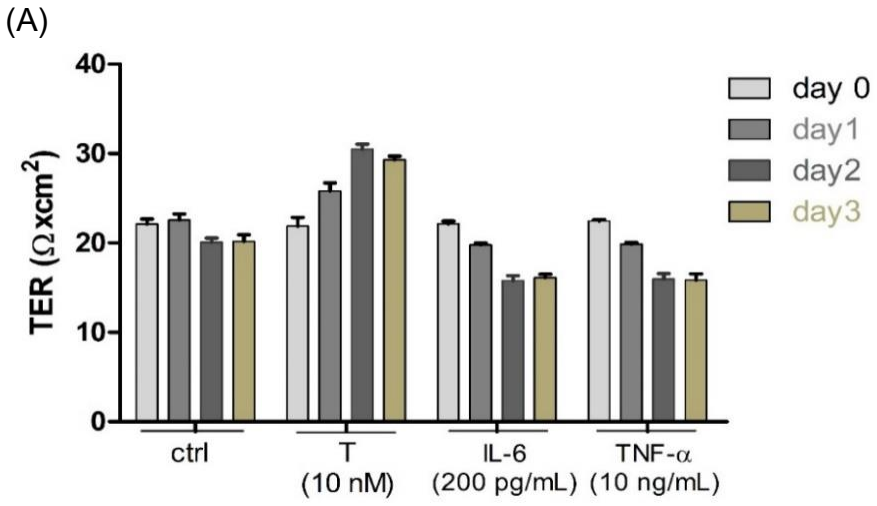

(B)

Comparison between control and all treatments and between all days of the treatments

Treatments	ctrl (a)	T (b)	IL-6 (c)	TNF-α (d)		
day0		n.s	n.s	n.s		
day1		a/b <0.001	n.s	n.s		
day2		a/b <0.0001	a/c <0.001	a/d <0.001		
day3		a/b <0.0001	a/c <0.0001	a/d <0.001		
days	**d0/d1**	**d0/d2**	**d0/d3**	**d1/d2**	**d1/d3**	**d2/d3**
ctrl	n.s	n.s	n.s	n.s	n.s	n.s
T	<0.001	<0.0001	<0.0001	n.s	<0.01	n.s
IL-6	n.s	<0.0001	<0.0001	<0.001	<0.001	n.s
TNF-α	n.s	<0.0001	<0.0001	<0.001	<0.001	n.s

Ctrl, control; T, testosterone; d, day. Comparison was done with the Tukey test.

(C)

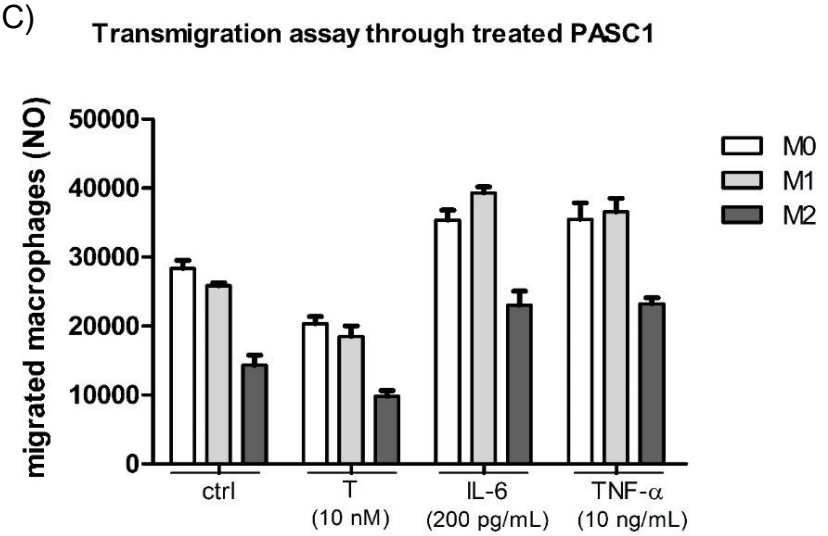

(D)

Comparison between ctrl and all treatments and between transmigrated macrophages in each treatment

Treatment	ctrl (a)	T (b)	IL-6 (c)	TNF-α (d)
M0		a/b < 0.01	a/c < 0.01	a/d < 0.01
M1		a/b < 0.01	a/c < 0.0001	a/d < 0.001
M2		a/b < 0.0001	a/c < 0.01	a/d < 0.001
Macrophages	**M0/M1**	**M0/M2**	**M1/M2**	
ctrl	n.s	< 0.0001	< 0.0001	
T	n.s	< 0.001	< 0.01	
IL-6	n.s	< 0.0001	< 0.0001	
TNF-α	n.s	< 0.0001	< 0.0001	

Ctrl, control; T, testosterone. Comparison was done with the Tukey test.

Figure 21. Characterization of PASC1 transmigration after treatment with different cytokines.

Treating PASC1 with T increased the TER values time-dependently on days 1-3 compared to the untreated controls. Treatment of a confluent monolayer of PASC1 with IL-6 or TNF-α decreased TER values time-dependently on days 1-3 compared to the untreated controls (A). T significantly increased the TER values specially in day 2,3, (A) whereas IL-6 or TNF-α significantly decreased TER values compared to day 0 or to the control (B). As shown in the controls (ctrl) and treatments more M0 and M1 macrophages significantly transmigrated compared to M2 macrophages (C). Each bar represents the mean ± SEMs of three independent experiments performed in duplicates. Statistical analysis for Fig. 21C is given in Fig. 21D and showed significance in reducing the numbers of transmigrated macrophages after T treatment, whereas IL-6 and or TNF-α significantly increased the transmigrated macrophages through PASC1. Moreover, significantly less M2 macrophages transmigrated compared to M0 or M1 (D).

3.3 Contribution of the classical AR or Zrt- and Irt-like protein 9 ZIP9 on TJ formation between PASC1 cells

As recently published, ZIP9 and not the AR mediated T signaling in the immature rat Sertoli cell line 93RS2 in vitro, in terms of phosphorylation of transcription factors (cAMP response element-binding protein (CREB), extracellular signal-regulated kinases1/2 (Erk1/2) and Activating transcription factors-1 (ATF-1)), and upregulation of the tight junction proteins ZO-1, Cldn-1 and -5 (Möller et al., 2021). In the presented study, T had positive effects on the integrity of the TJ barrier of PASC1 and on the expression of the tight junction proteins JAM3 and ZO-1. This is why we sought to investigate which of the both receptors, AR or ZIP9, is mediating signaling of T in PASC1.

3.3.1 Silencing AR or ZIP9 expression by siRNA to investigate their role in androgen signaling

It was required to specifically mute the expression of both androgen receptors in order to determine whether either one might have contributed in the studies that followed. As Fig. 22A shows, the expression of AR-specific mRNA and protein expression was greatly suppressed by AR-siRNA (Fig. 22B,C). ZIP9-directed siRNA was similarly successful in preventing expression of ZIP9-mRNA (Fig. 23A) or protein (Fig. 23B,C).

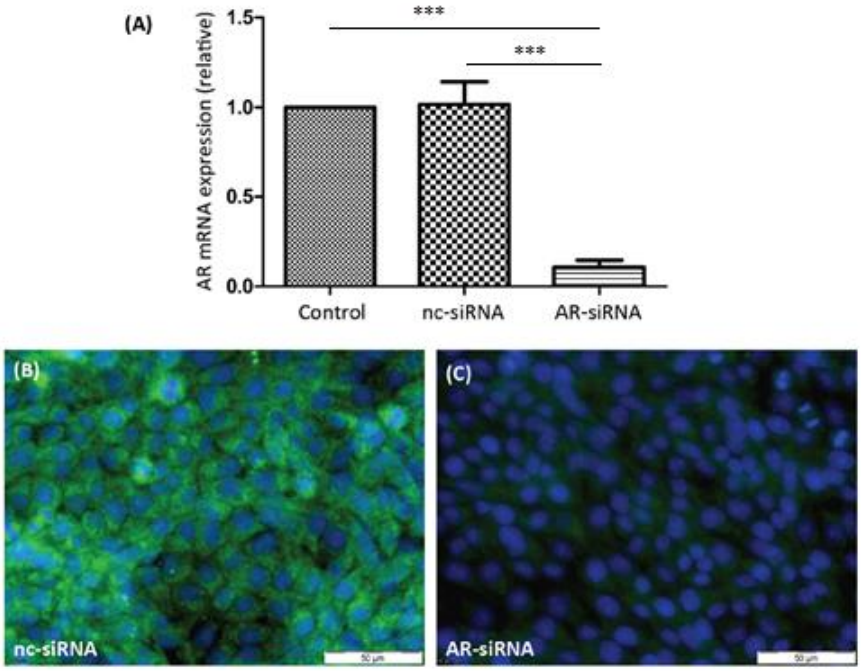

Figure 22. Detection of AR mRNA or protein in PASC1 cells.

Cells were treated with either nc-siRNA or AR-siRNA. (A) qRT-PCR showed expression of AR-specific mRNA. (B) Detection of AR protein by immunofluorescence before and (C) after silencing AR-specific mRNA expression. Green fluorescence corresponds to AR and nuclei are stained blue. Each bar represents the means ± SEMs of three independent experiments performed in duplicates. Tukey's multiple comparison test was used for statistical analysis; ***p < 0.001.

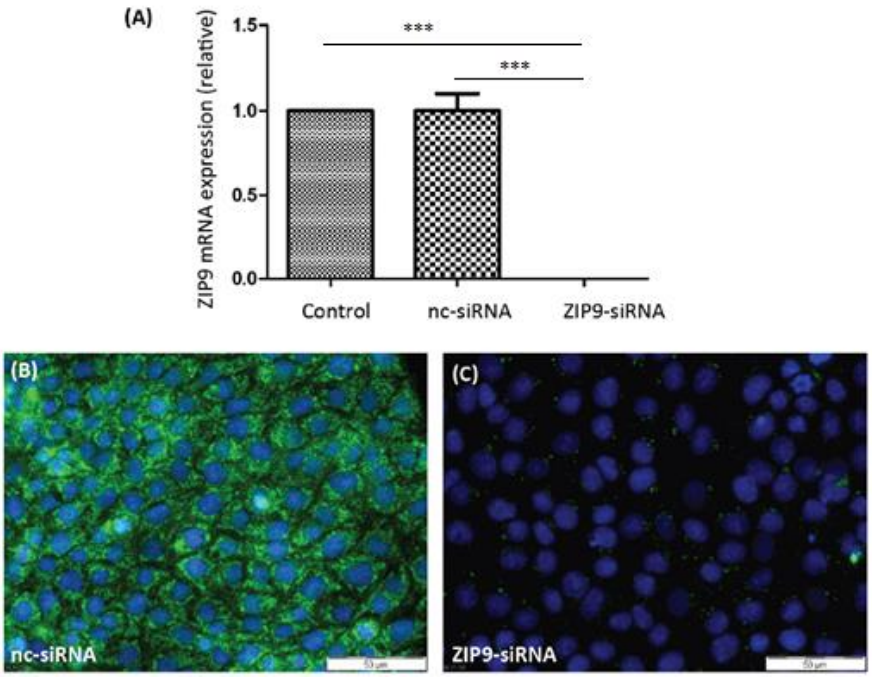

Figure 23. Detection of ZIP9 mRNA or protein in PASC1 cells.

Cells were treated with either nc-siRNA or ZIP9-siRNA. (A) qRT-PCR showed expression of ZIP9-specific mRNA/cDNA. (B) Detection of ZIP9 protein by immunofluorescence before and (C) after silencing ZIP9-specific mRNA expression. Green fluorescence corresponds to ZIP9 and nuclei are stained blue. Each bar represents the means ± SEMs of three independent experiments performed in duplicates. Tukey's multiple comparison test was used for statistical analysis; ***$p < 0.001$.

3.3.2 Investigation of the responsiveness of the PASC1 AR towards T or towards the ZIP9-targeting androgenic tetrapeptide IAPG

According to recent reports, the traditional AR is a transcription factor that responds to testosterone (T) or dihydrotestosterone (DHT) by dimerization and translocation from the cytosol to the nucleus, where gene expression is regulated (Zhou, 2010; Davey & Grossmann, 2016). In order to confirm that the AR of PASC1 is responsive to T and does not interact with the ZIP9-targeting IAPG peptide, we therefore focused on the ability of the AR of PASC1 to translocate into the nucleus in response to T or IAPG treatment.

As seen in Fig. 24A, in untreated PASC1, green fluorescence-stained AR was found in the cytoplasm and partially within the nucleus. The AR of PASC1 is responsive, as evidenced by the localization of all green fluorescence within the nuclei after T exposure (Fig. 24B). When PASC1 was treated with IAPG, AR translocation was not observed (Fig. 24C), despite the peptide being employed at a 1000-fold higher concentration (10 M) than T (10 nM).

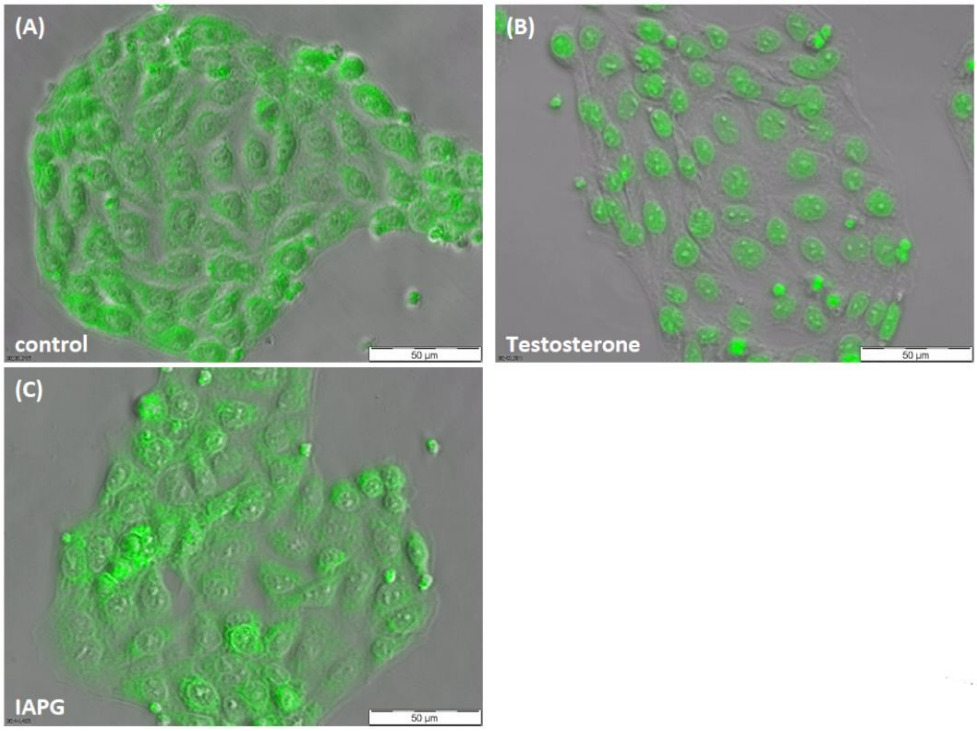

Figure 24. Localization of AR in PASC1 cells with T or IAPG treatment.

Cells were treated with T or IAPG for 2 hrs. (A) AR (green) was distributed in the cytoplasm and in the nuclei in the untreated control. (B) After exposure to 10 nM T, AR translocated into the nuclei. (C) There was no change in AR localization with 10 µM IAPG.

3.3.3 Binding of the IAPG peptide or of T to the androgen binding site of ZIP9

The fluorescent T analogue testosterone-BSA-FITC (T-BSA-FITC) is frequently employed to identify membrane-bound T receptors with an extracellular androgen binding site (Benten et al., 1999; Bulldan et al., 2017; Malviya et al., 2021). Prior studies using labeling of the ZIP9 androgen binding site in 93RS2 and L6 myoblasts demonstrated that this binding can be blocked by either T or by certain tetrapeptides like IAPG that are modeled to fit the ZIP9 androgen binding site (Bulldan et al., 2017 ; Möller et al., 2021).

As Fig. 24A shows, T-BSA-FITC labeled the surface of the adult rat Sertoli cells PASC1. The labeling corresponds to the binding of the T moiety of T-BSA-FITC, because the BSA-FITC compound as a negative control fails to label the membrane structure since it lacks T (Fig. 25B). Silencing of ZIP9 revealed the presence of an extracellularly accessible androgen binding site, because T-BSA-FITC binding is prevented (Fig. 25C).

We could also show that both, IAPG and T, can specifically interact with membrane-bound ZIP9 of PASC1 and displace T-BSA-FITC from its androgen binding site (Fig. 25D,E). The quantification of the bound compounds based on green fluorescence is summarized in Fig. 25F.

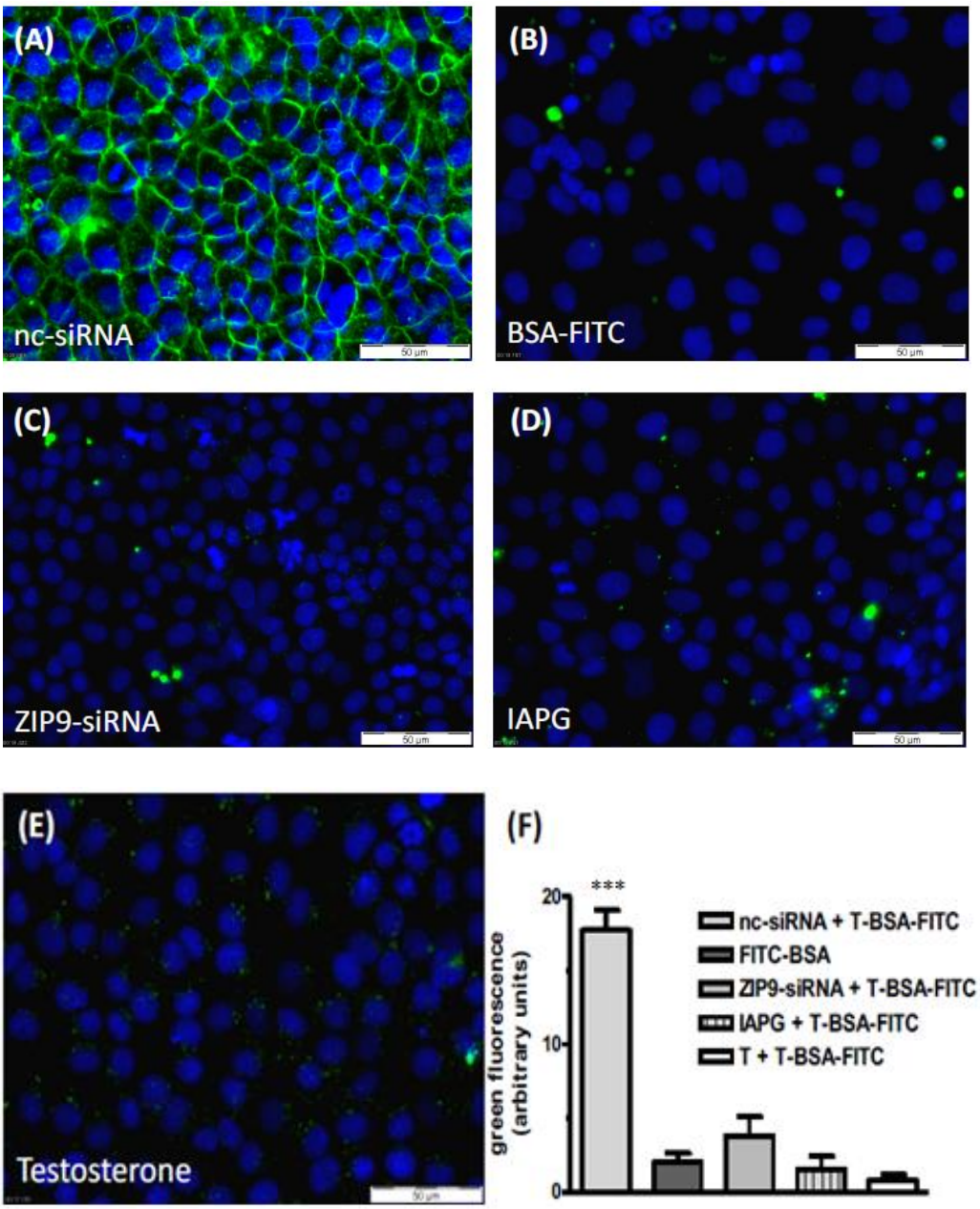

Figure 25. Testosterone-BSA-FITC (T-BSA-FITC) membrane labeling of PASC1 cells.

T-BSA-FITC or BSA-FITC are visualized as green fluorescence and nuclei are stained blue. (A) T-BSA-FITC labeled membranes of cells treated with nc-RNA. (B) BSA-FITC lacking the T moiety did not stain the membranes. (C) There was also no staining after ZIP9 knockdown. (D) IAPG (10 µM) or (E) T (10 nM) prevented membrane labeling by T-BSA-FITC. (F)

Statistical analysis of green fluorescence shown in panels A-E (n = 3 × 25; means ± SEM; *** $p < 0.001$).

3.3.4 Stimulation of Erk1/2 phosphorylation by T or IAPG

One of the important elements of the non-classical signaling pathway of T is the activation by phosphorylation of Erk1/2 (Shihan et al., 2014; 2015). It has been recently reported (Möller et al., 2021), that T stimulated phosphorylation of Erk1/2 with an EC50=0.411 ± 1.54 nM in the Sertoli cell line 93RS2 which is lacking the classical AR. The IAPG peptide stimulated phosphorylation of Erk1/2 with an EC50=1.39 ± 1.36 µM. The maximum of Erk1/2 phosphorylation was noted at 10 nM T or 10 µM IAPG.

This is why we sought to address T and IAPG impacts on Erk1/2 also in the adult rat Sertoli cells PASC1 and to compare it with the immature rat Sertoli cell line 93RS2. As presented in Fig. 26A,B, T or IAPG do not affect expression of Erk1/2 total protein, but on the other hand, they stimulate within 30 min Erk1/2 phosphorylation in a concentration-dependent manner. The EC50 values are 0.35 ± 1.29 nM for T and 1.02 ± 1.36 µM for IAPG (Fig. 26C,D), which are similar values obtained for Erk1/2 phosphorylation in the rat Sertoli cell line 93RS2. The same was also noticed regarding the concentrations needed for maximum stimulation of Erk1/2 phosphorylation which here was also achieved by either 10 nM T or 10 µM IAPG (Fig. 26). Thus, all further experiments were carried out by these concentrations of T or IAPG.

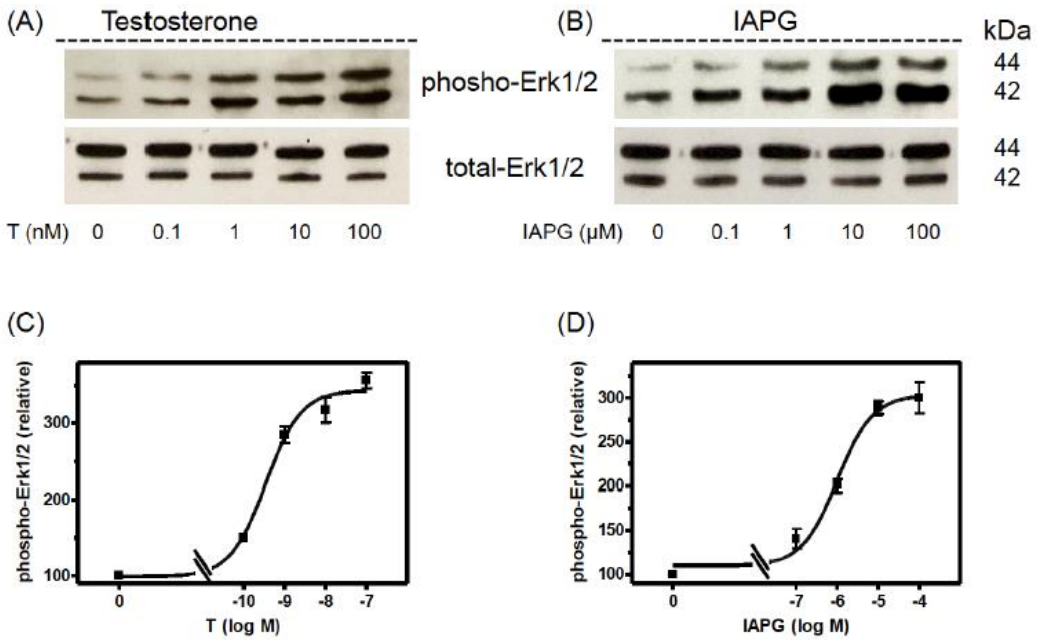

Figure 26. Western blot analysis of phospho-Erk1/2 after stimulation of PASC1 cells with various concentrations of T or IAPG for 24 hrs.

(A) Phospho-Erk1/2 detection after stimulation with T, and (B) after stimulation with IAPG. In (A) and (B) the total amount of Erk1/2 was not affected. (C) Semi-logarithmic plot of relative p-Erk1/2 signals revealed for T an EC50 of 0.35 ± 1.29 nM, and (D) for IAPG an EC50 of 1.02 ± 1.36 µM. For each diagram: n = 3; means ± SEM.

3.3.5 Identification of the receptor for androgen involved in Erk1/2 phosphorylation

In the next experiments, we wanted to test the possible participation of AR or ZIP9 in Erk1/2 stimulation in PASC1 after selectively silencing AR or ZIP9 expression by siRNAs. PASC1 that had received only nc-siRNA served as a control and demonstrated only a weaker staining of phosphorylated Erk1/2 (Fig. 27A) compared to the cells that received T (Fig. 27B) or IAPG (Fig. 27C). Silencing AR expression resulted in similar results: control cells displayed a weak signal of green fluorescence (Fig. 27D), whereas cells exposed to T (Fig. 27E) or IAPG (Fig. 27F) demonstrated stronger phosphorylation of Erk1/2. Moreover, the stimulatory effects of either T or IAPG on Erk1/2 phosphorylation in the presence of either nc-siRNA or AR-siRNA did not show remarkable differences from each other (Fig. 27J).

In contrast, silencing of ZIP9 expression entirely inhibited stimulation of Erk1/2 phosphorylation by T or IAPG. In the absence of either of the two substances (Fig. 27G) green fluorescence corresponding to p-Erk1/2 is on the basal level (Fig. 27A,D) and remained on that level regardless of treatment with either T (Fig. 27H) or IAPG (Fig. 27I).

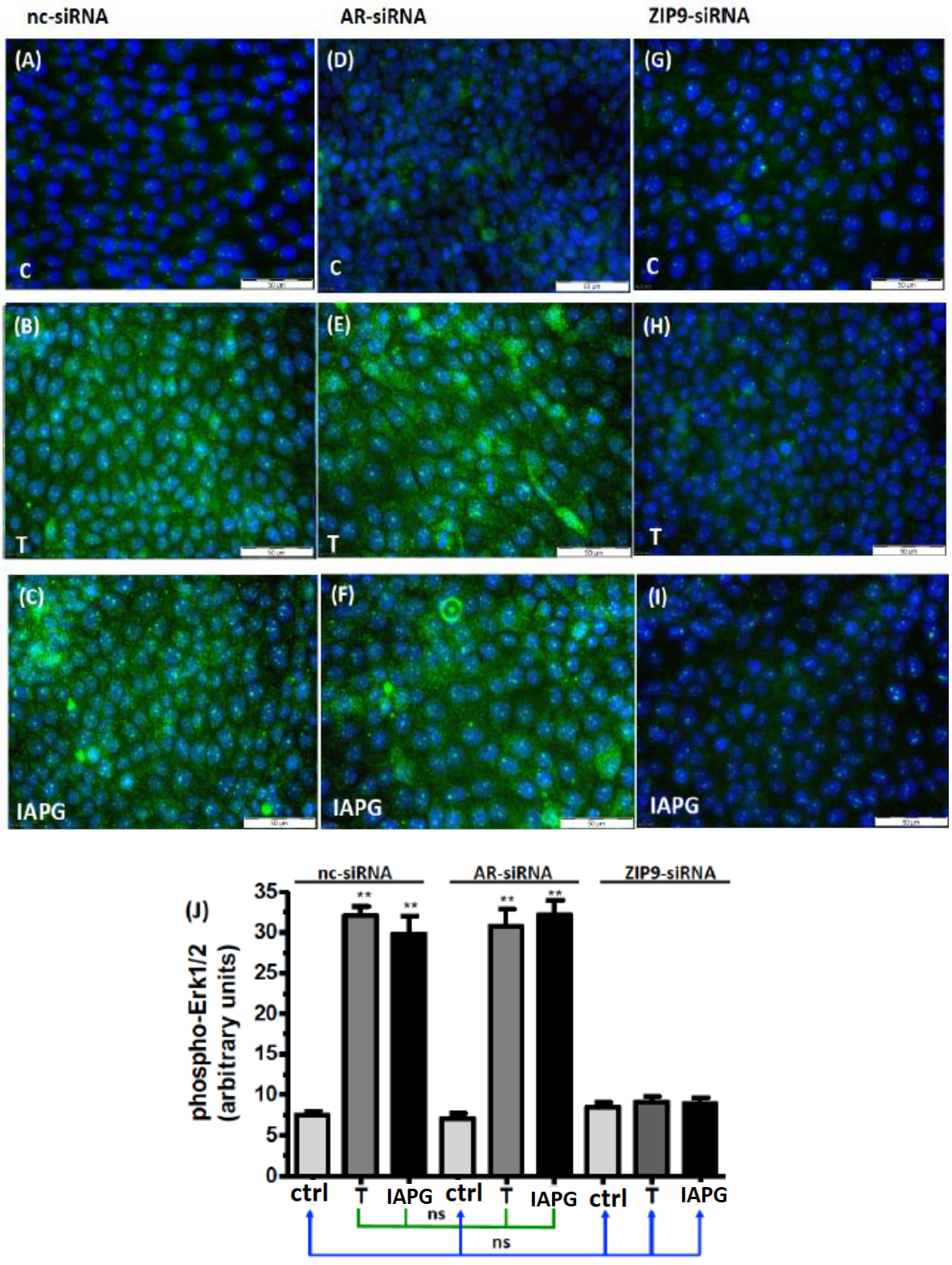

Figure 27. Immunofluorescence of phospho-Erk1/2 in PASC1 cells.

Incubation with vehicle (ctrl), 10 nM T, or 10 µM IAPG was carried out for 24 hrs. Nuclei are stained blue, and phospho-Erk1/2 is represented by green fluorescence. (A,B,C) Phospho-Erk1/2 in cells treated with nc-siRNA; (D,E,F) phospho-Erk1/2 in cells treated with AR-siRNA;

(G,H,I) phospho-Erk1/2 in cells treated with ZIP9-siRNA. (J) Statistical analysis of green fluorescence is shown in panel J for A-I (n = 3 × 25; means ± SEM; ** $p < 0.01$; ns = not significant).

3.3.6 Involvement of AR or ZIP9 in stimulation of CREB/ATF-1 phosphorylation by T or IAPG

Phosphorylation of the transcription factors CREB and ATF-1 is considered a trigger of the downstream non-classical signaling pathway of T (Cheng et al., 2007; Bulldan et al., 2016; Möller et al., 2021). It has been reported that the phosphorylation domains of CREB and ATF-1 are very similar, this is why, the antibody commonly used to detect them does not distinguish between them (Wen-Hua & Quirion, 2006; Möller et al., 2021).

PASC1 treated with nc-siRNA showed only a faint staining of CREB/ATF-1 phosphorylation, whereas T and IAPG stimulated CREB/ATF-1 phosphorylation in PASC1 (Fig. 28A-C). Similarly, PASC1 treated with AR-siRNA remained responsive to T- or IAPG-induced phosphorylation of CREB/ATF-1 (Fig. 28D-F) to the same extent as cells treated with nc-siRNA (Fig. 28J). However, T and IAPG failed to stimulate phosphorylation of CREB/ATF-1 in PASC1 treated with ZIP9-siRNA (Fig. 28G-I).

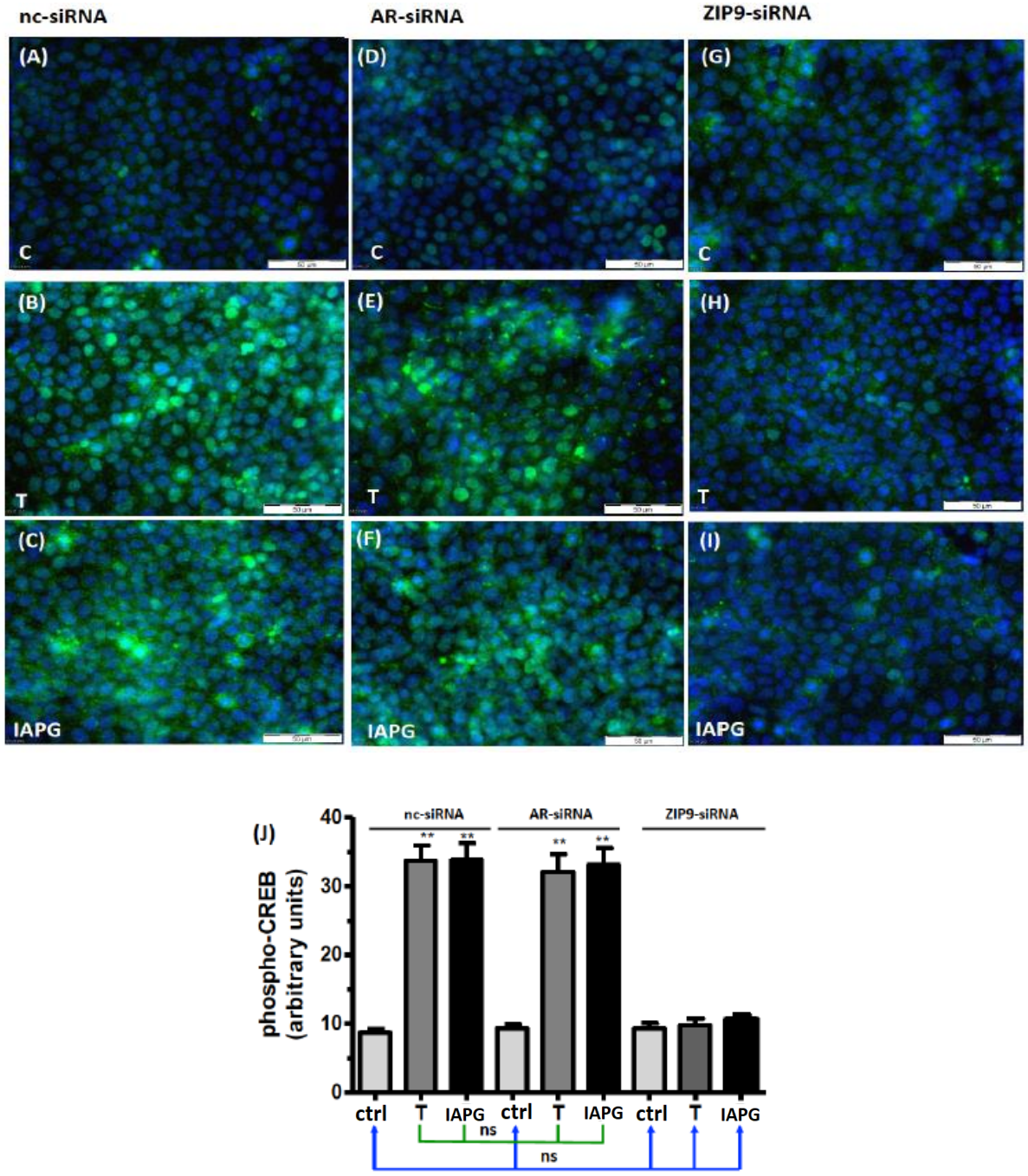

Figure 28. Immunofluorescence of p-CREB/p-ATF-1.

Incubation with vehicle (ctrl), 10 nM T, or 10 µM IAPG was carried out for 24 hrs. Nuclei are stained blue, and p-CREB/ATF-1 is green. (A,B,C) p-CREB/p-ATF-1 in cells treated with nc-siRNA. (D,E,F) p-CREB/p-ATF-1 in cells treated with AR-siRNA. (G,H,I) p-CREB/p-ATF-1 in cells treated with ZIP9-siRNA. (J) Quantification and statistical analysis of green fluorescence (n = 3 × 25; means ± SEM; ** $p < 0.05$; ns = not significant). Theses results go along with the results obtained in Fig.227.

3.3.7 Involvement of AR or ZiP9 in stimulation of ZO-1 expression by T or IAPG

ZO-1 is one of the tight junction proteins that interacts with other TJ-forming proteins like occludin, JAM, or claudins and links these with actin to the cytoskeleton (Stevenson et al., 1986; Ahn et al., 2016).

PASC1 cells incubated with nc-siRNA showed moderate to faint green fluorescence of ZO-1 on the cell membrane (Fig. 29A). The ZO-1 signal was much stronger in cells treated with T (Fig. 29B) or with IAPG (Fig. 29C), demonstrating that both compounds stimulated ZO-1 expression. Stimulation of ZO-1 was observed when cells were treated with AR-siRNA prior to their exposure to either T or IAPG (Fig. 29D-F). In contrast, the levels of ZO-1 fluorescence stimulated by T and IAPG in PASC1 cells were not significantly different from the non-treated ZIP9-siRNA PASC1 cells (Fig. 29G-J). The same applies for control cells treated with nc-siRNA or AR-siRNA and all ZIP9-siRNA-treated cells (Fig. 29J).

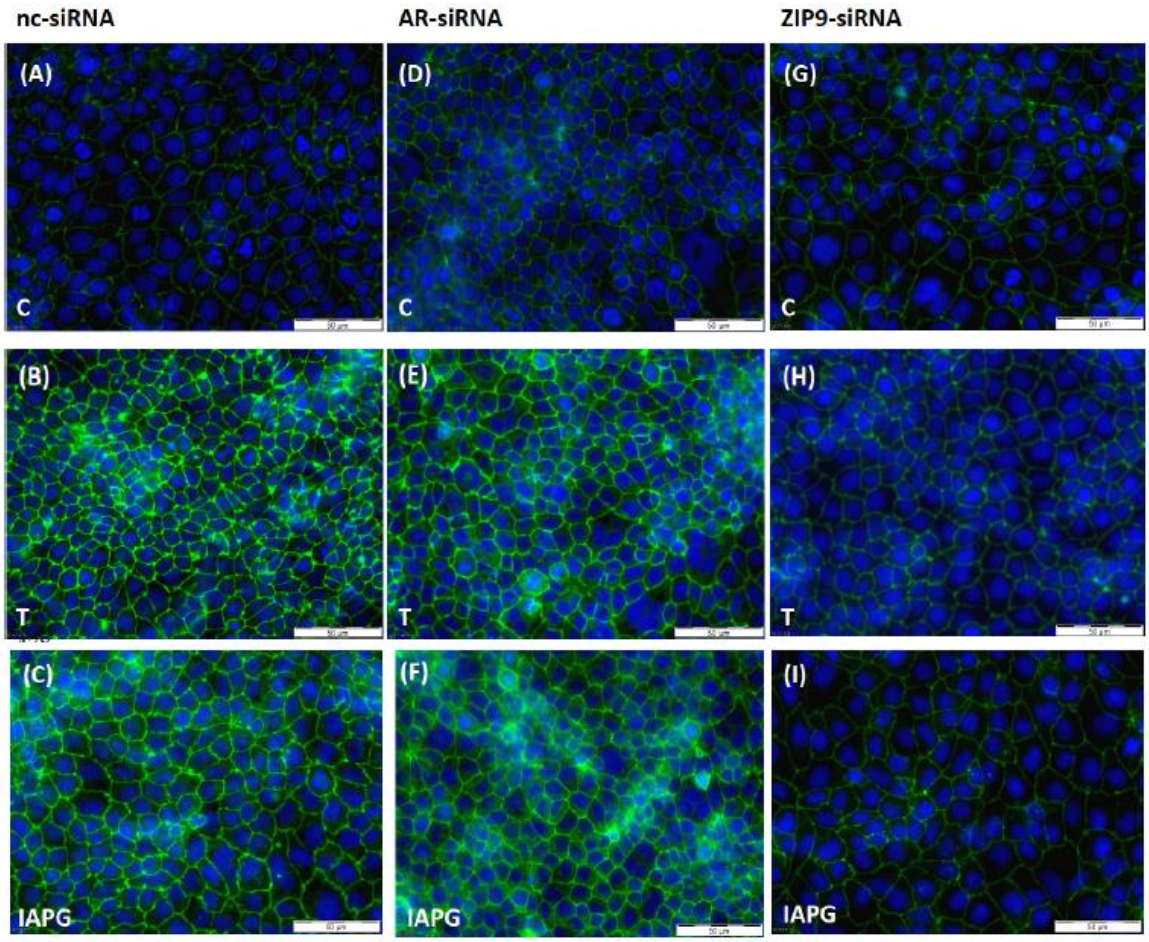

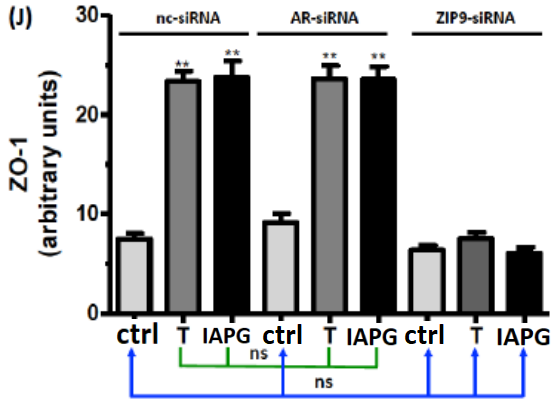

Figure 29. Immunofluorescence of ZO-1 expression in PASC1.

Cells were treated with vehicle (ctrl), 10 nM T, or 10 µM IAPG for 24 hrs. Nuclei are shown as blue, and ZO-1 in green. (A,B,C) ZO-1 in cells treated with nc-siRNA. (D,E,F) ZO-1 in cells treated with AR-siRNA. (G,H,I) ZO-1 in cells treated with ZIP9-siRNA. PASC1 stimulation with T or IAPG increased expression of ZO-1 (B,C) compared to contrl (A). This increase in ZO-1 expression was consistent after pre-treatment with AR si-RNA (E,F) compared to ctrl AR si-RNA (D) but it was not shown after ZIP9 si-RNA pre-treatment (G,H,I) . (J) Statistical analysis of green fluorescence shown in panels A-I (n = 3 × 25 cells TJ ; means ± SEM; ** $p < 0.01$; ns = not significant).

3.3.8 Participation of AR or ZIP9 in stimulation of Cldn-1 and JAM-3 expression by T or IAPG

Claudin-1 (Cldn-1) and JAM-3 are tight junctions expressed in the seminiferous tubule epithelia and are androgen dependent (Gye, 2003; Lui & Cheng, 2012; De Gendt et al., 2014; Bulldan et al., 2016; Möller et al., 2021). Both proteins interact with ZO-1 and contribute to the formation of TJ and the tightening of the BTB. T and IAPG stimulated expression of Cldn-1 in cells that had been treated with either nc-siRNA (Fig. 30A-C) or AR-siRNA (Fig. 30D-F), but failed to do so in cells where ZIP9 expression had been knocked down by ZIP9-siRNA (Fig. 30G-I).

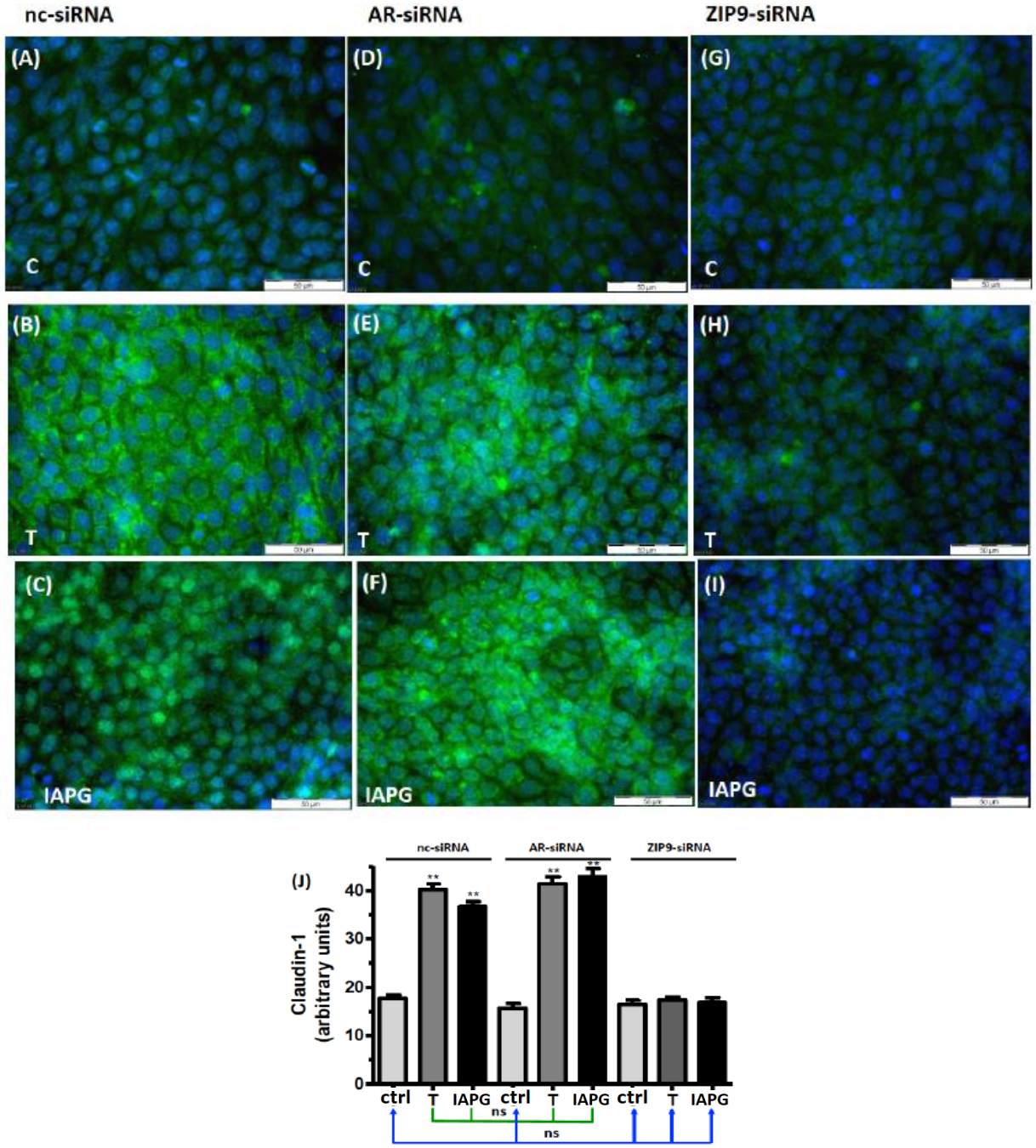

Figure 30. Detection of Cldn-1 by immunofluorescence.

Incubation with vehicle (ctrl), 10 nM T, or 10 µM IAPG was carried out for 24 hrs. Nuclei are stained as blue and Cldn-1 as green. (A,B,C) Cldn-1 in cells treated with nc-siRNA. (D,E,F) Cldn-1 in cells treated with AR-siRNA. (G,H,I) Cldn-1 in cells treated with ZIP9-siRNA. (J) Statistical analysis of green fluorescence shown in panels A-I (n = 3 × 25; means ± SEM; ** $p < 0.01$; ns = not significant).

The basal weak mRNA expression of JAM-3 in PASC1 cells treated with nc-siRNA, AR-siRNA, or ZIP9-siRNA (Fig. 31) was increased by T and IAPG only in cells that had been treated with nc-siRNA or AR-siRNA (Fig. 31). In cells that had been incubated with ZIP9-siRNA, JAM-3 mRNA expression remained at basal levels after IAPG or T treatment, like that observed in controls (Fig. 31).

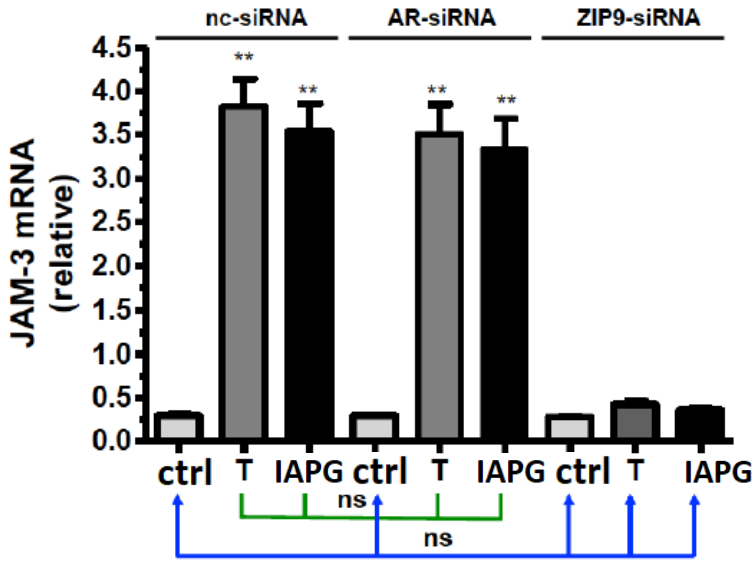

Figure 31. Detection of JAM-3-specific mRNA by qRT-PCR.

PASC1 cells were treated with nc-siRNA, AR-siRNA, or ZIP9-siRNA and afterwards incubated for 24 hrs with vehicle (ctrl), 10 nM T, or 10 µM IAPG. For each data point: n = 3 × 2; means ± SEM; ** $p < 0.01$; ns = not significant.

3.3.9 Investigation of the involvement of AR or ZIP9 in T- or lAPG-induced TJ formation

From the last results, we concluded that ZIP9 is significantly involved in the formation of the TJ barrier between Sertoli cells. TER measurements conducted over several days were consistent with this conclusion. T or IAPG stimulated PASC1 cells treated with nc-siRNA formed tighter TJs than the controls already after 1 day of treatment, as demonstrated by increased TER values (Fig. 32A). T and IAPG had the same effect on cells treated with AR-siRNA to knock down AR expression (Fig. 32B).

When ZIP9 expression was knocked down by ZIP9-siRNA, T and IAPG failed to stimulate TJ formation between the PASC1 cells (Fig. 32C).

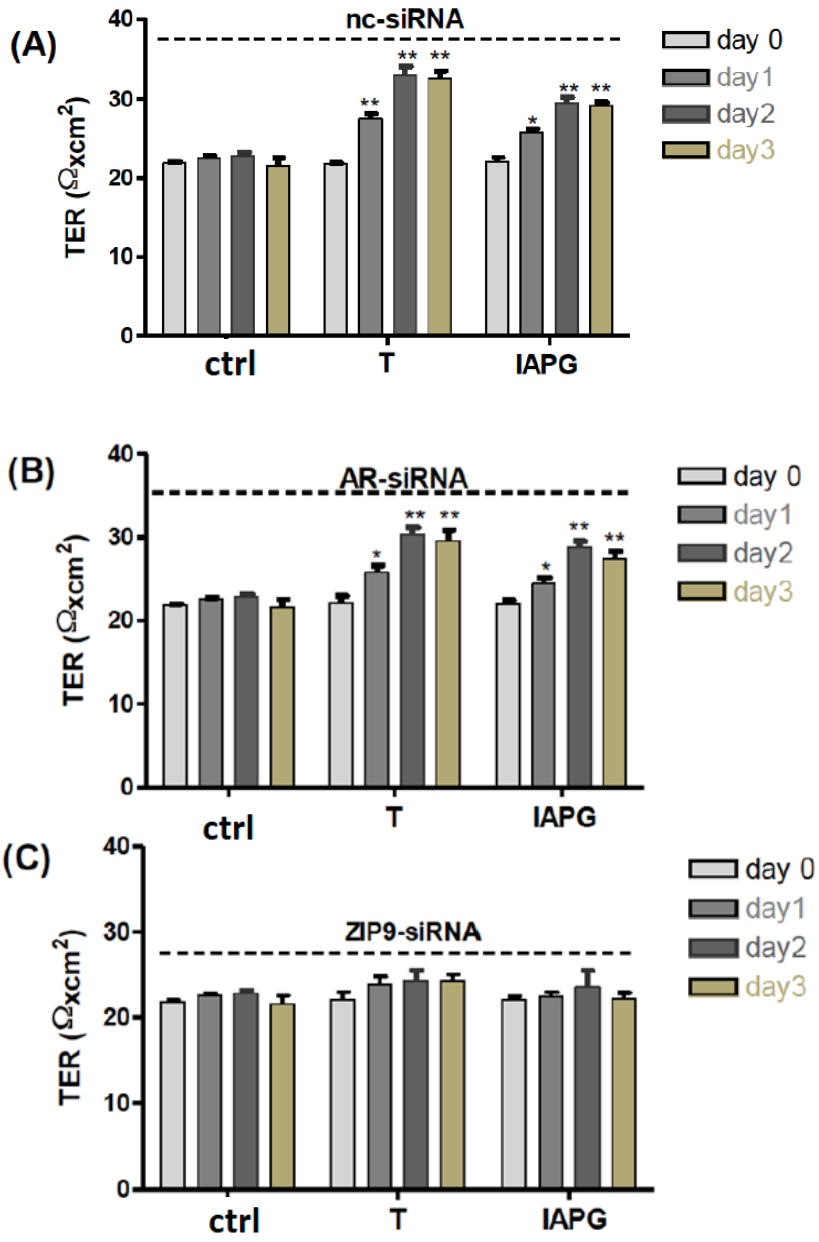

Figure 32. Transepithelial electrical resistance (TER) across adult Sertoli cell layers.

The PASC1 cells were treated with either nc-siRNA (A), AR-siRNA (B), or ZIP9-siRNA (C) before being exposed to vehicle (ctrl), 10 nM T, or 10 µM or IAPG. Measurements of TER were taken after 0, 24, 48, and 72 hrs. For each data point: n = 6; means ± SEM; * $p \leq 0.05$; ** $p < 0.01$.

4 Discussion

Studying SC has been mainly focused on understanding the role of SCs through different stages of prepubertal testis development (Chang et al., 2011; Mruk & Cheng, 2015). However, the functions of adult SC during sperm production after puberty or in sustaining the immune privileged environment have not been yet significantly addressed. The main reason is the difficulty of isolation and long-term propagation of primary adult SCs long enough to perform the required experiments. Moreover, very few protocols to isolate adult SCs have been published with limited success (Anway et al., 2003). In the present study, we established a fast and consistent new protocol for isolation and long-term maintenance of adult rat SCs based upon conditional reprogramming (Liu et al., 2012; 2017). We investigated the formation of tight junctions between adult SCs by testing its integrity and by elucidating the role of some testicular cytokines which (might) have an influence on the maintenance of the BTB. Additionally, we established a new protocol of isolation of rat blood monocytes and polarized them into M0, M1 or M2 macrophages, which in turn, were used in a transmigration assay through testicular cells to test the testicular immunological barrier with respect to immunological aspects. Finally, we also tested androgen signaling pathways in adult SCs and their influence on adult SC functions and the formation of tight junctions.

4.1 Isolation and characterization of the primary adult rat Sertoli cell line-1 (PASC1)

The conditionally reprogrammed PASCs were highly pure, viable and showed similar morphological and functional characteristics as SCs in vitro comparable to previous methods (Gautam et al., 2016). In addition to the remarkably lower number of animal sacrifices required for the execution of the protocol described here (only one animal) compared to other protocols (6-10 animals; Bhushan et al., 2016; Gautam et al., 2016), our protocol was more efficient in terms of enzymes used (~20-fold lower trypsin concentration) compared to other reports

(Hoeben et al., 1994; Bhushan et al., 2016) and less time consuming for the isolation of primary adult SCs (~2 hrs versus ~6-8 hrs). Despite the fact that other protocols also described fast and successful isolation of adult SCs (Anway et al., 2003; Ciller et al., 2016; Gautam et al., 2016), the method described here generated higher yields, which is possibly due to the fact that we used SC clusters instead of single SCs during the isolation process. On the other hand, we also observed that it was better to avoid any disturbance of the tubules especially in the beginning confirming the observations by Anway et al. (2003). As suggested by Liu et al. (2017), we used irradiated feeder cells and a complete CM for conditional reprogramming of SCs, but we found that the latter was preferable. However, it was important that either the irradiated 3T3-J2 mouse fibroblasts or conditioned medium generated from these cells were necessary to get rid of the other testicular cells (PCs, LCs, germ cells and immune cells) and thus to get highly pure epithelial Sertoli cells. Thus, up to date in our presented study, we established three viable adult SC cell lines of high purity and could maintain them over almost 11 months.

Furthermore, PASC1 were nearly 100% pure, expressed the SC-specific proteins SOX9, transferrin and clusterin, which are characteristic for SCs (Skinner & Griswold, 1980; Bailey & Griswold, 1995; Chang et al., 2011). Similarly, as shown for epithelial cells from other organs like breast, prostate, colon, and lungs (Saenz et al., 2014; Liu et al., 2017; Hynds et al., 2018) the conditionally reprogrammed PASC1 maintained their differentiation state even after passage 16 by expressing GATA1, a SC-maturation gene, in addition to a very weak expression of AMH, a typical marker of immature SCs (Yomogida et al., 1994; Fröjdman et al., 2000). In contrast to other immortalization methods, which have been reported to cause cell alterations and loss of cell characteristics over time like SV-40 large T antigen or hTERT (Konrad et al., 2005; Shay & Wright, 2005; Chapman et al., 2010), PASC1 maintained their differentiation state even after long-term propagation in vitro. We also showed that PASC1 were responsive to androgen treatment and they formed TJ barriers as an in vitro proxy of the BTB.

4.2 Establishment and characterization of the TJ barrier formed between PASC1

Next, we showed that the contribution of PCs to the tight junction barrier between PASC1 was negligible. These results complied with immature SCs/PCs co-cultures (Ailenberg et al., 1988; Legendre et al., 2010). We also showed that the barrier integrity was promoted by androgens (Mruk & Cheng, 2015). Since the AR expression in SCs was reported to be undetectable after using specific immortalization methods like SV40 (Konrad et al., 2005), our results showed convincingly that PASC1 maintained high level AR gene and protein expression in early and late passages. Furthermore, responsiveness to androgen treatment was also tested in later passages as demonstrated by increased expression of ZO-1 and JAM-3 and increased integrity of TJs after androgen treatment. This is a remarkable achievement and a clear difference to primary SCs, which most often loose AR expression and function after few passages in vitro (Sneddon et al., 2005). Previous literature indicated that the expression of ZO-1 and JAM-3 proteins is androgen-dependent and their mRNA expression was observed to begin around puberty (Gliki et al., 2004; Willems et al., 2010). Remarkably, ZO-1 was recently reported to associate with occludin and thus to contribute to the integrity of the BTB (Su et al., 2020). The involvement of ZO-1 and JAM3 in SC-SC cell-cell contacts and their androgen-dependent expression were also supported by our findings. PASC1 expressed next to the classical AR also ZIP9, a newly established membrane-bound androgen receptor of physiological and pathophysiological significance (Thomas et al., 2014; Bulldan et al., 2016; 2017; 2018). In 93RS2 rat Sertoli cells lacking AR, ZIP9 is the receptor that mediates testosterone signaling leading to expression of TJ-forming proteins (Bulldan et al., 2016).

4.3 Effects of some testicular cytokines on the TJ barrier of PASC1

Many cytokines are expressed in the testis and some of them have been described to be involved in the regulation of the BTB (Ghafouri-Fard et al., 2021). We addressed the effects of IL-6,

TGF-β3 and BMP2, three cytokines well-known to be presented in the testis. Particularly, IL-6 and TGF-β3 have been described to perturb the integrity of the BTB between immature rat SCs in vitro (Lui et al., 2003; Xia et al., 2009; Zhang et al., 2014). Our results with PASC1 complied with the results obtained with immature SCs regarding the reduction of the TJ barrier after treatment with IL-6 and TGF-β3. Up to date, BMP2 has been shown to be mainly implicated in immature spermatogonial cells and SC signaling and proliferation (Puglisi et al., 2004; Itman et al., 2008). Interestingly, our results showed for the first time that BMP2 negatively affected the TJ integrity in adult SCs. The involvement of BMP2 in the regulation of the testicular TJs is further supported by findings such as the disturbance of the intestinal mucosal barrier via occludin (Chen et al., 2014) or of the epithelial barrier in the lung by BMP2 (Helbing et al., 2013).

4.4 Studying the TJ barrier between PASC1 from an immunological aspect

It has been already published that the BTB is one of the tightest blood-tissue barriers (Cheng & Mruk , 2012). Recently in vivo studies have shown that even in the absence of SCs, only very few immune cells enter the seminiferous tubules when PCs were present (Rebourcet et al., 2014). Thus, in the current study, we have also evaluated the testicular barrier in vitro by addressing the transmigration of macrophages through SCs with and without PCs and with and without Matrigel.

Using the newly established PASC1 cell line, we demonstrated that adult SCs are the main constituent of the testicular barrier in vitro (Kabbesh et al., 2021). We further found that adult SCs are also the main cell type to attenuate transmigration of macrophages. No significant improvements of the barrier could be observed with PCs or matrigel used in different combinations with and without SCs. However, to achieve a suitable in vitro model of the BTB to study macrophage transmigration, we had to modify existing protocols.

In testis, anti-inflammatory M2 macrophages are considered to constitute the major subpopulation (≈80%) of testicular macrophages (TM), whilst pro-inflammatory M1 macrophages represent only a small TM subset (≈20%) supposed to originate mainly from circulatory monocytes (Wang et al., 1994). Thus, we isolated monocytes from rat blood, differentiated them into M0 macrophages and polarized them into M1 and M2 macrophages to be used for the transmigration assay. Therefore, rat blood derived monocytes (RBDMs) were freshly isolated from rat blood using gradual decreasing centrifugation and two washings to reduce contamination with lymphocytes. The final monocyte purification step was achieved by adherence to the plastic surface after 6 hrs by removing floating lymphocytes by washing (de Almeida et al., 2000). The purity of the RBDMs was quantified by detection of the monocyte-specific marker CD68 (Dijkstra et al., 1985; Grau et al., 2000). The high purity achieved with this protocol was similar to isolation of monocytes by Fluorescence-activated Cell Sorting (FACS) (Mossadegh-Keller et al., 2013; Spiller et al., 2016). Furthermore, we found a significant increase in the mRNA level of TNF-α in RBDMs after LPS treatment, which is an additional confirmation of monocytes characteristics (Van der Bruggen et al., 1999; de Almeida et al., 2000). After polarization of M0 macrophages into M1 and M2, gene expression of M1-specific markers, CXCL11 and TNF-α, and M2-specific markers, CCL17 and CCL22, was highly increased consistent with previous observations (Spiller et al., 2016).

MCP-1 is expressed in tissues during inflammation and is induced in a variety of cell types by pro-inflammatory mediators such as TNF-α, IL-1, or endotoxin (Proost et al., 1996; Sørensen et al., 2004). Importantly, MCP1 exerts its effects through the chemokine receptor type 2 (CCR2). Once activated CCR2 triggers a set of cellular reactions that result in IP3 formation, Ca^{2+} release, and activation of protein kinase C (Proost et al., 1996; Sallusto et al., 2008), which may promote changes in the cytoskeleton of macrophages and facilitate spreading and migration of cells (Larsson et al., 2006). The chemokine MCP1 was used in the present study as a

chemoattractant, which markedly increased migration of macrophages in a dose-dependent manner corresponding with previous observations (Green et al., 2012).

Inflammatory factors and multiple cell types exert suppressive activities on autoimmunity and tissue-specific immune cell infiltration, which is established in the juvenile testis and maintained through adulthood (Chan & Anderson, 2015). In our in vitro TIB model to study monocyte/macrophage transmigration, we showed that the TIB formation depends primarily on the SCs, whereas the contribution of PCs or MG to the TIB was negligible and did not improve the barrier in vitro.

Although our data showed that our in vitro cell transmigration model was reliable, the migration of macrophages through the BTB into the seminiferous tubules lumen seems to be nearly completely inhibited in vivo (Chan & Anderson, 2015). Similarly, Rebourcet et al. (2014) could demonstrate that testicular cells (peritubular cells, germ cells ….) form a relatively strong BTB even in the absence of SCs in vivo. Only very few immune cells infiltrated the seminiferous tubules. However, one has to keep in mind that in our transmigration model we used a very high number of macrophages (~1.0×10^5 macrophages on 2.0×10^5 SCs) in contrast to lower numbers of monocytes-macrophages normally found in the adult testis in vivo (7.9×10^6 monocytes-macrophages: 3×10^7 SCs) (Bortolussi et al., 1990; Hedger, 1997). Nevertheless, with our transmigration model the contribution of all testicular cell types and of immune-suppressive molecules can be tested in vitro.

4.5 Effects of different testicular cytokines on transmigration of macrophages through the TJ barrier between PASC1

Finally, we evaluated the transmigration model after treatment with pro-inflammatory cytokines such as TNF-α, IL-6 and the sex hormone T, which are known to regulate the barrier integrity (Li et al., 2006; Zhang et al., 2014; Kabbesh et al., 2021). The effects of TNF-α, IL-6 and T on

the integrity of the barrier quantified by TER values corresponded with the results obtained from macrophage transmigration. Remarkably, in all cases M2 macrophages demonstrated the weakest transmigration rate through PASC1 barrier as well. This can be reasoned by the secretion of inflammatory cytokines by M1 only e.g., IL-1β, IL-6, IL-17a, TNF-α etc. (Li et al., 2006; Zhang et al., 2014; Pérez et al., 2014) which have negative effects on the integrity of the BTB, which in turn, allows more transmigration of M1 macrophages compared to M2.

4.6 Investigation of the involvement of the classical AR or ZIP9 in androgen signaling and TJ formation in PASC1

Later in our investigation, we addressed the involvement of the classical AR or ZIP9 in the non-classical signaling pathway of testosterone and in the stimulation of TJ protein expression and TJ formation in PASC1 cells. We showed that PASC1 cells express both the classical AR and ZIP9. Testosterone and the tetrapeptide IAPG designed to fit into the androgen binding site of ZIP9 (Malviya et al., 2021; Möller et al., 2021), were used as stimulants. The peptide was shown previously to induce ZIP9-mediated androgenic effects (Malviya et al., 2021; Möller et al., 2021).

We addressed the ability of ZIP9 to recognize not only testosterone but also the peptide IAPG. Both molecules prevented labeling of the PASC1 membrane surface by T-BSA-FITC which is a testosterone analogue that cannot pass through the plasma membrane. The plasma membrane was not labeled by T-BSA-FITC when ZIP9 expression was silenced by siRNA, indicating that ZIP9 is possibly the only androgen receptor in PASC1 cell membranes with an extracellularly accessible androgen binding site.

The classical AR is an androgen-activated transcription factor localized in the cytosol or nuclei. When stimulated by testosterone or dihydrotestosterone, cytosolic AR form dimers that move into the nuclei to regulate gene expression (Zhou, 2010; Davey & Grossmann, 2016). Our

results showed that the AR of PASC1 cells responds to testosterone accordingly; it moves from the cytosol to the nucleus, thus demonstrating that PASC1 cells express a functioning AR. In contrast, the peptide IAPG didn't cause a similar translocation of the AR, suggesting that the peptide is highly specific towards the androgen binding site of ZIP9 and not interacting at all with the AR. These two experiments demonstrated that testosterone binds to the androgen binding site of both AR and ZIP9, whereas the peptide IAPG only interacts with the androgen binding site of ZIP9.

Testosterone and IAPG stimulate in a concentration-dependent manner Erk1/2 phosphorylation in PASC1 cells, testosterone with an EC_{50} of 0.35 ± 1.29 nM, and IAPG with an EC50 of 1.02 ± 1.36 µM. These values are within the same range as those obtained under similar conditions in the 93RS2 Sertoli cell line (Möller et al., 2021). Maximal effects were obtained in both cases at 10 nM testosterone or 10 µM IAPG.

Activation of Erk1/2 in Sertoli cells is part of the Src/c-Raf/Erk1/2/CREB (ATF-1) signaling module that promotes expression and formation of TJs (Bulldan et al., 2016; Möller et al., 2021). Testosterone and IAPG were found to stimulate phosphorylation of Erk1/2 and CREB/ATF-1 only in the presence of ZIP9, whereas the AR is not important for the phosphorylation of these proteins.

4.7 Investigation of the involvement of either the classical AR or ZIP9 in PASC1 androgen signaling in stimulation of Cldn-1 or JAM-3 and of the TJ integrity

Similar observations as described above were made with respect to the stimulation of the expression of TJ-associated ZO-1 and TJ-forming Cldn-1 or JAM-3. Thus, the presence of ZIP9 was pivotal for the stimulation of expression of the three TJ-associated proteins addressed in this investigation. These results showed that TJ formation fully depends on the presence of ZIP9 and is completely independent of the AR.

ZO-1, claudins, and JAM-3 are essential for the formation and maintenance of the BTB. Ensuring the dual functionality of this structure as a physical and immunological barrier is an absolute presupposition for the protection of male fertility (Cavicchia et al., 1996; Cheng & Mruk, 2012). BTB defects that weaken its integrity are associated with impaired spermatogenesis and testicular dysgenesis syndrome; malfunctioning of the BTB may also be linked to idiopathic male infertility observed in 30-40% of men with abnormal semen parameter (Cavicchia et al., 1996; Jiang et al., 2014). Taken together, these observations and the findings of the current investigation imply that there is a direct connection between ZIP9/androgen signaling and TJ protein expression and TJ formation in Sertoli cells and establish ZIP9 as a significant player in rat male fertility.

Findings from an earlier publication based upon experiments involving selective ablation of AR in mouse Sertoli cells might indirectly support the conclusions of the current investigation. In this SCARKO (selective ablation of AR in SC knockout mice) animal model, ablation of AR expression affected Sertoli cell maturation, barrier formation, and cytoskeletal development (Willems et al., 2010). Nevertheless, barrier formation was affected only to some degree and in fact was delayed by 5–10 days compared with that of control animals, whereas ZO-1 expression was only slightly affected. These findings suggested that the classical AR is not the sole promoter of TJ formation. The minor effects on TJ formation reported by Willems et al. (2010) may be also associated with the negative influence of AR ablation on SC maturation. Based on their findings, the authors came to the conclusion that the targeted ablation of AR did not completely prevent the formation of an anatomical and functional barrier defining basal and adluminal compartments within the seminiferous epithelium (Willems et al., 2010). On the other hand, Cldn-3, which is reported by Meng et al. (2005) to be a direct transcriptional target of the androgen receptor signaling was downregulated in SCARKO mice in addition to other tight junction proteins ZO-1, ZO-2, Cldn-13 and Cldn-25, which led to the assumption that the

AR is pivotal for the TJ remodeling in mice (Chakraborty et al., 2014). Moreover, testes of AR deficient mice contained high levels of immunoglobulin G (IgG) in addition to higher numbers of macrophages, monocytes and eosinophils in the interstitial space compared to the control animals (Meng et al., 2011). At that time, however, ZIP9 was unknown as a physiologically relevant androgen receptor of rat Sertoli cells.

Testosterone is undoubtedly a major parameter of male physiology. Not only is it essential for the establishment and maintenance of the male phenotype, behavior, and fertility, it also protects male fertility by regulating TJ dynamics at the blood–testis barrier. Nevertheless, testosterone replacement therapy prescribed for low endogenous testosterone levels is not necessarily the best way to treat BTB defects in order to restore fertility. Not only can exogenous testosterone induce severe side effects such as polycythemia, cardiac hypertrophy, and myocardial infarction, it also unfavorably affects male fertility (Payne et al., 2004; Nascimento & Medei, 2011). In a hypogonadal mouse model, although administration of androgens triggered TJ formation and also initiated in some tubules the production of post-meiotic elongated spermatids, spermatozoa were not obtained (Walker, 2010). This is because exogenous testosterone, by inducing negative feedback on the hypothalamic–pituitary–gonadal axis, prevents GnRH release from the hypothalamus and FSH and LH from the pituitary, leading to the impairment of testosterone production in Leydig cells (Basaria, 2014). As a result, germ cell production under these conditions is impaired (Patel et al., 2019).

4.8 ZIP9, the non-classical androgen receptor and its future therapeutic application

Based on the results of the investigation presented here, stimulation of the expression of TJ-associated or TJ-forming proteins by the ZIP9-specific, androgenic peptide IAPG might help to segregate BTB-stimulating events from the negative effects of testosterone on spermatogenesis. Although the expression patterns for TJ proteins appear to be stage- and species-specific

(Morrow et al., 2010), there is some overlap between species. The importance of claudins, ZO-1, and occludin for the maintenance of the BTB has also been demonstrated in humans. Thus, a recent study dealing with the integrity of the blood–testis barrier in terms of adhesion molecules in nonobstructive azoospermia identified the above proteins as critical parameters not only for BTB formation but also male fertility (Aydin et al., 2020). Moreover, Cldn-11 was reported to be expressed in mouse, rat and human, to play a vital role in spermatogenesis and seems to be essential in the BTB in humans (Stammler et al., 2016).

Based on the above, one can expect that the selective targeting of ZIP9 by the androgenic peptide IAPG may prove advantageous in the treatment of BTB-associated male infertility. In a first step in that direction, the hypogonadal mouse (Ebling et al., 2006) could be an appropriate model to investigate this possibility.

4.9 Conclusion

Collectively, our study showed the effectiveness of conditional reprogramming as an immortalization method, in which adult rat SCs maintained their differentiation and most importantly, AR receptor expression even after long term in vitro cultivation. Secondly, we have shown that adult SCs are the main contributors to the TJ barrier in vitro and the main testicular cells to attenuate transmigration of macrophages in a newly established transmigration model. Lastly, we demonstrated that ZIP9 was the main player in mediation of androgen signaling in PASC1 cells.

On the other hand, it was not possible to establish a "tighter" TJ barrier as we hypothesized that adult SCs could form a stronger barrier in contrast to immature SCs. Although this might be due to missing cells, certain immunological factors or even the absence of other circulatory cytokines or hormones in our in vitro model compared to in vivo conditions, we and others never could establish a very tight BTB in vitro. Thus, after many years of BTB research, one

has to critically ask whether the BTB is really a very tight barrier. Additionally, compared to other in vitro models of different tissue barriers, the TER values of our established in vitro BTB were clearly weaker (~20 Ω×cm^2 of PASC1 barrier (Kabbesh et al., 2021) compared to the high values in other cell types1400-2400 Ω×cm^2 of the gastric intestinal barrier between human epithelial colon cell line Caco-2 (Endorf et al., 2000) or even up to ~5900 Ω×cm^2 in rat blood brain barrier (Lippmann et al., 2014)).

Furthermore, transmigration of macrophages through the TJ barrier between PASC1 cells could not be completely stopped. Maybe other immune tolerance mechanisms are involved in testis immune privilege or in activating immune tolerance mechanisms of SCs.

Moreover, we have shown that the AR is not the sole receptor to promote TJ in Sertoli cells but the ZIP9 was shown to be the main player to mediate androgen signaling and TJ formation in adult rat Sertoli cells.

All in all, we have succeeded in isolating functional adult rat SCs and showed that these cells could be used as an in vitro model to study the TJ barrier and androgen signaling in adult rat SCs.

5 Summary

Despite numerous studies performed to analyze the BTB in vitro, very few were focused on its establishment or the key cells of its formation. Recent research demonstrated that not only SCs are contributing to establishment of the BTB but also other testicular cells like PCs. As recently published, ZIP9 is the sole receptor to mediate the non-classical pathway of T signaling in immature rat SCs. The aim of this study was to investigate which testicular cell(s) are contributing to formation of the BTB between adult rat SCs and the establishment of a transmigration model to study the TIB in vitro. We also aimed to uncover the mechanism of testosterone signaling in adult rat SCs.

We were successful in establishing an isolation protocol of adult rat SC and created the pure PASC1 line using enzymatic digestion and conditional reprogramming. PASC1 showed the main characteristics of SCs by maintaining expression of SC-specific and maturation markers in addition to the AR even after long propagation time. Our results have also revealed that SCs are the main contributors to formation of the BTB in vitro. We were also successful in establishing a transmigration model of macrophages through the barrier between SC after using a modified protocol to isolate rat monocytes from rat blood and polarizing them into M0, M1 and M2 macrophages. The results also showed that our in vitro BTB did only attenuate transmigration of macrophages but did not completely stop them. Of note, M2 macrophages transmigrated less efficiently compared to M0 or M1 macrophages. Lastly, we demonstrated that the regulation of the tight junction proteins Cldn-1, JAM-3 and ZO-1 is androgen-dependent. The ZIP9 is the only mediator of the non-classical pathway of androgen signaling represented by TJ formation and regulation in PASC1.

Taken together, we proved that SCs but not PCs are the main contributors to the BTB formation in vitro. Co-culturing both SCs and PCs with or without Matrigel did not have a significant effect to the BTB integrity. In addition, we showed that ZIP9, but not the AR, is the main

mediator of the non-classical pathway of androgen signaling in adult rat SC. Furthermore, we propose that other local immunological factors in vivo contribute to the formation of the TIB as we were unable to stop transmigration of macrophages through the PASC1 barrier. Our study paves the way for further investigations to understand the mechanism of testis immune privilege during spermatogenesis and the possible future therapeutic use of ZIP9 as a possible target of androgens.

6 Zusammenfassung

Trotz zahlreicher Studien, die durchgeführt wurden, um die BTB in vitro zu analysieren, konzentrierten sich nur sehr wenige auf die Etablierung oder die Schlüsselzellen seiner Bildung. Jüngste Forschungen zeigten, dass nicht nur SCs zur Etablierung des BTB beitragen, sondern auch andere Hodenzellen wie PCs. Kürzlich würde veröffentlicht, dass ZIP9 der einzige Rezeptor ist, der den nicht-klassischen Weg der T-Signalgebung in unreifen Ratten-SCs vermittelt. Das Ziel dieser Studie war es zu untersuchen, welche Hodenzelle(n) zur Bildung der BTB zwischen adulten Ratten-SCs beitragen, und die Etablierung eines Transmigrationsmodells zur Untersuchung der TIB in vitro. Unser Ziel war es auch, den Mechanismus der Testosteron-Signalübertragung in adulten Ratten-SCs aufzudecken.

Wir waren erfolgreich bei der Etablierung eines Isolationsprotokolls für adulte Ratten-SC und erstellten die reine PASC1-Linie unter Verwendung von enzymatischem Verdau und der bedingten Reprogrammierung. PASC1 behielt die Hauptmerkmale von SCs bei, indem es die Expression SC-spezifischer und SC-Reifungsmarker zusätzlich zum AR auch nach langer kultiviert aufrechterhielt. Unsere Ergebnisse zeigten auch, dass SCs den Hauptbeitrag zur Bildung der BTB in vitro leisten. Wir waren auch erfolgreich bei der Gewinnung eines Transmigrationsmodells von Makrophagen durch die Barriere zwischen SCs, nachdem wir ein

modifiziertes Protokoll verwendeten, um Rattenmonozyten aus Rattenblut zu isolieren und sie dann in M0, M1 und M2 Makrophagen zu polarisieren. Die Ergebnisse zeigten auch, dass unser in vitro BTB die Transmigration von Makrophagen nur verringerte, aber nicht vollständig stoppte. Bemerkenswert ist, dass M2-Makrophagen im Vergleich zu M0- oder M1-Makrophagen weniger effizient transmigrierten. Schließlich haben wir gezeigt, dass die Regulation der Tight-Junction-Proteine Cldn-1, JAM-3 und ZO-1 Androgen-abhängig ist. Das ZIP9 ist der einzige Mediator des nicht-klassischen Wegs der Androgensignalisierung, der durch die TJ-Bildung und -Regulierung in PASC1 repräsentiert wird.

Zusammengenommen haben wir demonstriert, dass SCs, aber nicht PCs, die Hauptverursacher der BTB-Bildung in vitro sind. Die Co-Kultivierung von sowohl SCs als auch PCs mit oder ohne Matrigel trugen nicht signifikanten zur Integrität der BTB bei. Darüber hinaus haben wir gezeigt, dass ZIP9, aber nicht der AR, der Hauptmediator des nicht-klassischen Wegs der Androgen-Signalübertragung in erwachsenen Ratten-SCs ist. Darüber hinaus schlagen wir vor, dass andere lokale immunologische In-vivo-Faktoren zur Bildung der TIB beitragen, da wir die Transmigration von Makrophagen durch die PASC1-Barriere nicht vollständig stoppen konnten. Unsere Studie ebnet den Weg für weitere Untersuchungen, um den Mechanismus der Immunprivilegien der Hoden während der Spermatogenese und den möglichen zukünftigen therapeutischen Einsatz von ZIP9 als möglichen Hauptziel von Androgen zu verstehen.

7 References

Abe M, Kurosawa M, Ishikawa O, Miyachi Y, Kido H. Mast cell tryptase stimulates both human dermal fibroblast proliferation and type I collagen production (1998). Clin Exp Allergy 28:1509-1517.

Ahn C, Shin DH, Lee D, Kang SM, Seok JH, Kang HY, Jeung EB (2016). Expression of claudins, occludin, junction adhesion molecule A and zona occludens 1 in canine organs. Mol Med Rep 14:3697-3703.

Ailenberg M, Tung PS, Pelletier M, Fritz IB (1988). Modulation of Sertoli cell functions in the two-chamber assembly by peritubular cells and extracellular matrix. Endocrinology 122:2604-2612.

Anway MD, Folmer J, Wright WW, Zirkin BR (2003). Isolation of Sertoli cells from adult rat testes: an approach to ex vivo studies of Sertoli cell function. Biol Reprod 68:996-1002.

Arck P, Solano ME, Walecki M, Meinhardt A (2014). The immune privilege of testis and gravid uterus: same difference? Mol Cell Endocrinol. 382:509-520.

Arukwe A, Nordtug T, Kortner TM, Mortensen AS, Brakstad OG (2008). Modulation of steroidogenesis and xenobiotic biotransformation responses in zebrafish (Danio rerio) exposed to water-soluble fraction of crude oil. Environ Res 107:362-370.

Asano K, Takahashi N, Ushiki M, Monya M, Aihara F, Kuboki E, Moriyama S, Iida M, Kitamura H, Qiu CH, Watanabe T, Tanaka M (2015). Intestinal CD169(+) macrophages initiate mucosal inflammation by secreting CCL8 that recruits inflammatory monocytes. Nat Commun. 21:7802.

Aydin S, Billur D, Kizil S, Ozkavukcu S, Topal Celikkan F, Aydos K, Erdemli E (2020). Evaluation of blood-testis barrier integrity in terms of adhesion molecules in nonobstructive azoospermia. Andrologia 52:e13636.

Bailey R, Griswold MD (1995). Clusterin in the male reproductive system: localization and possible function. Mol Cell Endocrinol 151:17-23.

Banchereau J, Steinman RM. Dendritic cells and the control of immunity (1998). Nature 392:245-252.

Basaria S (2014). Male hypogonadism. Lancet 383:1250-1263.

Beau C, Rauch M, Joulin V, Jégou B, Guerrier D (2000). GATA-1 is a potential repressor of anti-Müllerian hormone expression during the establishment of puberty in the mouse. Mol Reprod Dev 56:124-138.

Benhar I, London A, Schwartz M (2012). The privileged immunity of immune privileged organs: the case of the eye. Front Immunol 3:296.

Benten WP, Lieberherr M, Giese G, Wrehlke C, Stamm O, Sekeris CE, Mossmann H, Wunderlich F (1999). Functional testosterone receptors in plasma membranes of T cells. FASEB J 13:123-33.

Berg AH, Rice CD, Rahman MS, Dong J, Thomas P (2014). Identification and characterization of membrane androgen receptors in the ZIP9 zinc transporter subfamily: I. Discovery in female atlantic croaker and evidence ZIP9 mediates testosterone-induced apoptosis of ovarian follicle cells. Endocrinology 155:4237-4249.

Bhushan S, Tchatalbachev S, Lu Y, Fröhlich S, Fijak M, Vijayan V, Chakraborty T, Meinhardt A (2015). Differential activation of inflammatory pathways in testicular macrophages provides a rationale for their subdued inflammatory capacity. J Immunol 194:5455-5464.

Bhushan S, Aslani F, Zhang Z, Sebastian T, Elsässer HP, Klug J (2016). Isolation of Sertoli cells and peritubular cells from rat testes. J Vis Exp 108:e53389.

Bhushan S, Meinhardt A. The macrophages in testis function (2017). J Reprod Immunol. 119:107-112.

Bilinska B (2006). Hormonal status of male reproductive system: androgens and estrogens in the testis and epididymis in vivo and in vitro approaches. Reprod Biol 1:43-58.

Bortolussi M, Zanchetta R, Belvedere P, Colombo L (1990). Sertoli and Leydig cell numbers and gonadotropin receptors in rat testis from birth to puberty. Cell Tissue Res 260:185-191.

Brown Z, Strieter RM, Neild GH, Thompson RC, Kunkel SL, Westwick J (1992). IL-1 receptor antagonist inhibits monocyte chemotactic peptide 1 generation by human mesangial cells. Kidney Int 42:95-101.

Bulldan A, Dietze R, Shihan M, Scheiner-Bobis G (2016). Non-classical testosterone signaling mediated through ZIP9 stimulates claudin expression and tight junction formation in Sertoli cells. Cell Signal 28:1075-1085.

Bulldan A, Malviya VN, Upmanyu N, Konrad L, Scheiner-Bobis G (2017). Testosterone/bicalutamide antagonism at the predicted extracellular androgen binding site of ZIP9. Biochim Biophys Acta Mol Cell Res 1864:2402-2414.

Bulldan A, Bartsch JW, Konrad L, Scheiner-Bobis G (2018). ZIP9 but not the androgen receptor mediates testosterone-induced migratory activity of metastatic prostate cancer cells. Biochim Biophys Acta Mol Cell Res 1865:1857-1868.

Carson JA, Manolagas SC (2015). Effects of sex steroids on bones and muscles: Similarities, parallels, and putative interactions in health and disease. Bone 80**:** 67-78.

Cavicchia JC, Sacerdote FL, Ortiz L (1996). The human blood-testis barrier in impaired spermatogenesis. Ultrastruct Pathol 20:211-218.

Cera MR, Del Prete A, Vecchi A, Corada M, Martin-Padura I, Motoike T, Tonetti P, Bazzoni G, Vermi W, Gentili F, Bernasconi S, Sato TN, Mantovani A, Dejana E (2004). Increased DC trafficking to lymph nodes and contact hypersensitivity in junctional adhesion molecule-A-deficient mice. J Clin Invest 114:729-738.

Chakraborty P, Buaas FW, Sharma M, Smith BE, Greenlee AR, Eacker SM, Braun RE (2014). Androgen-dependent Sertoli cell tight junction remodeling is mediated by multiple tight junction components. Mol Endocrinol 29:1055-1072.

Chan AY, Anderson MS (2015). Central tolerance to self revealed by the autoimmune regulator. Ann N Y Acad Sci 1356:80-89.

Chang YF, Lee-Chang JS, Panneerdoss S, MacLean JA 2nd, Rao MK (2011). Isolation of Sertoli, Leydig, and spermatogenic cells from the mouse testis. Biotechniques 51:341-344.

Chapman S, Liu X, Meyers C, Schlegel R, McBride AA (2010). Human keratinocytes are efficiently immortalized by a Rho kinase inhibitor. J Clin Invest 120:2619-2626.

Chen K, Xie W, Luo B, Xiao W, Teitelbaum DH, Yang H, Zhang K, Zhang C (2014). Intestinal mucosal barrier is injured by BMP2/4 via activation of NF-κB signals after ischemic reperfusion. Mediators Inflamm 2014:901530.

Chen S, So EC, Strome SE, Zhang X (2015). Impact of detachment methods on M2 macrophage phenotype and function. J Immunol Methods 426:56-61.

Cheng J, Watkins SC, Walker WH (2007). Testosterone activates mitogen-activated protein kinase via Src kinase and the epidermal growth factor receptor in Sertoli cells. Endocrinology 148:2066-2074.

Cheng CY, Mruk DD (2012). The blood-testis barrier and its implications for male contraception. Pharmacol Rev 64:16-64.

Ciller IM, Palanisamy SK, Ciller UA, McFarlane JR (2016). Postnatal expression of bone morphogenetic proteins and their receptors in the mouse testis. Physiol Res 65:673-682.

Cooper TG (2007). Sperm maturation in the epididymis: a new look at an old problem. Asian J Androl 9:533-9.

Coutinho AE, Chapman KE (2011). The anti-inflammatory and immunosuppressive effects of glucocorticoids, recent developments and mechanistic insights. Mol Cell Endocrinol 335**:** 2-13

Cutolo M (2009). Androgens in rheumatoid arthritis: when are they effectors? Arthritis Res Ther 11:126.

Dambaki C, Kogia C, Kampa M, Darivianaki K, Nomikos M, Anezinis P, Theodoropoulos PA, Castanas E, Stathopoulos EN (2005). Membrane testosterone binding sites in prostate carcinoma as a potential new marker and therapeutic target: study in paraffin tissue sections. BMC Cancer 5:148.

Davey RA, Grossmann M (2016). Androgen receptor Sstructure, function and biology: from bench to bedside. The Clinical Biochemist. Reviews 37:3-15.

de Almeida MC, Silva AC, Barral A, Barral Netto M (2000). A simple method for human peripheral blood monocyte isolation. Mem Inst Oswaldo Cruzn 95:221-3.

de Gendt K, Verhoeven G, Amieux PS, Wilkinson MF (2014). Genome-wide identification of AR-regulated genes translated in Sertoli cells in vivo using the RiboTag approach. Mol Endocrinol 28:575-91.

de Kretser DM, Loveland K, Meinhardt A, Simorangkir D, Wreford N (1998). Spermatogenesis. Hum Reprod. 1:1-8.

de Kretser DM, Bryan M, Loveland K (2016). In: Spermatogenesis. Endocrinol: Adult & Pediatric 7:2325-53.e9.

Di Agostino S, Botti F, Di Carlo A, Sette C, Geremia R (2004). Meiotic progression of isolated mouse spermatocytes under simulated microgravity. Reproduction 128:25-32.

Dietze R, Shihan M, Stammler A, Konrad L, Scheiner-Bobis G (2015). Cardiotonic steroid ouabain stimulates expression of blood-testis barrier proteins claudin-1 and -11 and formation of tight junctions in Sertoli cells. Mol Cell Endocrinol 405:1-13.

Dijkstra CD, Döpp EA, Joling P, Kraal G (1985). The heterogeneity of mononuclear phagocytes in lymphoid organs: distinct macrophage subpopulations in the rat recognized by monoclonal antibodies ED1, ED2 and ED3. Immunology 54:589-599.

Drummond AE (2006). The role of steroids in follicular growth. Reprod Biol Endocrinol 4:16.

Ebling FJ, Nwagwu MO, Baines H, Myers M, Kerr JB (2006). The hypogonadal (hpg) mouse as a model to investigate the estrogenic regulation of spermatogenesis. Hum Fertil (Camb) 9:127-135.

Endorf C, Spahn-Langguth H, Regårdh CG, Lipka E, Amidon GL, Langguth P (2000). Caco-2 versus Caco-2/HT29-MTX co-cultured cell lines: permeabilities via diffusion, inside- and outside-directed carrier-mediated transport. Journal of Pharma Scie 89:63-75.

Estrada M, Espinosa A, Muller M, Jaimovich E (2003). Testosterone stimulates intracellular calcium release and mitogen-activated protein kinases via a G protein-coupled receptor in skeletal muscle cells. Endocrinology 144: 3586-3597.

Fallarino F, Luca G, Calvitti M, Mancuso F, Nastruzzi C, Fioretti MC, Grohmann U, Becchetti E, Burgevin A, Kratzer R, van Endert P, Boon L, Puccetti P, Calafiore R (2009). Therapy of experimental type 1 diabetes by isolated Sertoli cell xenografts alone. J Exp Med 206:2511-26.

Fijak M, Meinhardt A (2006). The testis in immune privilege. Immunol Rev 213:66-81.

Fröjdman K, Harley, V, Pelliniemi L (2000). Sox9 protein in rat Sertoli cells is age and stage dependent. Histochemistry 113:31–36.

Fijak M, Damm LJ, Wenzel JP, Aslani F, Walecki M, Wahle E, Eisel F, Bhushan S, Hackstein H, Baal N, Schuler G, Konrad L, Rafiq A, O'Hara L, Smith LB, Meinhardt A (2015). Influence of Testosterone on Inflammatory Response in Testicular Cells and Expression of Transcription Factor Foxp3 in T Cells. Am J Reprod Immunol 74:12-25.

Fink C, Weigel R, Fink L, Wilhelm J, Kliesch S, Zeiler M, Bergmann M, Brehm R (2009). Claudin-11 is over-expressed and dislocated from the blood-testis barrier in Sertoli cells associated with testicular intraepithelial neoplasia in men. Histochem Cell Biol 131:755-764.

Florin A, Maire M, Bozec A, Hellani A, Chater S, Bars R, Chuzel F, Benahmed M (2005). Androgens and postmeiotic germ cells regulate claudin-11 expression in rat Sertoli cells. Endocrinology 146:1532-40.

Forrester JV, Xu H, Lambe T, Cornall R (2008). Immune privilege or privileged immunity? Mucosal Immunol 1:372-81.

Fu R, Liu J, Fan J, Li R, Li D, Yin J, Cui S (2012). Novel evidence that testosterone promotes cell proliferation and differentiation via G protein-coupled receptors in the rat L6 skeletal muscle myoblast cell line. J Cell Physiol 227: 98-107.

Furuse M, Sasaki H, Fujimoto K, Tsukita S (1998). A single gene product, claudin-1 or -2, reconstitutes tight junction strands and recruits occludin in fibroblasts. J Cell Biol. 19:391-401.

Furuse M, Hata M, Furuse K, Yoshida Y, Haratake A, Sugitani Y, Noda T, Kubo A, Tsukita S (2002). Claudin-based tight junctions are crucial for the mammalian epidermal barrier: a lesson from claudin-1-deficient mice. J Cell Biol 156:1099-1111.

Gao X, Liu Z, Song J, Zhang Y, Jiang H, Ma D, Wang J, Yuan P, Li R, Bai J, Wang T, Wang S, Liu J, Liu X (2020). Berberine is sufficient to restore the destroyed seminiferous tubule structure and hypospermatogenesis in diabetes mellitus. Clin Transl Med 10:e193.

Gautam M, Bhattacharya I, Devi YS, Arya SP, Majumdar SS (2016). Hormone responsiveness of cultured Sertoli cells obtained from adult rats after their rapid isolation under less harsh conditions. Andrology 4:509-519.

Ghafouri-Fard S, Shoorei H, Mohaqiq M, Raza SHA, Taheri M (2021). The role of different compounds on the integrity of blood-testis barrier: A concise review based on in vitro and in vivo studies. Gene 780:145531.

Gliki G, Ebnet K, Aurrand-Lions M, Imhof BA, Adams RH (2004). Spermatid differentiation requires the assembly of a cell polarity complex downstream of junctional adhesion molecule-C. Nature 431:320-324.

Gow A, Southwood CM, Li JS, Pariali M, Riordan GP, Brodie SE, Danias J, Bronstein JM, Kachar B, Lazzarini RA (1999). CNS myelin and sertoli cell tight junction strands are absent in Osp/claudin-11 null mice. Cell 10:649-659.

Grau V, Scriba A, Stehling O, Steiniger B (2000). Monocytes in the rat. Immunobiology 202:94-103.

Green TD, Park J, Yin Q, Fang S, Crews AL, Jones SL, Adler KB (2012). Directed migration of mouse macrophages in vitro involves myristoylated alanine-rich C-kinase substrate (MARCKS) protein. J Leukoc Biol 92:633-639.

Guazzone VA, Hollwegs S, Mardirosian M, Jacobo P, Hackstein H, Wygrecka M, Schneider E, Meinhardt A, Lustig L, Fijak M (2011). Characterization of dendritic cells in testicular draining lymph nodes in a rat model of experimental autoimmune orchitis. Int J Androl 34:276-89.

Gye MC (2003). Expression of claudin-1 in mouse testis. Arch Androl 49:271-279.

Hall PF (1985). Role of cytochromes P-450 in the biosynthesis of steroid hormones. Vitam Horm 42: 315-368.

Haverfield JT, Meachem SJ, O'Bryan MK, McLachlan RI, Stanton PG (2013). Claudin-11 and connexin-43 display altered spatial patterns of organization in men with primary seminiferous tubule failure compared with controls. Fertil Steril 100:658-66.

Hedger M (1997). Testicular leukocytes: what are they doing?. Rev Reprod 2:38-47.

Hedger M, Hals D (2006). Immunophysiology of the man reproductive tract. In: Knobil and Neill's Physiology of Reproduction (3rd) 1:1195-1286.

Heffner D, Schust D (2010). In: The reproductive system at a glance. 3rd edition.

Helbing T, Herold EM, Hornstein A, Wintrich S, Heinke J, Grundmann S, Patterson C, Bode C, Moser M (2013). Inhibition of BMP activity protects epithelial barrier function in lung injury. J Pathol 231:105-116.

Hoeben E, Deboel L, Rombauts L, Heyns W, Verhoeven G (1994). Different cells and cell lines produce factors that modulate Sertoli cell function. Mol Cell Endocrinol 101:263-275.

Holstein A, Schulze W, Davidoff M (2003). Understanding spermatogenesis is a prerequisite for treatment. Reprod Biol Endocrinol 1:107.

Hussein MR, Abou-Deif ES, Bedaiwy MA, Said TM, Mustafa MG, Nada E, Ezat A, Agarwal A (2005). Phenotypic characterization of the immune and mast cell infiltrates in the human testis shows normal and abnormal spermatogenesis. Fertil Steril 83:1447-1453.

Hynds RE, Vladimirou E, Janes SM (2018). The secret lives of cancer cell lines. Dis Model Mech 11:dmm037366.

Ilani N, Armanious N, Lue YH, Swerdloff RS, Baravarian S, Adler A, Tsang C, Jia Y, Cui YG, Wang XH, Zhou ZM, Sha JH, Wang C (2012). Integrity of the blood-testis barrier in healthy men after suppression of spermatogenesis with testosterone and levonorgestrel. Hum Reprod 27:3403-11.

Itman C, Loveland KL (2008). SMAD expression in the testis: an insight into BMP regulation of spermatogenesis. Dev Dyn 237:97-111.

Jaguin M, Houlbert N, Fardel O, Lecureur V (2013). Polarization profiles of human M-CSF-generated macrophages and comparison of M1-markers in classically activated macrophages from GM-CSF and M-CSF origin. Cell Immunol 281:51-61.

Jiang C, Hall SJ, Boekelheide K (1997). Development and characterization of a prepubertal rat Sertoli cell line, 93RS2. J Androl 18:393-9.

Jiang XH, Bukhari I, Zheng W, Yin S, Wang Z, Cooke HJ, Shi QH (2014). Blood-testis barrier and spermatogenesis: lessons from genetically-modified mice. Asian J Androl 16:572-580.

Jezek D, Banek L, Hittmair A, Pezerović-Panijan R, Goluza T, Schulze W (1999). Mast cells in testicular biopsies of infertile men with 'mixed atrophy' of seminiferous tubules. Andrologia 31:203-210.

Jégou B, Sharpe RM (1993). Paracrine mechanisms in testicular control. In: Molecular biology of the male reproductive system pp 271-310. de Krester DM (ed), Academic Press, New York.

Kabbesh H, Riaz MA, Jensen AD, Scheiner-Bobis G, Konrad L (2021). Long-term maintenance of viable adult rat Sertoli cells able to establish testis barrier components and function in response to androgens. Cells 10:2405.

Kabbesh H, Riaz MA, Jensen AD, Scheiner-Bobis G, Konrad L (2022). Transmigration of macrophages through primary adult rat Sertoli cells. Tissue Barriers 20:2064179.

Kampa M, Nifli AP, Charalampopoulos I, Alexaki VI, Theodoropoulos PA, Stathopoulos EN, Gravanis A, Castanas E (2005). Opposing effects of estradiol- and testosterone-membrane binding sites on T47D breast cancer cell apoptosis. Exp Cell Res 307: 41-51.

Kampa M, Papakonstanti EA, Hatzoglou A, Stathopoulos EN, Stournaras C, Castanas E (2002). The human prostate cancer cell line LNCaP bears functional membrane testosterone receptors that increase PSA secretion and modify actin cytoskeleton. FASEB J 16:1429- 1431.

Kato S, Masuhiro Y, Watanabe M, Kobayashi Y, Takeyama KI, Endoh H, Yanagisawa, J (2000). Molecular mechanism of a cross-talk between oestrogen and growth factor signalling pathways. Gen to cells devoted to mol & cell mech 5: 593–601.

Kelsey TW, Li LQ, Mitchell RT, Whelan A, Anderson RA, Wallace WH (2014). A validated age-related normative model for male total testosterone shows increasing variance but no decline after age 40 years. PloS ONE 9:e109346.

Komljenovic D, Sandhoff R, Teigler A, Heid H, Just WW, Gorgas K (2009). Disruption of blood-testis barrier dynamics in ether-lipid-deficient mice. Cell Tissue Res 337:281-299.

Konrad L, Munir Keilani M, Cordes A, Völck-Badouin E, Laible L, Albrecht M, Renneberg H, Aumüller G (2005). Rat Sertoli cells express epithelial but also mesenchymal genes after immortalization with SV40. Biochim Biophys Acta 1722:6-14.

Kuo T, Harris CA, Wang JC (2013). Metabolic functions of glucocorticoid receptor in skeletal muscle. Mol Cell Endocrinol 380:79-88.

Lan P, Zhan W, Wang J, Yan L, Xiao L, Wu X (2001). Immune privilege induced by cotransplantation of islet and allogeneic testicular cells. Chin Med J (Engl) 114:1026-1029.

Larsson C (2006). Protein kinase C and the regulation of the actin cytoskeleton. Cell Signal 18:276-284.

Lee HM, Oh BC, Lim DP, Lee DS, Cho J, Lee G, Lee JR. Role of complement regulatory proteins in the survival of murine allo-transplanted Sertoli cells (2007). J Korean Med Sci 22:277-282.

Legendre A, Froment P, Desmots S, Lecomte A, Habert R, Lemazurier E (2014). An engineered 3D blood-testis barrier model for the assessment of reproductive toxicity potential. Biomaterials 31:4492-505.

Li MW, Xia W, Mruk DD, Wang CQ, Yan HH, Siu MK, Lui WY, Lee WM, Cheng CY (2006). Tumor necrosis factor {alpha} reversibly disrupts the blood-testis barrier and impairs Sertoli-germ cell adhesion in the seminiferous epithelium of adult rat testes. J Endocrinol 190:313-329.

Li N, Wang T, Han D (2012). Structural, cellular and molecular aspects of immune privilege in the testis. Front Immunol 3:152.

Lippmann ES, Al-Ahmad A, Azarin SM, Palecek SP, Shusta EV (2014). A retinoic acid-enhanced, multicellular human blood-brain barrier model derived from stem cell sources. Sci Rep 4:4160.

Liu X, Ory V, Chapman S, Yuan H, Albanese C, Kallakury B, Timofeeva OA, Nealon C, Dakic A, Simic V, Haddad BR, Rhim JS, Dritschilo A, Riegel A, McBride A, Schlegel R (2012). ROCK inhibitor and feeder cells induce the conditional reprogramming of epithelial cells. Am J Pathol 180:599–607.

Liu X, Krawczyk E, Suprynowicz FA, Palechor-Ceron N, Yuan H, Dakic A, Simic V, Zheng YL, Sripadhan P, Chen C, Lu J, Hou TW, Choudhury S, Kallakury B, Tang DG, Darling T, Thangapazham R, Timofeeva O, Dritschilo A, Randell SH, Albanese C, Agarwal S, Schlegel R (2017). Conditional reprogramming and long-term expansion of normal and tumor cells from human biospecimens. Nat Protoc 12:439–451.

Loveland KL, Klein B, Pueschl D, Indumathy S, Bergmann M, Loveland BE, Hedger MP, Schuppe HC (2017). Cytokines in male fertility and reproductive pathologies: immunoregulation and beyond. Front Endocrin (Lausanne) 8:307.

Lui WY, Lee WM, Cheng CY (2001). Transforming growth factor-β3 perturbs the inter-Sertoli tight junction permeability barrier *in vitro* possibly mediated via its effects on occludin, zonula occludens-1, and claudin-11. Endocrinology 142:1865-1877.

Lui WY, Lee WM, Cheng CY (2003). Transforming growth factor beta3 regulates the dynamics of Sertoli cell tight junctions via the p38 mitogen-activated protein kinase pathway. Biol Reprod 68:1597-1612.

Lui WY, Cheng CY (2012). Transcriptional regulation of cell adhesion at the blood-testis barrier and spermatogenesis in the testis. Adv Exp Med Biol 763:281-294.

Malviya VN, Bulldan A, Wende RC, Kabbesh H, Möller ML, Schreiner PR, Scheiner-Bobis G (2021). The effects of tetrapeptides designed to fit the androgen binding site of ZIP9 on myogenic and osteogenic cells. Biology (Basel) 11:19.

Mangelsdorf DJ, Thummel C, Beato M, Herrlich P, Schutz G, Umesono K, Blumberg B, Kastner P, Mark M, Chambon P, Evans RM (1995). The nuclear receptor superfamily: the second decade. Cell 83:835–839.

Mazaud-Guittot S (2011). Dissecting the phthalate-induced Sertoli cell injury: the fragile balance of proteases and their inhibitors. Biol Reprod 85:1091-1103.

Mayerhofer A (2013). Human testicular peritubular cells: more than meets the eye. Reproduction 145:R107-16.

Mellor AL, Munn DH (2008). Creating immune privilege: active local suppression that benefits friends, but protects foes. Nat Rev Immunol 8:74-80.

Meineke V, Frungieri MB, Jessberger B, Vogt H, Mayerhofer A (2000). Human testicular mast cells contain tryptase: increased mast cell number and altered distribution in the testes of infertile men. Fertil Steril 74:239-244.

Meinhardt A, Hedger MP (2011). Immunological, paracrine and endocrine aspects of testicular immune privilege. Mol Cell Endocrinol 335:60-68.

Meng J, Holdcraft RW, Shima JE, Griswold MD, Braun RE (2005). Androgens regulate the permeability of the blood-testis barrier. Proc Natl Acad Sci USA 102: 16696-16700.

Meng J, Mostaghel EA, Vakar-Lopez F, Montgomery B, True L, Nelson PS (2011). Testosterone regulates tight junction proteins and influences prostatic autoimmune responses. Horm Cancer 2:145-156.

Möller ML, Bulldan A, Scheiner-Bobis G (2021). Tetrapeptides modelled to the androgen Binding site of ZIP9 stimulate expression of tight junction proteins and tight junction formation in Sertoli cells. Biology (Basel) 11:55.

Moroi S, Saitou M, Fujimoto K, Sakakibara A, Furuse M, Yoshida O, Tsukita S (1998). Occludin is concentrated at tight junctions of mouse/rat but not human/guinea pig Sertoli cells in testes. Am J Physiol 274:C1708-1717.

Morita K, Sasaki H, Fujimoto K, Furuse M, Tsukita S (1999). Claudin-11/OSP-based tight junctions of myelin sheaths in brain and Sertoli cells in testis. J Cell Biol 3:579-588.

Morrow CM, Tyagi G, Simon L, Carnes K, Murphy KM, Cooke PS, Hofmann MC, Hess RA (2009). Claudin 5 expression in mouse seminiferous epithelium is dependent upon the transcription factor ets variant 5 and contributes to blood-testis barrier function. Biol Reprod 81: 871-879.

Morrow CM, Mruk D, Cheng CY, Hess RA (2010). Claudin and occludin expression and function in the seminiferous epithelium. Philos Trans R Soc Lond B Biol Sci 365: 1679-1696.

Mossadegh-Keller N, Sarrazin S, Kandalla PK, Espinosa L, Stanley ER, Nutt SL, Moore J, Sieweke MH (2013). M-CSF instructs myeloid lineage fate in single haematopoietic stem cells. Nature 497:239-243.

Mruk DD, Cheng CY (2004). Sertoli-Sertoli and Sertoli-germ cell interactions and their significance in germ cell movement in the seminiferous epithelium during spermatogenesis. Endocr Rev 25:747-806.

Mruk DD, Cheng CY (2015). The mammalian blood-testis barrier: Its biology and regulation. Endocr Rev 36:564-591.

Muto S, Hata M, Taniguchi J, Tsuruoka S, Moriwaki K, Saitou M, Furuse K, Sasaki H, Fujimura A, Imai M, Kusano E, Tsukita S, Furuse M (2010). Claudin-2-deficient mice are defective in the leaky and cation-selective paracellular permeability properties of renal proximal tubules. Proc Natl Acad Sci USA 107: 8011-8016.

Nascimento JH, Medei E (2011). Cardiac effects of anabolic steroids: hypertrophy, ischemia and electrical remodelling as potential triggers of sudden death. Mini Rev Med Chem 11:425-429.

New MI, White PC (1995). Genetic disorders of steroid hormone synthesis and metabolism. Baillieres Clin Endocrinol Metab 9: 525-554

Nitta T, Hata M, Gotoh S, Seo Y, Sasaki H, Hashimoto N, Furuse M, Tsukita S (2003). Size selective loosening of the blood-brain barrier in claudin-5-deficient mice. J Cell Biol 161: 653- 660.

Ochiai I, Matsuda K, Nishi M, Ozawa H, Kawata M (2004). Imaging analysis of subcellular correlation of androgen receptor and estrogen receptor α in single living cells using green fluorescent protein color variants. Mol Endocrinol 18:26–42.

Patel AS, Leong JY, Ramos L, Ramasamy R (2019). Testosterone is a contraceptive and should not Be used in men who desire fertility. World J Mens Health 37:45-54.

Payne JR, Kotwinski PJ, Montgomery HE (2004). Cardiac effects of anabolic steroids. Heart 90:473-475.

Pérez CV, Pellizzari EH, Cigorraga SB, Galardo MN, Naito M, Lustig L, Jacobo PV (2014). IL17A impairs blood-testis barrier integrity and induces testicular inflammation. Cell Tiss 358:885–898.

Petersen C, Soder O (2006). The sertoli cell--a hormonal target and 'super' nurse for germ cells that determines testicular size. Horm Res 66:153-161.

Proost P, Wuyts A, Van Damme J (1996). Human monocyte chemotactic proteins-2 and -3: structural and functional comparison with MCP-1. J Leukoc Biol 59:67-74.

Puglisi R, Montanari M, Chiarella P, Stefanini M, Boitani C (2004). Regulatory role of BMP2 and BMP7 in spermatogonia and Sertoli cell proliferation in the immature mouse. Eur J Endocrinol 151:511-20.

Rahman F, Christian HC (2007). Non-classical actions of testosterone: an update. Trends Endocrinol Metab 18:371-378.

Ramaswamy S, Weinbauer GF (2014). Endocrine control of spermatogenesis: role of FSH and LH/ testosterone. Spermatogenesis 4:e996025.

Randall VA (1994). Role of 5 alpha-reductase in health and disease. Baillieres Clin Endocrinol Metab 8:405-431.

Rebourcet D, O'Shaughnessy PJ, Monteiro A, Milne L, Cruickshanks L, Jeffrey N, Guillou F, Freeman TC, Mitchell RT, Smith LB (2014). Sertoli cells maintain Leydig cell number and peritubular myoid cell activity in the adult mouse testis. PLoS ONE 9:e105687.

Regadera J, Martínez-García F, González-Peramato P, Serrano A, Nistal M, Suárez-Quian C (2001). Androgen receptor expression in Sertoli cells as a function of seminiferous tubule maturation in the human cryptorchid testis. J Clin Endocrinol Metab 86:413-421.

Rival C, Lustig L, Iosub R, Guazzone VA, Schneider E, Meinhardt A, Fijak M (2006). Identification of a dendritic cell population in normal testis and in chronically inflamed testis of rats with autoimmune orchitis. Cell Tissue Res 324:311-318.

Saenz FR, Ory V, AlOtaiby M, Rosenfield S, Furlong M, Cavalli LR, Johnson MD, Liu X, Schlegel R, Wellstein A, Riegel AT (2014). Conditionally reprogrammed normal and transformed mouse mammary epithelial cells display a progenitor-cell-like phenotype. PLoS ONE 9:e97666.

Sallusto F, Baggiolini M (2008). Chemokines and leukocyte traffic. Nat Immunol 9:949-962.

Sanjuan PM, Langenbucher JL, Hildebrandt T (2016). Mood symptoms in steroid users: the unexamined role of concurrent stimulant Use. J Subst Use 21: 395-399.

Schell C, Albrecht M, Spillner S, Mayer C, Kunz L, Kohn F, Schwarzer U, Mayerhofer, A. (2010). 15-Deoxy-delta 12-14-prostaglandin-J2 induces hypertrophy and loss of contractility in human listicular peritubular cells: implications for human male fertility. Endocrinol 151:1257-1268.

Scobey M, Bertera S, Somers J, Watkins S, Zeleznik A, Walker W (2001). Delivery of a cyclic adenosine 3',5'-monophosphate response element-binding protein (creb) mutant to seminiferous tubules results in impaired spermatogenesis. Endocrinology 142:948-954.

Sette C, Barchi M, Bianchini A, Conti M, Rossi P, Geremia R (1999). Activation of the mitogen-activated protein kinase ERK1 during meiotic progression of mouse pachytene spermatocytes. J Biol Chem 274:33571-33579.

Sewer MB, Li D (2008). Regulation of steroid hormone biosynthesis by then cytoskeleton. Lipids 43:1109-1115.

Shay JW, Wright WE (2005). Senescence and immortalization: role of telomeres and telomerase. Carcinogenesis 26:867-874.

Shihan M, Bulldan A, Scheiner-Bobis G (2014). Non-classical testosterone signaling is mediated by a G-protein-coupled receptor interacting with Gnalpha11. Biochim Biophys Acta 1843:1172-1181.

Shihan M, Chan KH, Konrad L, Scheiner-Bobis G (2015). Non-classical testosterone signaling in spermatogenic GC-2 cells is mediated through ZIP9 interacting with Gnalpha11. Cell Signal 27:2077-2086.

Silvius JR (2003). Role of cholesterol in lipid raft formation: lessons from lipid model systems. Biochim Biophys Acta 1610: 174-183

Sipione S, Simmen KC, Lord SJ, Motyka B, Ewen C, Shostak I, Rayat GR, Dufour JM, Korbutt GS, Rajotte RV, Bleackley RC (2006). Identification of a novel human granzyme B inhibitor secreted by cultured sertoli cells. J Immunol 177:5051-5058.

Skinner MK, Griswold MD (1980). Sertoli cells synthesize and secrete transferrin-like protein. J Biol Chem 255:9523-9535.

Smith BE, Braun RE (2012). Germ cell migration across Sertoli cell tight junctions. Science 9:798-802.

Sneddon SF, Walther N, Saunders PTK (2005). Expression of androgen and estrogen receptors in Sertoli cells: studies using the SK11 cell line. Endocrinology 146:5304-5312.

Sørensen TL, Ransohoff RM, Strieter RM, Sellebjerg F (2004). Chemokine CCL2 and chemokine receptor CCR2 in early active multiple sclerosis. Eur J Neurol 11:445-449.

Spiller KL, Wrona EA, Romero-Torres S, Pallotta I, Graney PL, Witherel CE, Panicker LM, Feldman RA, Urbanska AM, Santambrogio L, Vunjak-Novakovic G, Freytes DO (2016). Differential gene expression in human, murine, and cell line-derived macrophages upon polarization. Exp Cell Res 347:1-13.

Stammler A, Müller D, Tabuchi Y, Konrad L, Middendorff R (2013). TGFβs modulate permeability of the blood-epididymis barrier in an in vitro model. PloS ONE 8:e80611.

Stammler A, Lüftner BU, Kliesch S, Weidner W, Bergmann M, Middendorff R, Konrad L (2016). Highly conserved testicular localization of claudin-11 in normal and impaired spermatogenesis. PLoS ONE 11:e0160349.

Stevenson BR, Siliciano JD, Mooseker MS, Goodenough DA (1986). Identification of ZO-1: a high molecular weight polypeptide associated with the tight junction (zonula occludens) in a variety of epithelia. J Cell Biol 103:755-766.

Su L, Mruk DD, Lie PP, Silvestrini B, Cheng CY (2012). A peptide derived from laminin-γ3 reversibly impairs spermatogenesis in rats. Nat Commun 3:1185.

Su L, Wang Z, Xie S, Hu D, Cheng YC, Mruk DD, Guan Y (2020). Testin regulates the blood-testis barrier via disturbing occludin/ZO-1 association and actin organization. J Cell Physiol 235:6127-6138.

Suarez-Pinzon W, Korbutt GS, Power R, Hooton J, Rajotte RV, Rabinovitch A (2000). Testicular sertoli cells protect islet beta-cells from autoimmune destruction in NOD mice by a transforming growth factor-beta1-dependent mechanism. Diabetes 49:1810-1818.

Thomas P, Pang Y, Dong J, Berg AH (2014). Identification and characterization of membrane androgen receptors in the ZIP9 zinc transporter subfamily: II. Role of human ZIP9 in testosterone-induced prostate and breast cancer cell apoptosis. Endocrinology 155: 4250- 4265.

Valverde MA, Parker MG (2002). Classical and novel steroid actions: a unified but complex view. Trends Biochem Sci 27: 172-173.

Van der Bruggen T, Nijenhuis S, van Raaij E, Verhoef J, van Asbeck BS (1999). Lipopolysaccharide-induced tumor necrosis factor alpha production by human monocytes involves the raf-1/MEK1-MEK2/ERK1-ERK2 pathway. Infect Immun 67:3824-3829.

Walker WH (2009). Molecular mechanisms of testosterone action in spermatogenesis. Steroids 74: 602-607.

Walker, W.H (2010). Non-classical actions of testosterone and spermatogenesis. Philos Trans R Soc Lond B Biol Sci 365:1557-1569.

Walker WH (2011). Testosterone signaling and the regulation of spermatogenesis. Spermatogenesis 1:116-120.

Wang J, Wreford NG, Lan HY, Atkins R, Hedger MP (1994). Leukocyte populations of the adult rat testis following removal of the Leydig cells by treatment with ethane dimethane sulfonate and subcutaneous testosterone implants. Biol Reprod 51:551-561.

Welsh M, Saunders P, Atanassova N, Sharpe R, Smith L (2009). "Androgen action via testicular peritubular myoid cells is essential for male fertility". FASEB J 23:4218-4230.

Welter H, Kampfer C, Lauf S, Feil R, Schwarzer J, Kohn F, Mayerhofer A (2013). Partial loss of contractile marker proteins in human testicular peritubular cells in infertility patients. Andrology 1:318-324.

Wen-Hua Z, Quirion R (2006). Insulin-like growth factor-1 (IGF-1) induces the activation/phosphorylation of Akt kinase and cAMP response element-binding protein (CREB) by activating different signaling pathways in PC12 cells. BMC Neuroscience 7:51.

Wenes M, Shang M, Di Matteo M, Goveia J, Martín-Pérez R, Serneels J, Prenen H, Ghesquière B, Carmeliet P, Mazzone M (2016). Macrophage Metabolism Controls Tumor Blood Vessel Morphogenesis and Metastasis. Cell Metab 24:701-715.

Willems A, Batlouni SR, Esnal A, Swinnen JV, Saunders PTK, Sharpe RM, Franca LR, De Gendt K, Verhoeven G (2010). Selective ablation of the androgen receptor in mouse Sertoli cells affects Sertoli cell maturation, barrier formation and cytoskeletal development. PloS ONE 5:e14168.

Winnall WR, Hedger MP (2013). Phenotypic and functional heterogeneity of the testicular macrophage population: a new regulatory model. J Reprod Immunol 97:147-158.

Xia W, Wong EW, Mruk DD, Cheng CY (2009). TGF-beta3 and TNFalpha perturb blood-testis barrier (BTB) dynamics by accelerating the clathrin-mediated endocytosis of integral membrane proteins: a new concept of BTB regulation during spermatogenesis. Dev Biol 327:48-61.

Yan HH, Mruk DD, Lee WM, Cheng CY (2008). Blood-testis barrier dynamics are regulated by testosterone and cytokines via their differential effects on the kinetics of protein endocytosis and recycling in Sertoli cells. FASEB J 22:1945-1959.

Yomogida K, Ohtani H, Harigae H, Ito E, Nishimune Y, Engel JD, Yamamoto M (1994). Developmental stage- and spermatogenic cycle-specific expression of transcription factor GATA-1 in mouse Sertoli cells. Development 120:1759-1766.

Zhang H, Yin Y, Wang G, Liu Z, Liu L, Sun F (2014). Interleukin-6 disrupts blood-testis barrier through inhibiting protein degradation or activating phosphorylated ERK in Sertoli cells. Sci Rep 4:4260.

Zhao S, Zhu W, Xue S, Han D (2014). Testicular defense systems: immune privilege and innate immunity. Cell Mol Immunol 11:428-437.

Zhou X (2010). Roles of androgen receptor in male and female reproduction: lessons from global and cell-specific androgen receptor knockout (ARKO) mice. J Androl 31: 235-243.

8 Acknowledgements

First and foremost, I would like to thank my both advisors PD Dr. Lutz Konrad and Prof. Dr. Georgios Scheiner-Bobis. I consider myself fortunate to be a mutual member of their both research groups. I was extremely lucky to have this team of supervisors who cared so much about my work, and who responded to all my questions and queries so promptly and gave me the chance to use both of their labs. It was a privilege for me to share of their both exceptional scientific knowledge but also of their extraordinary human qualities. I appreciate all their contributions of time, ideas, advice, patience, motivation, positive attitude, and immense scientific knowledge. Their guidance helped me in all the time of research and writing of this thesis.

A very special gratitude to my past and present group members whom contributed immensely to my personal and professional time on the workplace. I worked alongside with Dr. Raimund Dietze, Dr. Pradeep Kumar Kudipudi, Dr. Mazen Shihan, Herbert Kirch and Frau Hof with special mention to Dr. Muhammad Assad Riaz who was like my bigger brother joining and guiding me in almost all of my lab work together with Dr. Ahmad Bulldan. Not forgetting my dear colleagues Agnes and Jane. The group has been always a source of friendship, joy, and collaboration.

I gratefully acknowledge the funding sources that made my PhD work possible. I was funded by the Deutsche Forschungsgemeinschaft (DFG) for 3,5 years, and it is an honor to be a member of the IRTG group between Giessen and Melbourne which I received much appreciated support through my PhD work.

I would also like to thank my parents and all of my family members for their love, support, and encouragement throughout my study. I also thank my dear friends here in Germany whom made my life easier during the hard times of my PhD work.

9 Declaration

I declare that I have completed this dissertation single-handedly without the unauthorized help of a second party and only with the assistance acknowledged therein. I have appropriately acknowledged and cited all text passages that are derived verbatim from or are based on the content of published work of others, and all information relating to verbal communications. I consent to the use of an anti-plagiarism software to check my thesis. I have abided by the principles of good scientific conduct laid down in the charter of the Justus-Liebig-University Giessen „Satzung der Justus-Liebig-Universität Gießen zur Sicherung guter wissenschaftlicher Praxis“ in carrying out the investigations described in the Dissertation.

10 Erklärung

Ich erkläre: Ich habe die vorgelegte Dissertation selbstständig und ohne unerlaubte fremde Hilfe und nur mit den Hilfen angefertigt, die ich in der Dissertation angegeben habe. Alle Textstellen, die wörtlich oder sinngemäß aus veröffentlichten Schriften entnommen sind, und alle Angaben, die auf mündlichen Auskünften beruhen, sind als solche kenntlich gemacht. Ich stimme einer evtl. Überprüfung meiner Dissertation durch eine Antiplagiat-Software zu. Bei den von mir durchgeführten und in der Dissertation erwähnten Untersuchungen habe ich die Grundsätze guter wissenschaftlicher Praxis, wie sie in der „Satzung der Justus-Liebig-Universität Gießen zur Sicherung guter wissenschaftlicher Praxis“ niedergelegt sind, eingehalten.

Gießen, den ……. Hassan Kabbesh

Own publications:

- Kabbesh H, Riaz MA, Jensen AD, Scheiner-Bobis G, Konrad L. Long-Term maintenance of viable adult rat Sertoli cells able to establish testis barrier components and function in response to androgens. Cells 2021 13;2405.
- Malviya VN, Bulldan A, Wende RC, Kabbesh H, Möller ML, Schreiner PR, Scheiner-Bobis G. The effects of tetrapeptides designed to fit the androgen binding site of ZIP9 on myogenic and osteogenic cells. Biology (Basel) 2021 23;19.
- Kabbesh H, Riaz MA, Jensen AD, Scheiner-Bobis G, Konrad L. Transmigration of macrophages through primary adult rat Sertoli cells. Tissue Barriers 2022 20:2064179.
- Kabbesh H, Bulldan A, Konrad L, Scheiner-Bobis G. The Role of ZIP9 and Androgen Receptor in the Establishment of Tight Junctions between Adult Rat Sertoli Cells. Biology (Basel) 2022 11:668.

Conference abstracts:

- 12th GGL annual conference; Gießen, Germany. (04-05 Sep 2019) [Poster presentation]
- Science day des Forschungscampus Mittelhessen 2019- mind, brain and behavior; Marburg, Germany. (2 Oct 2019) [Poster presentation]
- First Digital GGL annual conference; Gießen, Germany. (29-30 Sep 2020) [Oral presentation]
- 12th International, 11th European and 32nd German Congress of Andrology; (online). (01-05 Dec 2020) [Poster presentation]
- 14th GGL annual conference; Gießen, Germany. (29-30 Sep 2021) [Poster presentation]
- Science day 2021 FB11; Gießen, Germany. (12 Nov 2021) [Poster presentation]